UNIVERSITÉ DU QUÉBEC À TROIS-RIVIÈRES

MODÉLISATION AVANCÉE ET COMMANDE D'UN BRAS ROBOT MANIPULATEUR INDUSTRIEL

MÉMOIRE PRÉSENTÉ

COMME EXIGENCE PARTIELLE DE LA

MAÎTRISE EN INGÉNIERIE-CONCENTRATION GÉNIE MÉCANIQUE

PAR

MEHDI FAZILAT

NOVEMBRE 2022

Université du Québec à Trois-Rivières

Service de la bibliothèque

Avertissement

L'auteur de ce mémoire ou de cette thèse a autorisé l'Université du Québec à Trois-Rivières à diffuser, à des fins non lucratives, une copie de son mémoire ou de sa thèse.

Cette diffusion n'entraîne pas une renonciation de la part de l'auteur à ses droits de propriété intellectuelle, incluant le droit d'auteur, sur ce mémoire ou cette thèse. Notamment, la reproduction ou la publication de la totalité ou d'une partie importante de ce mémoire ou de cette thèse requiert son autorisation.

UNIVERSITÉ DU QUÉBEC À TROIS-RIVIÈRES

ADVANCED MODELLING AND CONTROL OF INDUSTRIAL ROBOTIC MANIPULATOR ARM

A DISSERTATION

SUBMITTED TO THE DEPARTMENT OF MECHANICAL ENGINEERING IN

PARTIAL FULFILLMENT OF THE REQUIREMENTS FOR

THE DEGREE OF MASTERS IN MECHANICAL ENGINEERING

BY

MEHDI FAZILAT

NOVEMBER 2022

UNIVERSITÉ DU QUÉBEC À TROIS-RIVIÈRES

Maîtrise en ingénierie-concentration génie mécanique (M. Sc. A.)

Direction de recherche :

Prof. Nadjet Zioui, Département de Génie Mécanique, UQTR

Prénom et nom — Directrice de recherche

Jury d'évaluation

Prof. Nadjet Zioui, Département de Génie Mécanique, UQTR

Prénom et nom — Directrice de recherche

Prof. Sasan Sattarpanah Karganroudi, Département de Génie Mécanique — Président

Prénom et nom — Fonction du membre de jury

Prof. Mohamed Tadjine, École Nationale Polytechnique d'Alger, Algérie — Évaluateur externe

Prénom et nom — Fonction du membre de jury

Résumé

Au cours des dernières décennies, des recherches importantes ont été proposées concernant la modélisation des robots manipulateurs et la commande de mouvement. La commande de mouvement a des applications critiques dans de nombreux domaines, notamment la robotique industrielle et les systèmes autonomes. Un modèle mathématique précis d'un bras robotique articulé manipulateur à 6-DOF spécifique comprend le modèle cinématique et dynamique du robot représenté. Cette étude compare trois modèles dynamiques d'un bras robotique articulé. Des modèles CAO à trois niveaux de détail ont été développés à l'aide de SOLIDWORKS pour simuler la dynamique du bras robotique à six articulations ABB IRB-140. Les trois modèles différents sont conçus pour extraire des valeurs précises des paramètres de masse et d'inertie. Le premier modèle est très détaillé et proche de la conception réelle du robot. Le deuxième modèle est approximatif, utilisant des parallélépipèdes avec un choix de densité qui permet aux masses de correspondre aux masses des corps. Le troisième modèle est simplifié et considère les liens comme des tiges. Cette dernière approche est utilisée par plusieurs travaux dans la littérature en raison de sa simplicité. Les modèles ont été comparés en termes de prédictions de couple au niveau des articulations et en termes de consommation d'énergie par ces articulations et par le robot dans son ensemble. Les modèles géométriques directe et inverse ainsi que le modèle cinématique ont été utilisés pour déterminer les paramètres dynamiques et calculer le couple dans chaque articulation. Les modèles intégraient les spécifications techniques du bras ainsi que la représentation simplifiée, semi-détaillée ou détaillée des structures de liaison. Nous comparons ces modèles en tant que prédicteurs

de couple et de consommation d'énergie. Nous avons constaté que ces trois modèles produisaient des graphiques de vitesse angulaire, de couple et de consommation d'énergie avec des différences de profil relativement mineures. Ils semblaient tous être des prédicteurs adéquats des performances du robot au cours d'une tâche de 30 secondes. La consommation d'énergie des trois modèles évalue l'impact des différents modèles conçus, soulignant l'adéquation de chaque modèle à différentes situations. La différence globale de consommation d'énergie des trois modèles est de 0,53 % de moins pour le modèle détaillé et de 6,8 % de moins pour le modèle simplifié par rapport au modèle semi-détaillé. Sur la base de ces résultats, les trois modèles dynamiques testés dans cette étude semblent dignes de confiance pour prédire la consommation d'énergie pour les bras robotiques articulés.

L'algorithme de commande par modes de glissement est utilisé pour le contrôle de mouvement, avec et sans perturbations, afin de minimiser l'impact des erreurs de modélisation et de mesure et d'évaluer la robustesse pour les trois modèles de robot manipulateur. Les résultats de la simulation montrent que la méthode de commande par mode glissant est robuste et fonctionne de manière satisfaisante même en cas de perturbations externes. La commande par mode glissant offre des performances adaptées pour contrôler des modèles de robots avec des perturbations non modélisées. Généralement, les résultats des contrôleurs examinés sur trois modèles (détaillé, semi-détaillé et simplifié) sont proches avec une légère différence en pourcentage. Le contrôleur sous perturbation avait également des résultats relativement proches par rapport au contrôleur sans perturbation. La méthodologie de commande en mode glissant a une réponse dynamique appropriée et une performance d'erreur de suivi minimale à partir des résultats de simulation. L'inconvénient le plus important de cette technique est l'effet du phénomène de broutage avec l'entrée de contrôle, mais les résultats globaux pour les modèles sont satisfaisants.

Mots-clés *: Robots manipulateurs industriels, Conception assistée par ordinateur (CAO), Représentation D-H, Modèle dynamique et simplifications, Consommation d'énergie, Commande robuste, SMC, Cinématique Simulink, dynamique, Théorème de stabilité de Lyapunov, suivi de trajectoire*

Abstract

In recent decades, significant research has been proposed regarding manipulator modeling and motion control. Motion control has critical applications in many areas, including industrial robotics, autonomous systems, etc.

A precise mathematical model of a specific 6-DOF manipulator articulated robotic arm includes the kinematic and dynamic model of the robot represented. This study compares three dynamic models of an articulated robotic arm. CAD models at three levels of detail were developed using SOLIDWORKS to simulate the dynamics of the six-jointed robotic arm ABB IRB-140. The three different models are designed to extract precise values of the mass and inertia parameters. The first model is very detailed and close to the actual robot design. The second model is approximate, using parallelepipeds with a density choice that allows the masses to match the link masses. The third model is simplified and considers the links as rods, an approach repeatedly appearing in the literature because of its simplicity. The models were compared in terms of their predictions of torque in the proximal joints and energy consumption by these joints and by the robot overall. Forward and inverse kinematics and differential kinematics were used to model the dynamic parameters and compute torque in each joint. The models incorporated the technical specifications of the arm along with the simplified, semi-detailed, or detailed representation of the link structures. We compare these models as predictors of torque and energy consumption. We found that these three models yielded graphs of angular velocity, torque, and energy consumption with relatively

minor differences in profile. They all appeared to be adequate predictors of robot performance during a 30-second task. Energy consumption of the three models evaluates the impact of the various designed models, highlighting the suitability of each model for different situations. The overall difference in energy consumption of the three models is 0.53% less for the detailed model and 6.8% less for the simplified model compared to the semi-detailed one. Based on these results, the three dynamic models tested in this study appear to be worthy of confidence for predicting energy consumption by articulated robotic arms.

The Sliding mode controller algorithm is employed for motion control, with and without disturbances, to minimize the impact of the error in the property inputs to the controller and evaluate the model's robustness for three robot manipulator models. The simulation results show that the sliding mode control method is robust and performs satisfactorily even in external disturbances. Sliding mode control offers suitable performances for controlling robot models with unmodeled disturbances. Generally, the controller results examined on three models (detailed, semi-detailed, and simplified) are close with a slight percentage difference. The controller under disturbance also had relatively close results compared to the controller without disturbance. The sliding mode control methodology has an appropriate dynamic response and minimum tracking error performance from simulation results. The most significant disadvantage of this technique is the chattering phenomenon effect with control input, but the overall results for the models are satisfactory.

Keywords: *Industrial robot manipulators, Computer-aided Design (CAD), D-H representation, Dynamic model and simplifications, Energy consumption, Robust Control, SMC,Simulink kinematics, dynamics,Lyapunov stability theorem, trajectory tracking*

Acknowledgements

I would like to express my immense gratitude to Prof. Dr. Nadjet Zioui for her supervision and encouragement. Her enthusiasm and brilliance greatly motivated me throughout this pursuit. Her support and compassion have helped me overcome the challenging obstacles along the way.

Dedicate to the memory of my Mother, Maryam.

Contents

Abstract vi

Acknowledgments viii

List of Figures xii

List of Tables xvi

Abbreviations xvii

Nomenclature xviii

Introduction 1

Chapter 1. Control design methods 9

1.1 Industrial serial manipulators 10

1.2 Control for Robotics 13

1.2.1 PD and PID Control 17

1.2.2 Intelligent controllers 18

1.2.3 Feedback Linearization Control 19

1.2.4 Lyapunov Based Control 20

1.2.5 Robust Control 21

Chapter 2. Related Works 26

2.1 General Overview 27

2.2 Sliding Modes Control (SMC) 31

2.3 SMC For Robotic Manipulator Arms 33

2.4 Control Of Chattering Levels 39

Chapter 3. Tools and Methods 46
3.1. Robotic-arm presentation 47
3.2. Robot models 49
3.2.1. Forward and inverse kinematics 49
3.2.1.1. Forward kinematics 49
3.2.1.2. Inverse kinematics 51
3.2.2. Forward and inverse differential kinematics 53
3.2.2.1. Forward differential kinematics 54
3.2.2.2. Inverse differential kinematics 56
3.2.3. Dynamic model 57
3.3. Mathematical models of the robot 58
3.4. CAD designs of the robot 70
3.5. Evaluation of robot performance 73
3.6. Control Strategy - Sliding Mode Control (SMC) 73

Chapter 4. Results and Discussion 79
4. 1. Impact of simplifications on dynamics model of the robot 80
4. 2. Robust controller results 88

Conclusion 105

References 110

List of Figures

Fig 1: Manipulator with Revolute and Prismatic Joints [59]. 13

Fig 2: Block diagram of a closed-loop control system [59]. 15

Fig 3: Robotic system with motion control system, inner and outer loop controller [80]. 19

Fig 4: Standard robust control problem [85]. 21

Fig 5: The ABB IRB 140 robot located in the UQTR automation laboratory. 47

Fig 6**:** D-H parameters and link assignments for a rotational joint. 49

Fig 7**:** Configurations of the three proximal joints of the IRB 140 manipulator arm. 52

Fig 8**:** ABB IRB 140 frame assignments. 58

Fig 9**:** Projection of the second and third links on the x–y plane of the tool center point. 62

Fig 10: Z-Y-X Euler rotations of the distal joints. 64

Fig 11: Detailed SolidWorks model of the ABB IRB 140 robotic arm. 71

Fig 12: Semi-detailed rectangular SolidWorks model of the ABB IRB 140 robotic arm. 71

Fig 13: Simplified SolidWorks model of the ABB IRB 140 robotic arm. 71

Fig 14: IRB 140 robot proximal joint angle variations. 80

Fig 15: IRB 140 robot proximal joint angular velocity. 81

Fig 16: IRB 140 robot proximal joint angular acceleration. 81

Fig 17: Torque variations for the first proximal joint of the IRB 140 robotic arm. 82

Fig 18: Torque variations for the second proximal joint of the IRB 140 robotic arm. 82

Fig 19: Torque variations for the third proximal joint of the IRB 140 robotic arm. 83

Fig 20a **:** Energy consumption by the proximal joint 1 based on three models. 85

Fig 20b **:** Energy consumption by the proximal joint 2 based on three models. 86

Fig 20c **:** Energy consumption by the proximal joint 3 based on three models. 86

Fig 21: Energy consumption by the IRB 140 robotic arm, based on three models. 87

Fig 22: Simulink Model of Robot Manipulator. 89

Fig 23: Simulink Trajectory Model of Robot Manipulator. 89

Fig 24: Projection of X-Y Trajectory of Robot Manipulator. 90

Fig 25: Projection of X-Y-Z Trajectory of Robot Manipulator. 90

Fig 26a : Angular position of joint One for Detailed Model using SMC. 92

Fig 26b : Angular position of joint Two for Detailed Model using SMC. 92

Fig 26c : Angular position of joint Three for Detailed Model using SMC. 92

Fig 27a : Angular position of joint One for Semi-Detailed Model using SMC. 93

Fig 27b : Angular position of joint Two for Semi-Detailed Model using SMC. 93

Fig 27c : Angular position of joint Three for Semi-Detailed Model using SMC. 93

Fig 28a : Angular position of joint One for Simplified Model using SMC. 94

Fig 28b : Angular position of joint Two for Simplified Model using SMC. 94

Fig 28c : Angular position of joint Three for Simplified Model using SMC. 94

Fig 29a : Angular position tracking error of joint One for Detailed Model using SMC. 95

Fig 29b : Angular position tracking error of joint Two for Detailed Model using SMC. 95

Fig 29c : Angular position tracking error of joint Three for Detailed Model using SMC. 95

Fig 30a : Angular position tracking error of joint One for Semi-Detailed Model using SMC. 96

Fig 30b : Angular position tracking error of joint Two for Semi-Detailed Model using SMC. 96

Fig 30c : Angular position tracking error of joint Three for Semi-Detailed Model using SMC. 96

Fig 31a : Angular position tracking error of joint One for Simplified Model using SMC. 97

Fig 31b : Angular position tracking error of joint Two for Simplified Model using SMC. 97

Fig 31c : Angular position tracking error of joint Three for Simplified Model using SMC. 97

Fig 32: Sliding surfaces for Detailed Model. 98

Fig 33: Sliding surfaces for Semi- Detailed Model. 98

Fig 34: Sliding surfaces for Simplified Model. 99

Fig 35 : Angular position of joints for Detailed Model with disturbance. 100

Fig 36 : Angular position of joints for Semi-Detailed Model with disturbance. 100

Fig 37 : Angular position of joints for Simplified Model with disturbance. 100

Fig 38 : Angular position tracking error of joints for Detailed Model with disturbance. 101

Fig 39: Angular position tracking error of joints for Semi-Detailed Model with disturbance. 101

Fig 40 : Angular position tracking error of joints for Simplified Model with disturbance. 101

Fig 41: Sliding surfaces with disturbance for Detailed Model. 102

Fig 42: Sliding surfaces with disturbance for Semi-Detailed Model. 102

Fig 43: Sliding surfaces with disturbance for Simplified Model. 102

List of Tables

Table 1: Classification of the SMC methods. 45

Table 2: Joint limits of the ABB IRB 140 robot. 48

Table 3: DENAVIT-HARTENBERG parameters for the ABB IRB 140 robotic arm. 59

Table 4: Mass property results of each model provided using SolidWorks software. 72

Table 5 : Performance of SMC of angular position for the models. 91

Table 6 : Performance of SMC of angular position for models under disturbance. 103

Abbreviations

AC	Alternating Current
ANN	Artificial Neural Network
CAD	Computer-Aided Design
CAM	Computer Aided Manufacturing
CAO	Computer-Assisted Ordering
CL	Close-Loop
CTC	Computed Torque Control
DC	Direct Current
DOF	Degree Of Freedom
DH	Denavit Hartenberg
FLC	Fuzzy Logic Controllers
GA	Genetic Algorithm
HOSM	Higher Order Sliding Mode Control
ISM	Industrial Serial Manipulators
MIMO	Multiple Input/Multiple Output
NTSMC	Non-Singular Terminal Sliding Mode Control
OL	Open-Loop
PD	Proportional Derivative
PID	Proportional Integral Derivative
RIA	Robot Institute of America
SMC	Sliding Mode Control
STSMC	Super-Twisting Sliding Mode Controller
TSMC	Terminal Sliding Mode Control
UQTR	University of Quebec at Trois Rivieres
VSS	Variable Structure Switching
VSCS	Variable Structure Control System

Nomenclature

r(t)	Reference input or the setpoint of the closed-loop
y (t)	Output or the measured value
$G_P(s)$	Plant transfer function
$G_c(s)$	Controller transfer function
e(t)	Error of the closed-loop
$D_t(s)$	Disturbance variables of the closed-loop
H(s)	Sensor transfer function
$H\infty$	H-infinity methods in control theory
Inv(j)	Jacobian matrix inverse
K(s)	Controlled signal
S(x)	Sliding surface
sgn	Signum function
U	Control signal
sat (S/Φ)	Saturation function
α_{i-1}	Twist angle between joint axes z_i and z_i - 1 measured about x_{i-1}
a_{i-1}	Distance between joint axes z_i and z_{i-1} measured along the standard normal
θ_i	Joint angle between joint axes x_i and x_{i-1} calculated about z_i
d_i	Link offset between axes x_i and x_{i-1} measured along z_i
${}^{i-1}_{i}T$	Homogeneous transformation matrix
$\dot{p}_e$	End-effector linear velocity vector

$\dot{q}$	Joint velocity vector
v_e	End-effector velocity
J	Jacobian matrix
J^{-1}	Inversion of the Jacobian matrix
ω_e	Angular joint velocity
ω_c	Joint angular velocity
$\ddot{q}$	Joint acceleration vector
M	Inertia matrix
Vi	Coriolis vector
G	Gravitational vector
τ	Force and torque vector
$R_z(\alpha)$	Rotation around axis z by the α
$R_y(\beta)$	Rotation around axis y by the β
$R_x(\gamma)$	Rotation around axis x by the γ
S	Sliding surface
${}^{i}p_{ci}$	Mass center position
${}^{i}I_i$	Inertia matrices
E_i	Energy consumption
c_{θ_i}	Cosine of angles θ_i
s_{θ_i}	Sine of angles θ_i

Introduction

Nowadays, industrial robots perform in various industries. Any repetitive operation is an excellent job for a robot, especially if it's difficult or dangerous. The application of robots in manufacturing industries is precious. Robots have been employed for high-volume production, but as the technological advancements reduced the cost of industrial robots, more choices and possibilities are extended for wide-range industrial processes. In the last decades the growth of digital technologies, new techniques and new technologies in industries also their implementation in production lines motivates the industries worldwide to always observe these advancements and modernization and development in automation of their production procedures to stay competitive. The fourth technological revolution "Industry 4.0" can be labeled in many ways as intelligent factories, smart industry, or advanced manufacturing refers to the execution of production technologies, funded by different digital technologies and new materials, sensor technology that reinforces the evolution of robotic technologies [1]. The development of digital technology and the development of other technologies are contributing to the growth of automated industrial technology so that each year the representation of service robots for logistics in the production process is being expanded and improved [2]. An increase in representation will continue. It can be predictable will reach around 1000.000 robot units with constant growth in 2020 [3].

The modeling and control issues are required to ensure the performance of any task according to the expected input with minimum error. Proper control systems are essential to high-performing industrial manipulators, and good models are necessary for well-functioning control systems. Control of robotics arms has been considerably investigated in the literature. Authors have presented various control methods such as PD and PID Control, Intelligent controllers, Feedback Linearization Control, Lyapunov Based Control, and Robust Control.

Between the methods, Sliding mode control is an overall robust control technique in robotics that addresses parameter uncertainty and bounds disturbances. SMC method is based on the Lyapunov stability theory [4]. It mainly attempts to specify the nominal feedback control law and a disciplinary control action that leads the controlled system to the desired operation, expressed as the sliding surface. In literature, various forms of the sliding mode controller for different manipulator arms types were studied.

A four-linked SCARA robot manipulator with uncertain parameters includes a non-singular-terminal sliding mode control proposed for the SMC strategy's efficiency by Shankar J et al. [5]. A robust nonlinear control technique with an uncertainty analyzer is employed to track position within the robot's workspace to a cinematically redundant mobile manipulator with four degrees-of-freedom robotic arm mounted on three mobile bases examined by Mishra et al. [6]. A smooth sliding mode control and primary approach for a flexible joint robotic manipulator with constrained motion and force control were presented by Huang et al. [7]. A suggested continuous control integrated with a genetic algorithm guarantees stability and quick convergence discussed by Wang and Sun [8].

The nonlinear sliding manifolds' analysis focuses on two objectives, improving the transient effects on the control input. Second, it delivers a finite convergence time of the sliding system on the manifold, which is not met by the classic linear manifold design. Much less work is currently in the literature concerning investigating nonlinear sliding functions among the research on decreasing or eliminating chattering in sliding mode control. Between the analysis of nonlinear functions, research on Terminal Sliding Mode Control (TSMC) on nonlinear sliding functions is developed to provide a fast convergence of the tracking error in a finite time [9-13].

Si et al. [14] stimulated the dynamic model of the two-link flexible manipulator with payload using the Euler Lagrange equation. A fast NTSMC was suggested for the trajectory tracking problem of the two-link flexible manipulator. Moreno and Osorio introduced a Lyapunov-based approach for investigating the stability of a class of second-order sliding mode controllers called the super-twisting sliding mode controller (STSMC) [15]. A new terminal sliding mode for the control method of a typical robotic manipulator dependent on finite time and differential stability theory principle of inequality with the support of the model-based approach for robotic manipulators in mind, the TSMC technique to controlling robots was analyzed by Liu et al. [16]. Studied sliding operations with the variation of the parameters over time to improve the control's robustness and quick convergence presented by Choi et al. [17].

The primary problem of sliding mode control is the high-frequency chattering phenomenon arising from the control signals during the undertaking of this control system. Chattering is caused by an unsteady term in the sliding mode control law. Asif et al. [18] presented a terminal sliding mode control that configures a control law for trajectory tracking non-holonomic mobile robots to eliminate the chattering phenomenon and provide stability by utilizing the Lyapunov theory controlled by velocity inputs that enforce kinematic configurations. A new form of chatter-free sliding PID control principles for continuous mechanical plants, which ensures exponential convergence, is considered by Vicente et al. [19]. A nonlinear reaching law reduces the discontinuous gain and thus chattering when the sliding manifold is contacted, studied in [20,21]. Another technique employed by multiple researchers is increasing the degree of the sliding functions from one to a specific degree. Operating the virtual time derivative order of the control law suggested by [22]. Choosing discontinuous time derivative, then the actual control law is created by a series of integrals with continuous nature, ensures proven chattering avoidance by the

noted method. This technique has been employed by Hamerlain et al. on a specific robot trajectory tracking [23].

The two major subjects of this thesis are the study of analyzing the impact of dynamic models with different classes of detail and the control of the 6 degrees of freedom (DOF) robotic arm industrial manipulators. Suitable control systems are fundamental to high-performing industrial manipulators, and good models are essential to well-functioning control systems. Variable structure control is a way of controlling the dynamics of a model-based linear and the nonlinear system where the control law alters accordingly with some predefined rules in the control process and has various types based on the controlling strategy utilized among the sliding mode control that is widely employed in controlling a dynamic system with uncertainty and disturbance.

Considerable studies implementing robust control strategies utilize random, constant, or sine signals as modeling or measurement errors. To our knowledge, this is the first time that a realistic model (with real parameters of the robot) is employed along with simplified and semi-simplified models to obtain as close as possible to the real modeling errors, attempt to design and structure the real model of a specific robot to evaluate not only the errors but also the performances in terms of consumed energy and the implementation of the control strategy. Most control strategies are based on dynamic models, in which variables are embedded as torque or forces, depending on whether the joint is revolute or prismatic. Unlike robust controllers, precise controllers rely on the dynamic model's precision [24, 25]. Robust control strategies can be designed to yield the proper dynamic behavior when faced with modeling errors and unmodeled dynamics[26]. However, studies repeatedly show that the dynamic modeling of robots is highly challenging.

Adequate models are necessary for well-functioning control systems. The modeling problem is necessary before applying the control techniques to guarantee the execution of any task according

to the desired input with minimum error. The derivation of forwarding and inverse kinematics is an important step in robotic modeling based on the representation of Denavit Hartenberg (DH). Two basic methods of modeling a dynamic manipulator are the Newton-Euler formulation, in which each term is expressed separately, and the Euler-Lagrange formulation relies on mechanical systems' energy properties to compute the equations of motion [27], which defines the system as based entirely on potential energy and kinetic energy [28]. This application of the Euler-Lagrange formulation requires precise knowledge of the inertia and center of mass of each of the various links of the robot at any time. Some researchers, therefore, prefer approaches based on model parameter identification [29-37]. Others use approximation methods, considering links as parallelepipeds or rods having masses equal to the robot, to simplify the inertia and center of mass calculations [38-46]. It must be understood that parameter identification and approximation methods both generate the error due to measurement and noise in the former case and simplification in the latter point.

Robotic manipulator arms with more than three degrees of freedom have complex kinematic and dynamic equations with multiple variable elements. To study the motion of the robotic manipulator arm, such as speed and acceleration, path and trajectory planning, thorough analysis for force and torque computations, and also study critical issues such as energy for optimization of the manipulator robotic arms requires an analytical and mathematical model. Methods for modeling robot arms have been developed. In some methods, the actual model of the robot arm is simplified with assumptions for the robotics arm presented in classical calculations. Today, with the help of CAD/CAM engineering 3D design software, a 3D model of a robotic arm can be designed. With the abilities built into these types of software, the mass properties are also evaluated for the 3D model. An approximate result can be obtained from mass properties such as the center of mass and

inertia tensors of a complex chain mechanism such as a robotic arm. Despite these facilities provided by 3D engineering design software and powerful analytical math software, proper kinematic and dynamic models can be obtained and organized for the robotics arms. The more precise the robot's mathematical models are, the more complex the equations related to its torque and energy and more variable elements. To analyze and solve these equations, powerful and helpful software such as MATLAB can be used.

A precise mathematical model of a specific 6-DOF manipulator articulated robotic arm includes the kinematic and dynamic model of the robot represented. This study compares three dynamic models of an articulated robotic arm. CAD models were developed for this purpose using SOLID WORKS software. The three different models are designed to extract precise values of the mass and inertia parameters. The first model is very detailed and close to the actual robot design. The second model is approximate, using parallelepipeds with a density choice that allows the masses to match the link masses. The third model is simplified and considers the links as rods, an approach repeatedly appearing in the literature because of its simplicity [47]. We compare these models as predictors of torque and energy consumption.

For an actual application of a serial or parallel robot, the physical parameters of these systems should be identified in the best possible way. The data of mass, inertia matrices, mass centers, friction forces, etc., delivered for any software, implies an error percentage that must be considered in the calculus. MATLAB is an adequate tool for developing algorithms, evaluating and validating models, and simulating system responses. Still, the computational time for calculating algebraic operations in robotics is not very efficient. In some cases, the detailed level of modeling results is the heavy and slow simulation of path tracking with many points.

A robust controller is synthesized to overcome close-to-reality modeling errors and appreciate their performances. The Sliding mode controller algorithm is used for motion control, the developed basis of with and without disturbances to evaluate the model's robustness for three different robot manipulator models. The executed algorithm analyzes a thoroughgoing trajectory to prove the performance and conduct of the designed sliding mode controller of the robot to perform tasks undertaking the controller.

The impact of the three different dynamic models on the performances of the robot and some fundamental concepts related to torque equations and energy consumption on a movement path over a fixed time interval were examined and explored to evaluate the three dynamic models as predictors of the robot's performance. A control module and a robustness controller (SMC) were included to minimize the impact of the error in the property inputs to the controller implemented for three models to examine the effect of different models on the performance and dynamic response of three other models. In the end, the studies represented some significant outcomes based on comparing the different models.

Chapter One

Control design methods

1.1 Industrial serial manipulators

This chapter provides an introduction to industrial robots and control strategy, in particular the series manipulators. First, introduce some terminology, followed by a short overview of the demand for industrial robots and typical applications, to how industrial serial manipulators (ISM) are usually designed and controlled to associate with desirable characteristics for an ISM.

As the title indicates, robotics is the acknowledgment and investigation of robots. Karel Capek coined the robot, the Czech word “robota,” implying (forced labor) in 1921 [48]. Robots are artificial computerized machines that execute tasks by human controls and aim to make work more straightforward. According to RIA (RIA: Robot Institute of America), a robot is a "reprogrammable multifunctional manipulator developed to move materials, specialized parts, tools or devices through variable programmed motions to execute different tasks" [49].

In this thesis, the representation "robotic manipulator" is utilized. A scientist named George Devol, Jr. designed the first robotic arm in the 1950s, before which robotics mainly was a product of science fiction and imagination [50]. Numerous multiple functional scope exploration applications have been slowly developed by robotics. The importance of robots in assisting industrialization was not realized until the 1980s, when robotic arms were designed for use in automobiles and other manufacturing assembly lines [51]. The robotic arm's outcome has been molded to do the intended job, and it can be organized for almost any activity, such as gripping like a hand, tightening screws, creating works of art, etc. A robotic arm manipulator is an interconnected set of sensors, power supplies, control systems, and software that work independently to execute a task [52]. These robots can be stationary, such as on an assembly line, or they can be mobile and transported to different locations. Manipulator robotic arms have various forms and sizes but are often organized by the degree of freedom (DOF).

A robotic arm is a mechanical mechanism, usually programmable, similar to a human feature. The arm robot can be the entire mechanism or part of a more complex robot. Each direction of motion on the robot is assumed to be an axis of motion, and each axis is considered one degree of freedom. The typical joint motion of a robotic manipulator arm, yaw, pitch, and roll, allows locating the tools in a work space and are named position axes [53]. The manipulator's joints allow rotational motion (in the articulated robot) or translation (linear) motion. The links of the manipulator can be considered as a kinematic chain. The end of the manipulator driveline is named the end-effector and is similar to the human hand. According to the application, the end-effector or robotic tools can be designed to perform any chosen actions such as welding, gripping, spinning, Etc. Robotic arms perform various parts of welding, turning, and positioning in automotive assembly lines [54]. The robot manipulator field is one of the exciting areas in industrial, educational, and medical applications. The robot manipulator is one of the motivating disciplines in industry and academic applications and a critical branch to control sciences because of its intellectual aspects, non-linear characteristics, and real-time execution. It performs in unexpected, dangerous, and inhospitable cases which humans cannot reach. For example, working in chemical or nuclear reactors is extremely risky, while operating a robot instead of a human applies no risk to human life. It was developed to improve human work, such as manufacturing or manipulating heavy materials and unpredictable environments. Thus, modeling and analyzing the robotic manipulators and applying control strategies are essential before using them in these cases to work with high precision [55].

The robotic manipulator has immeasurable duties, so it is organized to be flexible in the general motions from which to proceed. There are three main subsystems in robot manipulators: mechanical, electrical, and control. The mechanical system of the robot includes all moving elements. It consists of a group of links (rigid bodies) connected by joints that allow the motion of

the selected link. The mechanical system moves the end-effector (the top link) to the XYZ position regarding the base frame [56]. This motion depends on the electrical system (ex., motors, power amplifiers, and other electronic circuits) and the movements performed by some rotations and translations towards the different links. Due to the group of assignments and duties in robot manipulators, their structure is split into two main classes: serial manipulators and parallel manipulators. The manipulator's arm consists of links attached in series, forming an open-loop chain. A single kinematic chain links the end effector to the base frame at the end of the chain. On the other hand, parallel manipulators form a closed-loop chain finished by the end effector and are connected to the base frame by two or more kinematic chains (e.g., arm or legs). The only drawback of the finite parallel manipulator and the serial manipulator is that the parallel robot manipulators suffer from a limited workspace compared with serial robot manipulators [57].

There are two specific joint types used on the industrial manipulator. The first type is described in texts by a cylinder, which only permits relative rotation between two links. This joint is called revolute, or rotary joint (e.g., human joints)and is the most regular type of joint in a robotic manipulator. The second type of joint is called a prismatic or sliding joint. A square box symbolizes it. This type of joint allows only relative linear motion between two links along its axis. Both types are described as R and P joints, respectively. The robot manipulator whose all joint variables are prismatic is known as a Cartesian manipulator, while the robot whose all joints are revolute is known as an articulated manipulator [58]. Figure 1 presents a schematic diagram of a robot manipulator. It consists of some joints, and each one of these joints will have a motor to actuate the expected link.

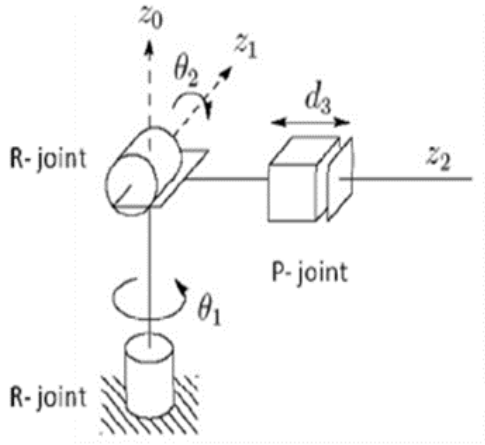

Figure 1: Manipulator with Revolute and Prismatic Joints [59].

The fundamental matter for investigating the robot manipulator issue has two sides. The first is the mathematical modeling of the manipulator and actuators, which contains the analysis of forwarding and inverse kinematics. Then the second issue is the control of the robot manipulator [60]. The robot motions' analysis is necessary before implementation in the existing system. Therefore, computer simulations are required to perform any controller, where developing a different mathematical model for any robot manipulator is crucial for running simulations [61]. In recent years, industrial and commercial systems with high efficiency and outstanding implementation have carried the advantage of robot technology. Many control classifications of research and multiple control applications were introduced during the last years, focusing on the control of robotic systems [62].

1.2 Control for Robotics

One of the most important and applicable matters in robotics is motion control. Because the robot's procedure must be accurate without affecting surrounding circumstances. Controlling

manipulators is a significant research scope to modify the time record of joint inputs demanded to move the end-effector to perform the critical task.

It is crucial to control and adapt the robot manipulator in the control system. Typically, two control systems are used, the open-loop (OL) control system and the closed-loop (CL) control system [63]. The controller sends a signal to the motor in the OL control system but does not estimate the error measure. On the other hand, in the CL control system, the controller sends the signal to the motor, and the output signal will be fed back to express the motor's present state. CL controller has some benefits over the OL controller, such as disturbance rejection like friction in motors, enhanced reference-tracking execution, and stabilization of an unstable operation. A control system consists of devices and tools like sensors, controllers, and actuating devices that provide a valid task to robot manipulators [64]. When the controller is proceeding, the robot manipulator during the working environment, the sensor or feedback system collects the data about the robot manipulator state and the surrounding circumstances. It then controls the information to modify and enhance the system's behavior. The Control system provides some functions for the mechanism (robot arm), such as:

1- Providing the ability to move the robot manipulator in the surrounding environments.
2- Collecting information about the robot manipulator in the working spaces.
3- Using this information gives a methodology to control the robot manipulator.
4- Storing the data, then providing it to the robot manipulator, then updating it instantly.

A controller is utilized to modify the conduct of the physical system based on the input value through analyses and motions. During the first decade, many control methods and methodologies were suggested to control the motion of robot manipulators, such as point-to-point, continuous trajectory sequence, velocity, and systematic movements [65].A variety of robot manipulators and

their architectures influence the control strategy. On the other hand, the mechanical design of the manipulator affects the sort of controller. Although manipulator robots have a variety of assignments in all applications, this is the case restricted behavior compared with humans. Therefore, the control technique should be used to obtain the preferred behavior. Every robot has a controller that continuously reads from sensors like motor encoder, force sensors, vision sensor, and depth sensor, which updates the actuator commands to achieve the desired robot behavior [66]. The fundamental structures of the closed-loop control system illustrated in Figure 2 include some significant elements.

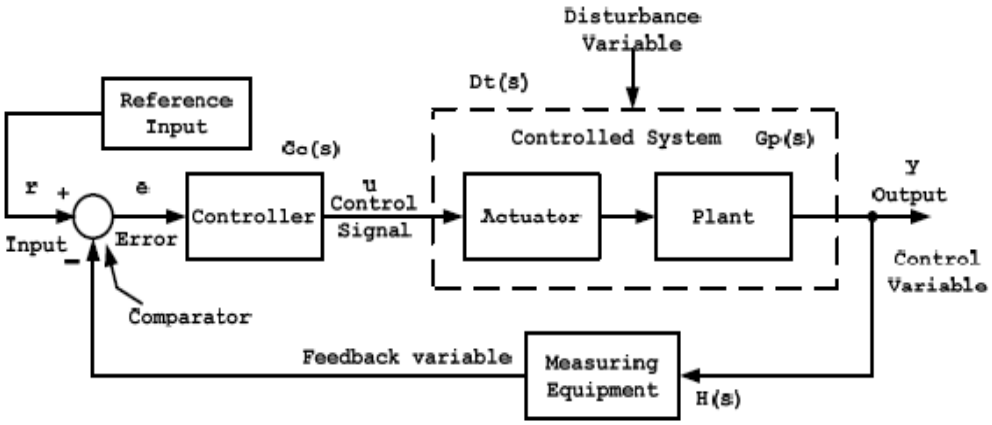

Figure 2: Block diagram of a closed-loop control system [59].

The closed-loop control system involved the reference input or the set point of the closed-loop, *r(t)*, the summer and comparator section, the controller, the controlled system including plant and actuator, the output or the measured value *y (t)*, and the feedback loop. The plant $G_P(s)$ is the mechanism like a robot manipulator, and it contains the actuators, gears, and mechanical components. The controller $G_c(s)$ is a tool that is utilized to correct the error signal *e(t) = r(t) - y(t)* and provide applicable input to modify the behavior of the mechanism and improve the features of the closed-loop system. The controller emphasizes reducing the error between the set

point and the feedback signal. Nevertheless, if the input signal and feedback signal are not equal, the controller will update the position signal until the difference between both signals is zero. Some unpredictable disturbance variables $D_t(s)$ may influence the output signal. The sensor *H(s)* is the instrument that evaluates the output signal. Many systems may be unstable due to nonlinearity, so an adequate control system must create control output to follow the desired response. The desired reaction for a control system ensures that the critical point in developing a control system is to ensure that the dynamic response of the closed-loop systems is steady and stable [67].

There are two approaches used in control theory to control systems, the linear method and the nonlinear method [68]. Operating linear control is relevant only when the controlled system can be modeled mathematically [69]. The fact is that most mechanisms have nonlinear aspects. Therefore, linear controllers fail to satisfy the requirements due to system nonlinearities. Nonlinear variations and parameters such as gear backlash, load variations, etc. parameters have unexpected effects on the controlled systems like a robot manipulator, decreasing the performance. Therefore, it can be supposed that the robotic manipulator is a linear model when working in a small space or has a high transmission ratio between the joints and their linkages. Nonlinear methods are considered a general case compared to linear methods because they can be applied successfully to linear methods [70]. Still, the linear approach is lacking in solving and controlling nonlinear problems. Standard processes are used to solve the nonlinearities in the control systems, such as sliding mode control and status feedback control.

Different controlling strategies employed to solve the optimal control issue include tracking the position and reducing the vibrations. The optimization algorithm controls and estimates its execution index like angular acceleration, force, torque, etc. [71]. Many numerical optimization methods have been developed to design more suitable mechanisms.

Advanced robot control laws can enhance the robot's operations. The improvement of the robot design itself may also donate substantially to the increase in execution and capabilities. Combining the proper controller with suitable sensors equips some sense and awareness of the workspace and enhances its precision and speed. Current challenges in the robotics application have influenced the research of robot control in several essential topics such as modeling, position and motion control, and robust control [72]. The issues can motivate robot modeling, simulation, and control design research. Therefore, position and trajectory control is fundamental research in robotic control. The motion control problem has received significant interest in robotics.

The arm robot manipulator trajectory tracking design and control requires more than kinematic and dynamic to enhance effectiveness and improve efficiency. Advanced control theorem and artificial intelligence can help reach the purpose, such as adaptive control. Artificial controls applied in trajectory tracking of an arm robot manipulators are Fuzzy logic controllers (FLC), Artificial Neural Network (ANN) and the combination of FLC and ANN and Genetic Algorithm (GA) [73]. The complications of kinematics and dynamics modeling can be avoided by using rules-based and learning based on artificial intelligence. The control of robotic manipulators using different controllers is discussed in the following subsections:

1.2.1 PD and PID Control

The PD (Proportional-Derivative) and PID (Proportional-Derivative-Integral) are the classic methods of controlling a system. The PID and PD controllers are the most utilized controls in various industrial applications as these are the first choices of an engineer for their simplicity, flexibility, and stability.

Despite all advantages of the PID, this controller is unable to control uncertainty for a non-linear system. A manipulator robotic arm is a non-linear system that different PID control such as PID and state feedback control methods, PD-FUZZY logic controller, intelligent PID controllers, H∞ PID control, and hybrid PD-PID control controller techniques are used to control the robot's trajectory and position [74]. A PID or PD controller can be experimentally implemented to control a manipulator arm robot considering the servo driver velocity and the actuator torque also suggest guaranteeing stabilization of the robot, which has higher dynamics and excessive noise. PID controllers are appropriate to eliminate the steady state error of the position. PD and PID present an integration action to the closed loop to enhance the execution tracking of a trajectory [75].

1.2.2 Intelligent controllers

An intelligent controller is a type of controller that is able to indicate the solution intelligently, relying upon the conditions, just like a human. These controllers anticipate keys for such a system that is complicated to illustrate, such as manipulator robotic arms. Developing a controller for such a system is difficult due to the impossibility of getting actual models. These issues can be resolved by enforcing intelligent controls like fuzzy logic and artificial ANN [76].

The fuzzy logic controller is a typically intelligent controller method with human decision-making characteristics. The fuzzy logic strategy can employ human experience knowledge that deals with indefinite and ambiguous details to control the optimal control problem. Even though Commonly fuzzy logic method controllers use IF-THEN rules to solve the issue, the method includes the degree of truth other than true and false or 1 and 0. A fuzzy logic-based controller is employed for the motion and position for tracking the trajectory and vibration control [77].

An Artificial Neural Network (ANN) controller is straightforward and quick to configure classification and predict without comprehending the problem behaviors of the mechanism. The ANN controller is an excellent tool for developing learning about the required output and input relations. ANN controllers, especially for mathematically undefined configurations, are suitable for escaping mathematical modeling complications. The architecture of ANN involves four main layers Input Layers, Hidden Layers, Custom layers, and Output Layers. Various Neural networks are used to control the rigid and flexible robotic arms presented to control the position, trajectory monitoring and tip distraction, motion regulation, and force and torque on the dynamic model [78].

1.2.3 Feedback Linearization Control

Applying the feedback linearization approach to solving robotics control problems is based on the computed torque technique. The feedback linearization control technique works according to inner-outer loop control techniques. The inner loop should linearize the mechanism, such as the manipulator's arm. On the other hand, the outer loop gains the standard conditions for the closed loop. Figure 3 depicts the control motion system (inner and outer control loops) of a manipulator robot arm manipulated by a DC motor [79].

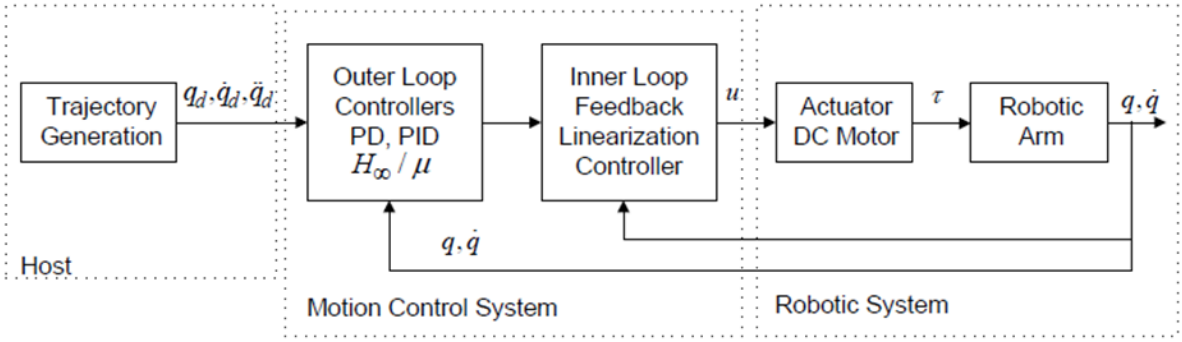

Figure 3: Robotic system with motion control system, inner and outer loop controller [80].

The Computed Torque Control (CTC) involves PD control at the outer loop to a linearized system by the feedback linearization control. In robotics, CTC is employed to implement the PD controllers separately for every joint at the outer loop [81]. The feedback linearization method has two critical features that require attention, model error and the outer loop controller configuration. The feedback linearization technique is based on the identical model of the mechanism. Hence, the controller is sensitive to modeling errors such as parameter errors and unmodeled dynamics. Robust control strategies or adaptive controllers generally manage parameter uncertainty. to estimate a limited quantity of parameters adaptive controllers can be a practical approach. The feedback linearization control continuously linearized the mechanism elements until the outcomes of the plant are considered a linear system. Thus, applying one or multiple linear control techniques is possible to reach the desired performance. Considerable controllers for the outer loop control are proposed, such as the standard PD loop of CTC, linear optimal control, sliding mode control, and $H \infty / \mu$ robust optimal controllers [82].

1.2.4 Lyapunov Based Control

An essential tool for controlling a mechanism is the Lyapunov stability theory based on the destruction of the energy function. Lyapunov stability theory is not formative to designing a controller, but a simple form of the equations of motion with some reasonable assumptions authorizes a derivation of stabilizing controllers [83]. These assumptions enclose bounded disturbances and bounded parameter deviations. The inertia-based control technique attempts to reshape the robot's energy function, setting an entirely different behavior like the CTC approach. Investigations indicated and presented the passivity controllers are more robust than CTC. Another

development of Lyapunov stability theory is the sliding mode control (SMC), which is regarded as a robust control approach [83,84].

1.2.5 Robust Control

To provide proper conduct of the closed loop robot, despite the errors and disturbances in models, it is expected to develop robust controllers. Modeling errors are typically divided into parameter errors and unmodeled dynamics that differently influence the closed loop system. The standard control algorithm considered in many studies in advanced controls is illustrated in Figure 4.

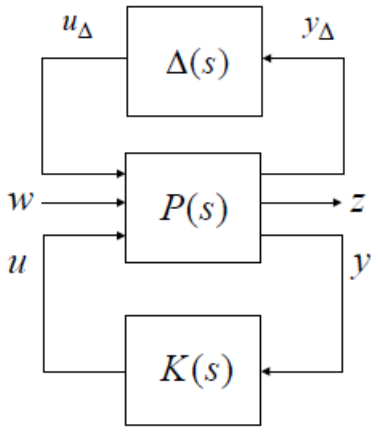

Figure 4: Standard robust control problem [85].

K(s) as controlled signal is supplied with measurement signals y and has to stabilize P(s) as plant signal deal with u as input signals. The p(s) is usually a generalized plant that includes weighting parametric and dynamic uncertainty, input signal thresholds, and the simulated robot's dynamic model [85].

The popular robust control strategy that is the primary and widely used type of variable structure control methodology for linear and nonlinear systems is the sliding mode control (SMC), also named Variable Structure Switching (VSS) control [86]. Sliding mode control is a popular robust control strategy in robotics that addresses parameter uncertainty and bounded disturbances. SMC method is based on the Lyapunov stability theory. It primarily attempts to define the nominal feedback control law and a corrective control action that leads the controlled system to the expected operation, described as the sliding surface. SMC is qualified to change the system's dynamics by applying a high-frequency switching control law even if the system has good feedback for nonlinear and discontinuous systems [87]. Many researchers have utilized various sliding mode control strategies for nonlinear multi-input and multi output systems. The system's stability in sliding mode control will be guaranteed if the matching condition is verified when there is uncertainty and external disturbance in the system. The main disadvantage of the SMC is the chattering effect on the system problem, which is harmful to actuators leading to low accuracy in trajectory tracking and causing wear and heat to the mechanical parts [88]. Many methods to reduce or eliminate a system's chattering problem are mainly into two branches: the estimated uncertainty method and the boundary layer saturation method. The advantages of SMC controls include their robustness concerning unspecified parameter deviations or disturbances once it is in the sliding mode. The SMC technique does not need a precise model. On the other hand, there are two principal drawbacks to the SMC control. One is the specification of the control law required to push the system to the switching surface and the other is the necessity to reduce chattering near the switching surface [89- 91].

By investigating and studying the research performed in the field of modeling and control concerning industrial robot arms in recent years, the present study, for the first time, deals with the

different levels of modeling in the field of industrial robots and aims to study the effects of simplification on models with different levels in details. The primary purpose of this research is to find a confirmation to prove the efficiency and acceptable accuracy of the fundamental modeling of a robot arm with fewer computational elements. Because the use of simplified models significantly impacts the number of calculations and, as a result, has a direct effect on an essential factor as calculation time.

The computational time for calculating algebraic equations in robotics is not very efficient. Another valuable result of this study is that the three models reach nearly the same values for the total energy consumption by the robot executing a path of movement over a single time interval, suggesting that they all could give acceptable results in different situations. For this reason, using a simplified state of the actual model improves and optimizes the calculus process. Its meaningful advantage is that it uses only a simplified model, significantly saving computing resources and time. This model could guide the development of simulation to be used in control and could also inform classical computing theory for robotic arm kinematics and dynamics modeling.

We compare these models as predictors of torque and energy consumption to analyze the effects of simplification in the results and the amount of difference in the final results for torque and energy in three different models at different levels of detail, to investigate and substantiate the suggestion of employing simplification in robotics calculous for more efficient computational time.

A control module and a robustness controller (SMC) included to minimize the impact of the error in the property inputs to the controller. The simulation results show that the sliding mode control method is robust and performs satisfactorily even in external disturbances. Sliding mode control offers suitable performances for control of robot models with unmodeled disturbances. Generally,

the controller results examined on three models (detailed, semi-detailed, and simplified) are close with a slight percentage difference. The sliding mode control methodology has an appropriate dynamic response and minimum tracking error performance from simulation results. The most significant disadvantage of this technique is the chattering phenomenon effect with control input, but the overall results for the models are satisfactory.

We found that these three models yielded graphs of torque and energy consumption with relatively minor differences in profile. Energy consumption of the three models evaluates the impact of the various designed models, highlighting the suitability and worth of confidence for predicting energy consumption by articulated robotic arms for each model in different situations. The overall difference in energy consumption of the three models is 0.53% less for the detailed model and 6.8% less for the simplified model compared to the semi-detailed one. The simulation outcomes indicate that the sliding mode control method is robust and performs satisfactorily even in external disturbances. Sliding mode control offers suitable performances for controlling robot models with unmodeled disturbances.

In this study, particularly for a specific industrial articulated robotic arm with six degrees of freedom, three different dynamics models, the detailed, semi-detailed, and simplified, will be developed. The effects of the three dynamic models will be examined and compared in terms of features related to the dynamic model, such as torque and energy consumption. The impact of implementing the advanced control technique has been accomplished by determining the proper classic sliding mode control to force the system's trajectory to slide along the desired trajectory with proper switching controls, which is determined by the equivalent controls method for three different models. State-of-the-art advanced control methods, specifically in the robotic field presented in Chapter Two, and general design procedures consist of mathematical models and

CAO design of the robot to obtain the three different models and system modeling for the design and implementation of the SMC controller are summarized and presented in Chapter Three. Chapter Four presents an analysis and comparison of the simulation results of the plan. Conclusions drawn from this study are presented in Chapter Five.

Chapter Two

Related Works

In the recent development in the control, advanced control strategies are well specified for the procedures under the effect of parametric uncertainties due to modeling error, nonlinearities, and external disturbances. Among the various robust control methods, sliding mode control (SMC) has made awareness of the control engineer due to its superiorities. SMC has procreated as a control corresponded to other robust control strategies. Its distinct components are insensitive to matched uncertainties, reduced order sliding mode equations, zero error convergence of closed loop system, and nonlinear control.

This section illustrates the literature review of SMC development in control technology. The development of SMC-based technique with the integration of intelligent control in control engineering has been investigated by assuming numerous applications. A general review of some well-known nonlinear control methods is presented, followed by a more detailed review of the sliding mode control, which concentrates on the work launched to date on reducing the high-frequency chattering problem and studying nonlinear sliding functions for robotic applications, especially on manipulator robots, which will put our research work into context. The following subsections present the basics of sliding mode control and concern the SMC implementation in different applications like process control, power electronics, and drives, especially Robotics. in this literature, the latest outcome of SMC, such as integration of SMC with different control techniques and progress in the SMC to make control strategy intelligent have been addressed.

2.1 General Overview

Nowadays, the exponential development of numerical computation tools authorizes an efficient execution of complex real-time control algorithms. Nonlinear digital controllers are increasingly utilized to handle complex systems among these algorithms. Several outcomes of nonlinear systems are described in detailed references, particularly in [92-95].Applications concerning these

nonlinear regulators are increasingly operated in industry and research. These controllers can also contain intelligent algorithms that perform at artificial neural networks [96] or fuzzy logic principles [97]. On the other hand, developed control techniques, e.g., fuzzy and neural networks and a combination of both is remarkable for concerning non-linear systems and also variable robotic manipulator dynamics [98-100].

In the classical nonlinear control strategies, feedback linearization control is a well-known technique in the scientific literature [94]. This method combines linearizing the system by balance and involving classic linear feedback control in the new linearized system. This approach carries a distinct form in robotic applications, known as the partitioned law or (computed torque approach) [101]. In actual applications, the feedback linearization approach is executed with some parameter adaptation methods to drive the robust control of modeling disturbances and uncertainties [102]. This technique can be integrated with intelligent strategies to provide robustness [103]. The backstepping control approach is another well-known nonlinear approach. This method is established on the advanced structure of Lyapunov functions developed from tracking errors [104,105]. However, this approach is appropriate for systems with triangular gable configurations, and the compiling of the control law evolves more complicated with the high order of the system. In scientific literature, this method is usually executed with adaptive techniques and with intelligent spectators and state estimators [106,107].

In the approaches noted above, sliding mode control remains an attractive nonlinear control technique to research, given its simplicity of performance and its natural robustness regarding disturbances and modeling uncertainties. Equivalent to previous approaches, sliding mode control can combine with intelligent techniques to enhance expected execution [108- 110]. The sliding mode control method is a robust control method for the complex higher order nonlinear systems

under parametric uncertainties and external effects. The sliding mode function was first emanated in variable configuration systems in the 1950s in the former Soviet Union [111 - 113].

In the early design phase, the variable structure system could not pay attention to the control field. The performance complexity, precisely the chattering problems with sensors, actuators, and switching systems. But there are some critical benefits to this method as it adjusts the system's dynamic conduct by choosing a suitable switching function, which creates the closed loop response insensitive to reached uncertainty in the system. Such a valuable component draws attention to the researchers for contribution to SMC evolution. In a recent development, SMC design approaches to the main issues like the elimination of chattering, the balance of the effect of unformed dynamics, adaptability in an uncertain system and enhancement in the dynamic execution of the closed loop system. The crucial benefit of selecting an SMC controller over the linear control like PID, as SMC supplies presence of stability and robustness execution in multiple uncertain systems where PID fails in the issue of an uncertain environment. Presently, sliding mode control (SMC) has been executed as the automatic controller for considerable applications like robotics, motion control problems, industrial process control, aerospace and power electronics applications [114-118].

The principal logic of SMC as a control strategy for different applications is due to the more proper execution for nonlinear systems, convenience to multiple input/output (MIMO) systems, and admits that it applies to discrete-time systems with an adequate strategy [119]. SMC method equips the excellent interpretation while negotiating with determinate uncertainties and disturbances and unmodeled dynamics [120,121] over the other specified techniques like robust adaptive control [122], H infinity control [123], and backstepping control [124]. The primary phase in developing the SMC is to set the switching function, which systems state on a sliding surface. After that, the

choice of proper control law makes system states on the sliding manifold in internal and external disturbances/uncertainties. However, the fundamental structure of the SMC is at the origin of the phenomenon of chattering under control [125]. Thus it is not appropriate in the actual procedure. The chattering appeared in some researchers then handled control, and there was a method named second order sliding. The refined classic SMC grew up in the 1980s when the “second order sliding” concept was presented [126]. Then in the following step of the evolution of SMC in the 2000s, higher order conceptions were acquired attention largely [127].

The need for evolution in the classic algorithm is due to the restrictions like the basic setup needs a relative degree of the system to be equal to the sliding variable. In addition, it makes it difficult to compensate for the high frequency switching control signal [128,129]. In advanced control, digital computers and microcontrollers increase due to digital control performance, and the algorithm is more efficient than analog methods. The first tries were taken for a discrete system variable control system in Russia in 1967. Regardless, the discrete-time sliding model was presented by Drakunov and Utkin firstly in control literature [130]. In the mid of 80s, the discrete sliding different researchers caused mode-control attention. [102,118,131-138] because of the switching-based control law and the absence of a switching function in the control law. One significant altercation with the classical SMC is that the system states it carries infinite time to reach stability. The researchers had the new inspiration to improve the system's performance in scrolling mode, and the system should reach equilibrium in a finite time. The new control name was terminal sliding mode control (TSMC) [139]. Despite the benefit of TSMC but system states take time to achieve stability if the initial condition is far away from the origin. Therefore the new evolved control algorithm as non-singular terminal sliding mode control (NTSMC) was emanated [140–142].

SMC execution is feasible nowadays in the rising technological world hence there are numerous applications encountered in the literature. Improvement in advanced control in the current decade has grown, and due to this, the usage of intelligent computers has attracted considerable attention. The feasibility of undertaking intricate control algorithms are achievable because of high-speed computers. Manipulator robots are used in various sectors in factories, surgery, laser cutting, painting, picking and positioning, warehouse storage, assembly, welding, etc., has attained comprehensive significance. The dynamics of the manipulator system are influenced by parametric uncertainties, nonlinearity, strong dynamic coupling and variable temporal structures [143]. SMC is beneficial in its elaborate set of features, and various SMC configurations have been used for industrial robot manipulators [144]. One class of nonlinear systems is under-actuated systems established in robotics and control theory with different fields of industry. The control of an under-actuated system is challenging because the system has a lower number of actuators than the number of variables to be controlled. The robustness is the exceptional point in controlling under-actuated systems, and SMC has been capable of controlling the under-actuated system with the influence of structured and unstructured uncertainties [145 -147].

2.2 Sliding Modes Control (SMC)

Sliding modes to control possibility came from later work on irregular structure systems [148]. Theoretically, it is handled by a control method that controls closed loop dynamical behavior corresponds to a sliding surface. Closed loop behavior is designed by selecting slide surfaces because closed-loop system dynamics elements control the whole system's behavior. The sliding surface can be illustrated as relation (1):

$$s = \dot{e} + \lambda e = 0 \; ; \; \lambda > 0 \quad (1)$$

Where trajectory error is indicated by e, exponential error convergence as (2):

$$\ddot{y} = \; f(y) + u \quad (2)$$

The system state y; u, the control law is presented as (3):

$$u = u_0 = -f + \ddot{y}_d - \lambda \dot{e} \quad (3)$$

Outcomes in $\dot{s}$ = 0 are, System converges exponentially for zero initial state s(t_0). The closed loop dynamics of the System are converged towards the sliding surface by adding a discontinuous term as $k.sgn(s)$ in control u0 for k > 0. At s = 0, the System will reach the sliding surface in finite time. An estimation on f, $\hat{f}$ is available in the presence of parametric uncertainties, then the control law becomes $\hat{u}$= k.Sgn(s) + u therefore,

$$u = -f + \ddot{y}_d - \lambda \dot{e} - k \; sgn(s)$$

that creates,

$$\dot{s} = f - \; \hat{f} \; - k \; sgn(s) \quad (4)$$

It will be possible to obtain the Lyapunov stability and convergence to sliding surface by selecting k > || $f - \; \hat{f}$|| [149].The classic SMC can provide an exponential stability with entire details about the system and also it delivers asymptotic stability of the system under the effect of uncertainties.

Terminal types of the SMC, TSMC and NTSMC are referenced to increase convergence properties of dynamical systems. Method focused on controlling robust robot functions in unstructured situations. Terminal sliding mode controller and fast finite time SMC modified types of classic SMC enforce finite time closed-loop convergence to equilibrium and convergence of tracking error

to zero [150]. The authors indicate that terminal sliders provide robustness to parametric uncertainty without recourse to high frequency switching control similar to conventional sliders. The concept of terminally sliding surfaces developed control synthesis of non-linear systems [151].

Most of the study papers on sliding mode control focus on two critical topics, chattering reduction on the control input and the study of nonlinear sliding manifolds. The chattering phenomenon originated from a discontinuous term in the control input, whose intent to absorb disturbances and matched or unmatched uncertainties and improve the control's robustness [152].The problem with chattering is that it implements the control input uncontrolled high-frequency commutations with very physical features or excite high-frequency dynamics on the closed loop system. Research endeavors on this subject have attempted to treat or prevent chattering while compromising on or keeping the identical level of robustness [153].

2.3 SMC For Robotic Manipulator Arms

It facilitated a specific method for developing a passivity-based terminal dynamic sliding mode control that ensures global finite time convergence for robot manipulators [154]. A new form of chatter-free sliding PID control regulation for continuous mechanical plants, which guarantees exponential convergence, is considered by Vicente et al. [19]. Regulated a non-linear integral control input for inertial and gravity dynamics, while proportional plus derivative control includes a closed-loop system trajectory stabilizer. A decentralized system model-free controller provides better performance than a model-based adaptive controller with or without finite-time convergence. A smooth sliding mode control and primary approach for a flexible joint robotic manipulator with constrained motion and force control presented by Huang et al. [7]. Few

components of reduced dynamics of constrained robots have been worked upon to zero the motion and tracking errors. It facilitated a specific method in [155] for developing a passivity-based terminal dynamic sliding mode control that ensures global finite time convergence for robot manipulators. In robotics, the terminal sliding mode control is an attractive approach. TSMC provides a more significant convergence accuracy to the robot's motion [156- 158]. A new terminal sliding mode for the control technique of a specific robotic manipulator dependent on finite time and differential stability theory principle of inequality with the support of the model-based method for robotic manipulators in mind, the TSMC approach to controlling robots was analyzed by Liu et al. [16]. The stability control of two flexible link manipulators investigated the subject of non-minimum phase problems and complicated dynamics and consequently suggested an optimized continuous non-singular terminal SMC control strategy. A recommended continuous control integrated with a genetic algorithm guarantees stability and quick convergence discussed by Wang and Sun [8].A four-linked SCARA robot manipulator with uncertain parameters contains a nonsingular-terminal sliding mode control presented to correspond to the efficiency of SMC strategy by Shankar J et al. [5]. Model-based proportional derivative and feedforward controller is also molded and employed to control the motion of a SCARA robot with high tracking precision. Studied a changeable fractional order for terminal sliding mode controller structured for handling robot manipulators with external disturbances and uncertainties by Nojavanzadeh and Badamchizadeh [159]. Lyapunov stability theorem demonstrates that adaptive control is utilized to evaluate the upper limit of uncertainties and stability of a closed loop system. The purpose of tracking in finite time is achieved. Razzaghian et al. [160] investigated the practical tracking control design of robot manipulators via continuous fractional order NTSMC according to time delay analysis. Time delay analysis applied to counterbalance unknown dynamics of robot

manipulators provoking a model-free structure and suggested controller can perform finite time stability in both achieving step and sliding phase prompting to control execution better as corresponded to using the boundary layer strategy. The research study of Zhu et al. [161] explored a terminal sliding mode control for the constant Markovian jumping manipulator systems, and numerical analysis is noted to define the practicality of the theoretical outcomes and also be able to guarantee the manipulator to track the excellent trajectory. Another method for the position analysis of the robotic manipulators presented in [162], in universal Extended Kalman Filter principles, which has a more reasonable outcome than classic Extended Kalman Filter in terms of convergence speed, robustness, and measure accuracy. Moreover, the position of each joint is set to use in a non-singular Fast TSMC.Therefore, using non-singular fast TSMC maintains finite time convergence and does not include the singularity problem of terminal sliding mode will be a better key for the preferred trajectory tracking of robotic manipulators. A finite time continuous terminal sliding mode controller with concern with respect to a Stewart platform which was planned to counterbalance for time varying external disturbances, model-free dynamics has shown by Luong et al. [163]. The simulation influences occurred with good tracking control results with evolution in model elements and time varying external disturbances and also, parametric investigation on developing parameters for the controller noted as future work.

Rsetam et al. [164] analyze the control motion of a single link flexible joint two Degree of freedom robot, a nonlinear and under-actuated fourth order system, employed hierarchical NTSMC. Based on the nature of the mechanism, a two-fold disintegration of the system is into rigid and flexible sub systems, respectively. The Lyapunov theorem is utilized to derive the presented control, qualified to stabilize both sub-systems in a finite time. Rapid multiple terminals switched sliding mode control techniques for robot manipulators having the effects of global high-speed

convergence delivering global non-singularity studied in [165]. Si et al. [14] facilitated the dynamic model of the two-link flexible manipulator with payload employing the Euler Lagrange equation. A fast NTSMC was suggested for the trajectory tracking problem of the two-link flexible manipulator. A substantial relative movement control in the multi robotic system with a specific approach named artificial potential field method for path planning, rapid adaptive gain NTSMC strategy for developing a robust controller has been offered by Nair et al. [166].

A robust nonlinear control approach with an uncertainty analyzer is used to track position within the robot's workspace to a cinematically redundant mobile manipulator with four degrees-of-freedom robotic arm mounted on three mobile bases examined by Mishra et al. [6]. It combines a decentralized PID control law for feedback part to raise the stability of the entire system, which improves performance temporary, a feedforward compensation used to support the control assignment by contrasting the results of known dissimilarities from recalled reference acceleration. This method provided no limit on the control design for lumped disturbances and mentioned can be improved for fast varying lumped disturbances in future work.

The design of adaptive control strategies for the robot, manipulators have been a practical field of research in recent decades. Energy-based views of organizing a robust adaptive control technique for robotic manipulators [167]. Using adaptive sliding control technique to balance supposed dynamics of the model and to overcome unmodeled dynamics achieved.

A PID fast terminal sliding mode dynamic inverse control technique for a mobile robots to balance nonlinear and non-holonomic effects for trajectory tracking of dynamic established by Mallem et al. [168]. The terminal sliding mode control technique is implemented to guarantee the finite time convergence of tracking errors.

A constructive fault tolerant control approach for an uncertain non-holonomic scheme employs the minimum dilation degree and auxiliary states transformation proposed in [169], a constructive terminal slide technique. Non-holonomic systems face the problem of being subject to non-integrable conditions whose behavior should yield with limitations. The robot parking problem describes the efficiency of operating the standard non-holonomic designs with a control strategy.

A hierarchical fast terminal sliding mode control approach, trained by Zheng et al. [170] based on the sliding-mode control methods' features. The control strategy efficiently maintains two wheeled robots counterbalanced, and tracks expected momentum by further studies per intensive sample outcome. Simultaneously, the control strategy avoided decreasing shaking through rough terrain and expected weather. Asif et al. [18] presented a terminal sliding mode control suggested the configuration of a control law for trajectory tracking non-holonomic mobile robots eliminate the chattering phenomenon and provide stability by utilizing the Lyapunov theory controlled by velocity inputs that enforce kinematic configurations. Khoo et al. [171] described the integral terminal sliding mode obliging control of multi-robot networks that supply finite time convergence for a first-order non-linear system with applied disturbances. The control mode used for collaborative consensus control of 2 degrees of freedom first ordered specific types of mobile robots. It demonstrated that finite-time consensus tracking of multi-robot networks could be achieved on sliding surfaces. Henghua et al. [172] suggested an NTSM control for position identification and synchronizing of multiple manipulator configurations. A limited time reaching law improves the cumulating rate and chattering avoidance. It delivers a steady state of NTSM with the existence of external disturbances. Multiple adaptive terminals sliding mode configuration with outcome recurring fuzzy wavelet neural networks provided for a set of networked heterogeneous multi-directional robots are given by Wu et al. [173]. Results of succeeding control

methods were confirmed via simulations. The studied technique would be an attractive case for research to perform experiments to validate the usefulness of the proposed approach and consider collision. The integral terminal sliding mode considers the adaptive synchronization control system for multiple robotic manipulators with actuator saturation combined by Dongya et al. [174]. Limited time stability is studied by considering Lyapunov theory, and simulation results have presented the methods' efficacy. A design of robust adaptive controller for parallel manipulators, on sliding mode a model-based adaptive control proposed by Bennehar et al. [175]. The adaption loop corresponds to the model-based control loop's varying time state and unspecified components. To estimate the efficacy of the studied controller, some practical investigations are performed on 4 DoF parallel robots. The train results have indicated enhanced tracking performance of the instructed controller. Future work suggested applying the proposed controller on redundantly actuated parallel manipulators with different internal joint forces. Illustrated a stable, adaptive, and rapid control strategy for controlling the n-DOF robotic manipulator in [176].The strategy for controlling was a Combination of multiple terminal sliding mode controllers and radial base neural networks to avoid modeling problems that ensure the robust performance of the robot, eliminate the chattering phenomenon, and enhance control performance. A control dysfunction in the application studied by Jun et al. [9] for a specific 6-DOF wire manipulated parallel robot (WD-PR).kinematic and dynamic equations for the wire parallel wired robot presented entirely, matching control law is developed by NTSM, continuous NTSM and stability estimation is considered by Lyapunov theory.

Much less work is currently in the literature regarding the study of nonlinear sliding functions among the research on the reduction or elimination of chattering in sliding mode control. Between the analysis of nonlinear functions, research on Terminal Sliding Mode Control (TSMC) on

nonlinear sliding functions is developed to provide a fast convergence of the tracking error in a finite time in [9-13]. An investigated sliding functions with the variation of the parameters over time to enhance the control's robustness and quick convergence presented by Choi et al [17].

2.4 Control Of Chattering Levels

The major issue of sliding mode control is the high-frequency chattering phenomenon occurring on the control signals during the execution of this control system. Chattering is generated by an unsteady term contained in the sliding mode control law. In a numerical implementation, the commutations made by the discontinuous period do not appear instantaneously, leading to Chattering.

A specific method to decrease chattering is to smoothen the discontinuous term using a saturation function. This technique is named the boundary layer approach [94]. The drawback of the approach is that the robustness of the control is decreased, and the system stays within a boundary of the sliding manifold. A nonlinear reaching law reduces the discontinuous gain and thus chattering when the sliding manifold is contacted, studied in [20,21].

Another method to reduce chattering consists of increasing the order of the system explored by Laghrouche et al. [177]. That is known as higher order sliding mode control (HOSM). A particular case of HOSM is second-order sliding mode control. Different applications of second order sliding mode control were proposed in many studies [177-187]. Nevertheless, the disadvantage of HOSM method is that the stability verifications are primarily based on geometrical forms. To handle this issue, Moreno and Osorio presented a Lyapunov-based technique for examining the stability of a

specific class of a second order sliding mode controller, named the super-twisting sliding mode controller (STSMC) [15].

The study of nonlinear sliding manifolds concentrates on two different goals, enhancing the transient impacts on the control input. Second, it provides a finite convergence time of the sliding system on the manifold, which is not met by the classic linear manifold design. use of sliding functions with time-varying parameters to enhance robustness and transient behavior of the control input explored by Choi et al. [17] and Stepanenko and Su [188]. Nowadays, the research focuses on terminal sliding mode control, where nonlinear sliding functions are designed to guarantee a fast and finite convergence time on the sliding surface [189-195].

The other chattering component is that the sliding surface is never exactly achieved in training. Chattering is typically disfavored because it can exhilarate unwanted dynamics in the mechanism. Nevertheless, in specific applications, for example, in power electronics, Chattering does not necessarily negatively affect as indicated by Slotine and Li [94].

In the scientific literature concerning sliding mode control, the primary research principle aims to reduce and eliminate the chattering phenomenon on the control inputs. Multiple techniques have been generated to prevent or stop chattering. in the best-known method, a methodology of softening the discontinuous term in the control law consists in replacing the periodical term of the control law $ksgn(S)$ with the term $k \cdot sat\ (S/\Phi)$ [94]. The sat function is described as follows :

$$sat\left(\frac{s}{\Phi}\right) = \begin{cases} 1\ for\ \frac{s}{\Phi} > 1 \\ \frac{s}{\Phi}\ for\ -1 \leq \frac{s}{\Phi} \leq 1 \\ -1\ elsewhere \end{cases} \quad (5)$$

With this method, chattering on the control input is eliminated. Regardless, the convergence of the error stays in residents of the sliding surface. The amplitude is straight conditional on the selected

value of Φ. Tracking performance is consequently influenced. Other functions that correspond to the (sign) function are also proposed and examined in the literature, such as using a sigmoid function instead of the sign function [196].

Another method used by considerable researchers is increasing the degree of the sliding functions from one to a specific degree. Utilizing the virtual time derivative order of the control law proposed by [22]. Choosing discontinuous time derivative, then the actual control law is formed by a series of integrals with continuous nature, guarantees proven chattering avoidance by the mentioned technique. This technique has been used by Hamerlain et al. on a typical robot trajectory tracking [23].

Focused on the second order to avoid chattering on the control input studied in [197,198]. Nevertheless, higher order sliding mode control requires forming a new sliding surface, which means the demand for studies. A typical approach of this method used only for sliding functions with second order is known as Super-Twisting, presented by Moreno and Osorio [15]. This approach provided eliminates chattering without having to use derivative sliding surface terms in the expression of the control law.

Reducing chattering with Different methods suggested in literature consists of modifying the conventional reaching law. A nonlinear reaching law permits a dynamic adaption to the control law with the variation of the sliding function organized by Alattas et al [199]. Therefore, the addition of the state vector from the sliding surface, the greater this gain is and tends to get the vector back to the surface. Thus, it is theoretically possible to decrease high-frequency switching in a steady state without concerning the convergence time or system tracking error. Two potential reaching laws to eliminate chattering were studied in [200].The first reaching law includes a term proportional in the sliding function to enable the system to reach the sliding surface quickly if far

from the surface. Also, the proportional representation decreases the effort needed by the discontinuity of sign function sgn(s), and hence enables the reduction of the chattering levels on the control input step. This reaching law is shown by :

$\dot{S} = -k.sgn(s) - Q.s$ (Q is the terms of equation determined by finite amount and time) (6)

The second suggested reaching law involved a fractional power of the sliding function that multiplies the sign of this one. The proposed reaching law function demonstrates that the reaching law generates a finite reaching time of the sliding surface if the term of alpha is real and between zero and one. The proposed reaching law function is presented as follows:

$\dot{S} = -k.|s|^{\alpha}sgn(s) \qquad (0 \leq \alpha \leq 1)$ (7)

Due to technological advances and the development of intelligent computers, the implementation of the advanced control algorithm is possible. The growth of advanced control algorithms, particularly the sliding mode control, is considered due to the competence and ease of implementation of linear and nonlinear systems. In this survey, general application areas of the SMC control, especially robotic applications, are considered. The different configurations of SMC methods for those applications have been studied. The generation of SMC controlling techniques with a robotic application point of view, such as second order sliding mode controllers, super twisting controllers, and arbitrary order sliding mode controllers, are explained. Also, the improvement of the SMC control method with the integration of other techniques was concerned.Recent advancements in the SMC control state that integrating and combining the different intelligent techniques with the SMC control strategy is the next step in sliding model-based control strategies. The adaptive and intelligent method based on the SMC strategy has

developed and is much more effective in uncertain systems with the effect of structured and unstructured uncertainty.

Sliding mode control remains an attractive nonlinear control technique to research, given its simplicity of performance and its natural robustness regarding disturbances and modeling uncertainties. Equivalent to previous approaches, sliding mode control can combine with intelligent techniques to enhance expected execution. The sliding mode control method is a robust control method for the complex higher order nonlinear systems under parametric uncertainties and external effects. Presently, sliding mode control (SMC) has been executed as the automatic controller for considerable applications like robotics, motion control problems, industrial process control, aerospace and power electronics applications. SMC method equips the excellent interpretation while negotiating with determinate uncertainties and disturbances and unmodeled dynamics over the other specified techniques like robust adaptive control, H infinity control, and backstepping control.

Classic SMC grew up when the “second order sliding” concept was presented. Then in the following higher order conceptions were acquired attention largely. One significant altercation with the classical SMC is that the system states it carries infinite time to reach stability. terminal sliding mode control (TSMC) had the new inspiration to improve the system's performance in scrolling mode, and the system due to reach equilibrium in a finite time.because of in TSMC execution, system states take time to achieve stability if the initial condition is far away from the origin. Therefore the new evolved control algorithm as non-singular terminal sliding mode control (NTSMC) was emanated. Terminal types of the SMC, TSMC and NTSMC are referenced to increase convergence properties of dynamical systems. Method focused on controlling robust robot functions in unstructured situations. Terminal sliding mode controller and also fast finite

time SMC as another strategy, modified types of classic SMC enforce finite time closed-loop convergence to equilibrium and convergence of tracking error to zero.

Improvement in advanced control in the current decade has grown, specially in Manipulator robots that are used in various sectors. The dynamics of the manipulator system are influenced by parametric uncertainties, nonlinearity, strong dynamic coupling and variable temporal structures because of the SMC is beneficial in its elaborate set of features, and various SMC configurations have been used for industrial robot manipulators most of the study papers on sliding mode control focus on two critical topics, chattering reduction on the control input and the study of nonlinear sliding manifolds.

Table 1 demonstrates a comprehensive classification of the methods selected in the literature reviewed in this the researchers' level of interest, and the mechanisms chosen for research in the field of sliding mode control. In general, different types of sliding mode control in the latest works in control of robotics are exciting and significant for researchers and the overall effort for the research conducted on the control of manipulator arms using sliding mode control indicates the effectiveness of this control method. The quality of the performance of this method in different forms for manipulator robotic arms shows the acceptable results and the capability of this control method. Among the forms of the sliding mode control method, the terminal sliding mode control method has received more attention from researchers. Significant convergence time and finite time convergence are the reasons for choosing the TSMC model in the sliding control. On the other side in the literature review, it can be concluded that other forms of sliding mode control, such as the classical form of the SMC and non-singular terminal SMC control , provide acceptable results and using the both methods has great interest to research. Table 1 also shows that most researchers

have used the classical form of the sliding mode control method to evaluate the performance and quality of the sliding mode control method.

Table 1: Classification of the SMC methods.

Method	Mechanism	Subjects/Target
Classical Sliding control	- Flexible joint robotic manipulator [7] - 3 DOF Manipulator [19][17] - 6 DOF Manipulator [165][167][173] - 4 DOF Manipulator [6][175] - Parallel manipulator [176]	- Compare model free/based adaptive controller [7] - Finite time convergence [19][17] - Track the trajectory [165][6] - Investigate efficiency of SMC strategy [167][173][175][176]
Terminal sliding mode control	- 3 DOF Manipulator [155] - 6 DOF Manipulator [156-158][163][171][9] - 4 DOF Manipulator [16][10] - SCARA robot [159][11-13] - Parallel manipulator [174] - Markovian manipulator systems [161] - Mobile robot [168][169][170][18]	- Significant convergence time [155-158] - Examine differential stability theory [16][174] - Studied handling with external disturbances [159] - Track the trajectory [161][163][169][170][171] - Finite time convergence [168][18][10-13] - Investigate efficiency of SMC strategy [9]
Non-singular terminal SMC control	- Two flexible link manipulators [8][14][166] - SCARA robot [5] - 6 DOF Manipulators [160][162][172] - Single link flexible joint [164]	- TSMC with a genetic algorithm guarantees convergence time[8] - Investigate efficiency of SMC strategy [5] - Finite time convergence [160] - Track the trajectory [162][164][14][166][172]

Another significant issue that attracts attention in the literature review and latest works related to sliding mode control is the combination of each form of sliding mode control with specific mathematical functions to control the chattering phenomenon. These functions are used in the part of the control law function. Among the essential methods of interest to researchers, we can mention the boundary layer approach, nonlinear reaching law, high order sliding mode control (second-order), and super twisting sliding mode. In general, in the literature review, it can be found that the mentioned methods have an acceptable ability to solve the chattering phenomenon in the sliding mode control method.

Chapter Three

Tools and Methods

3.1. Robotic-arm presentation

The robot considered in this study is the ABB IRB 140 (M2004), shown in Figure 5. Its 6-axis articulated structure is one of the most widely used in many industrial fields.

Figure 5: The ABB IRB 140 robot located in the UQTR automation laboratory.

According to the ABB technical documentation [201], this industrial robot can be mounted on the floor or a wall at any angle and even inverted for a wide variety of working ranges. It is used

mainly for arc welding, assembly, cleaning/spraying, machine tending, material handling, packing, and deburring. It weighs about 98 kg with an end effector weighing up to 5 kg, including a payload with a reach of about 810 mm that can be mounted on its mounting flange. Up to 1.5 kg of equipment can be mounted on its upper arm. Its joint limits allow ample functional workspace duty. These are summarized in Table 2 [201].

Table 2: Joint limits of the ABB IRB 140 robot.

Joint	**Type**	**Limits (°)**
1	Rotational	+180 to -180
2	Rotational	+110 to -90
3	Rotational	+50 to -230
4	Rotational	+200 to -200
5	Rotational	+120 to -120
6	Rotational	+400 to -400

The manipulator includes the IRC5 controller [202], a multi-robot controller with PC tool support that optimizes robot performance for short cycle times and precise movements, and RobotWare (Robot Studio), which allows ABB robot programming on a PC without shutting down production. A program can be built on the ABB Virtual Controller, an exact copy of the software that runs robots in production. Robot Studio allows very realistic simulations to be performed using simple robot programs and configuration files identical to those used in the field.

3.2. Robot models

3.2.1. Forward and inverse kinematics

3.2.1.1. Forward kinematics

The purpose of the forward kinematics model is to determine the position and orientation of the robot end-effector as a function of joint angle and displacement relative to the base frame or other reference. To achieve this mathematically, a global coordinate frame must be assigned to the base frame and a local reference frame given to each joint [203-205]. Homogeneous transformation 4×4 matrices are then computed for the robot joint axes using a formalism such as D-H (Denavit-Hartenberg) to define and interpret robot spatial geometry and end-effector location in a fixed reference system [205]. Figure 6 shows the D-H parameter and link assignments for a rotational joint.

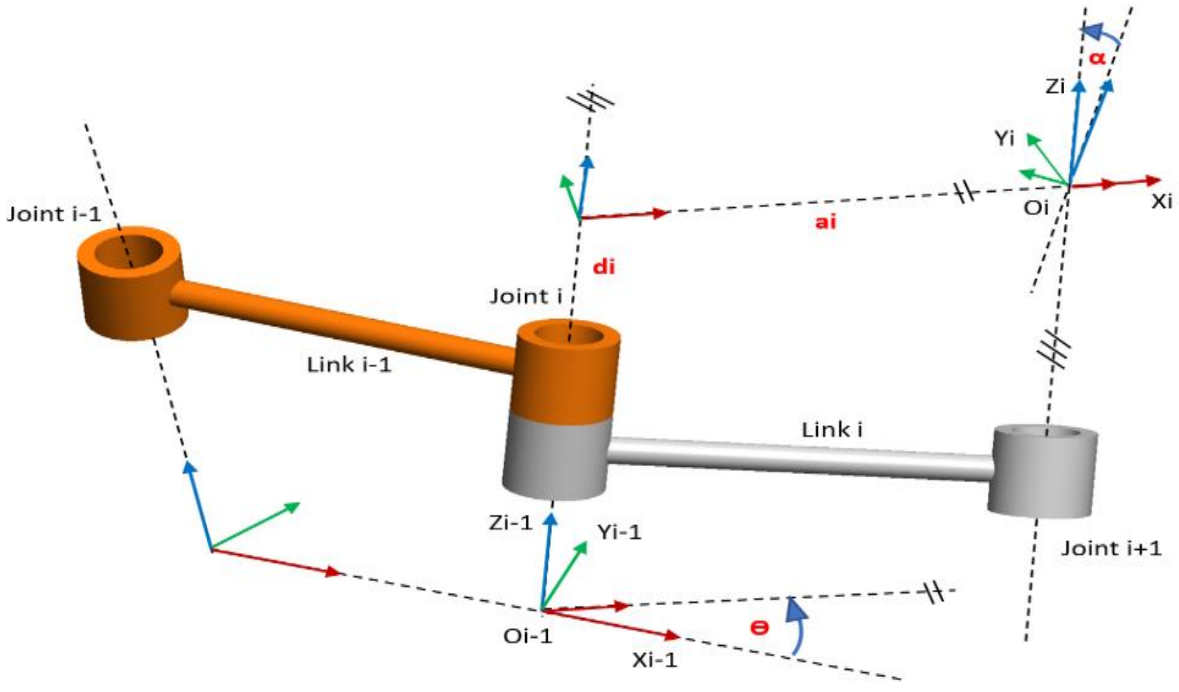

Figure 6**:** D-H parameters and link assignments for a rotational joint.

The kinematic function thus maintains a fixed relationship between the two successive joint axes it supports. This relationship can be defined using two parameters: link length a and link twist α. Link offset d and joint angle θ are used to describe the nature of the connection between adjacent links [204].

The D-H parameters can be defined as follows:

α_{i-1}: Twist angle between joint axes z_i and $z_i - 1$ measured about x_{i-1}

a_{i-1}: Distance between joint axes z_i and z_{i-1} measured along the standard normal

θ_i: Joint angle between joint axes x_i and x_{i-1} calculated about z_i

d_i: Link offset between axes x_i and x_{i-1} measured along z_i

The four transformations between the two axes can be defined as follows:

$$^{i-1}_{i}\mathrm{T} = \mathrm{Rot}(x_{i-1}, \alpha_{i-1}) \times Trans(x_{i-1}, a_{i-1}) \times \mathrm{Rot}(z_i, \theta_i) \times Trans(0, 0, d_i) \quad (8)$$

As indicated in relation (1) $^{i-1}_{i}T$ is the homogeneous transformation matrix, Rot (x_{i-1}, α_{i-1}) is rotation around an axis x by the Trans (x_{i-1}, a_{i-1}) is the transfer along axis x to the value of the a, Rot (z_i, θ_i) is rotation around axis z by the θ, Trans $(0,0,d_i)$ is the transfer along axis z to the value of the d.

Therefore, the following homogeneous transformation matrix can be obtained:

$$ {}^{i-1}_{i}T = \begin{pmatrix} c_{\theta_i} & -s_{\theta_i} & 0 & a_{i-1} \\ s_{\theta_i} c_{\alpha_{i-1}} & c_{\theta_i} c_{\alpha_{i-1}} & -s_{\alpha_{i-1}} & -d_i s_{\alpha_{i-1}} \\ s_{\theta_i} s_{\alpha_{i-1}} & c_{\theta_i} s_{\alpha_{i-1}} & c_{\alpha_{i-1}} & d_i c_{\alpha_{i-1}} \\ 0 & 0 & 0 & 1 \end{pmatrix} \quad (9) $$

Where c and s indicate the cosine and sine of angles θ_i and α_i.

3.2.1.2. Inverse kinematics

The inverse kinematics model is used to calculate the joint values and hence the collective joint configuration corresponding to the desired pose of the end effector. In a reference coordinate system, the variables representing each joint may be determined according to the location requirements of the manipulator end [206]. The first three joints proximal to the base frame of the IRB 140 determine the end-effector position and the remaining three determine effector orientation [205]. The inverse kinematics problem can be solved using analytical or numerical methods [207, 208]. Analytical solutions of joint variables are based on configuration data. Since a given end-effector position may be reached via multiple joint configurations, multiple values for each joint may be obtained as solutions. Figure 7 shows different configurations for the proximal joints. The primary joints determine the position of the end-effector [209].

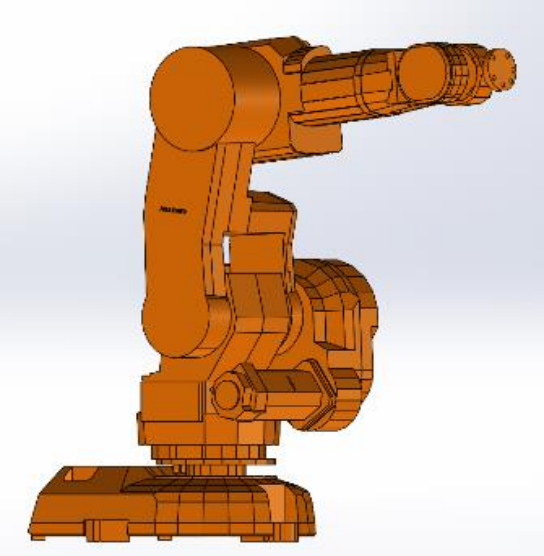

(a)

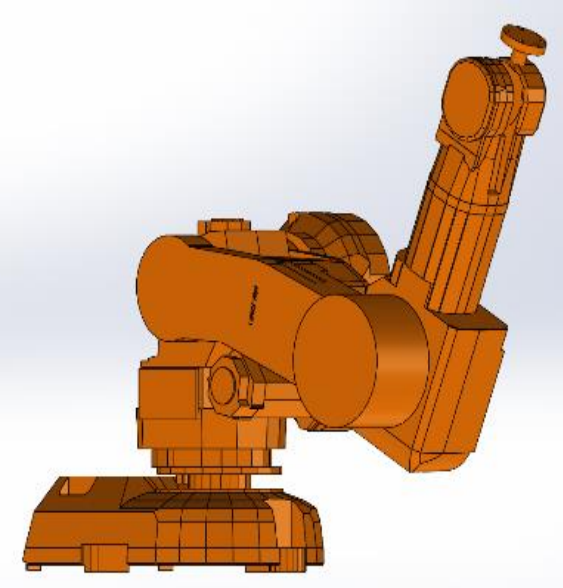

(b)

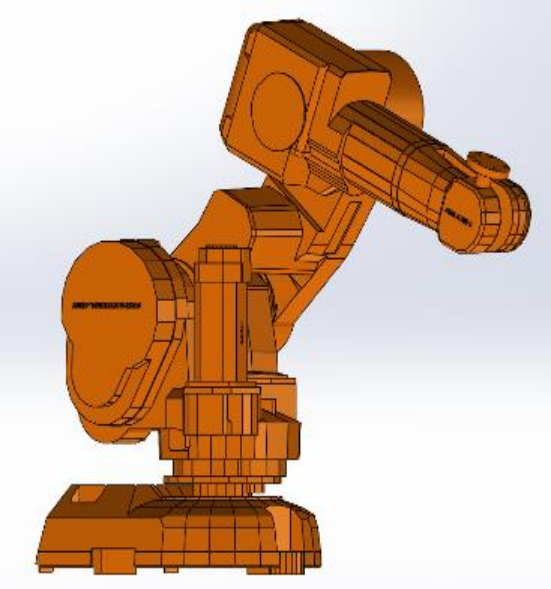

(c)

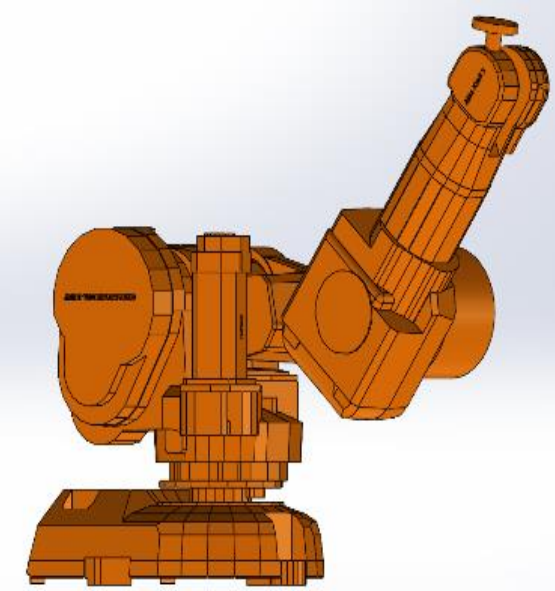

(d)

Figure 7**:** Configurations of the three proximal joints of the IRB 140 manipulator arm, A – Right and above; B – Right and below; C – Left and above; D – Left and below.

3.2.2. Forward and inverse differential kinematics

Differential kinematics define the relationship between joint angular velocities and the corresponding end-effector linear and angular velocity. The study of velocities and static forces leads to the Jacobian matrix of the manipulator, an essential tool for analyzing and controlling robotic motion, finding singularities and redundancy, determining inverse kinematics equations, and describing velocity and force manipulability ellipsoids [2].

A Jacobian matrix is a multidimensional form of the derivative. Depending on the number of joints, it can be of any dimension (including non-square). The number of rows in a Jacobian matrix equals the number of degrees of freedom in Cartesian space. For example, three if only robot position is considered, or six if position and orientation are considered. The number of columns corresponds to the number of joints comprising the manipulator.

Considering the end-effector linear velocity vector $\dot{p}_e$, the angular velocity vector ω_e and the joint velocity vector $\dot{q}$, J_p would then be the (3 × n) matrix that links the linear velocity vector to the joint speed vector and J_o would be the (3 × n) matrix that links the angular velocity vector to the joint speeds vector as expressed in equation (10.1) and (10.2) or in its compact form in equation (11) [210].

$$\dot{p}_e = J_p(q)\dot{q} \tag{10.1}$$

$$\omega_e = J_O(q)\dot{q} \tag{10.2}$$

$$v_e = \begin{pmatrix} \dot{p}_e \\ \omega_e \end{pmatrix} = J(q)\dot{q} \qquad J = \begin{pmatrix} J_P \\ J_O \end{pmatrix} \tag{11}$$

v_e presented the End-effector velocity, and J indicated The Jacobian matrix.

Equation (4) represents the manipulator differential kinematics equation. The (6 × n) matrix J is the manipulator geometric Jacobian, a function of the joint variables. Each joint is prismatic with linear velocity or revolute with angular velocity. It is convenient to proceed separately for linear and angular velocities [210]. The linear velocity-time derivative of $p_e(q)$ is expressed in equation (12), whereas angular velocity is expressed in equation (13).

$$\dot{p}_e = \sum_{i=1}^{n} \frac{\partial p_e}{\partial q_i} \dot{q}_i = \sum_{i=1}^{n} JP_i \dot{q}_i \qquad JP_i = z_{i-1} \times (p_e - p_{i-1}) \tag{12}$$

JP_i position components in the Jacobian matrix

$$\omega_e = \omega_n = \sum_{i=1}^{n} \omega_{i-1}, i = \sum_{i=1}^{n} JO_i \dot{q}_i \qquad JO_i = z_{i-1} \tag{13}$$

Jo_i orientation components in the Jacobian matrix

The Jacobian matrix can also be partitioned in equation 14 as follows:

$$J = \begin{pmatrix} JP_1 & & JP_n \\ & \dots & \\ JO_1 & & JO_n \end{pmatrix} \qquad \begin{pmatrix} JP_i \\ JO_i \end{pmatrix} = \begin{cases} \begin{bmatrix} z_{i-1} \\ 0 \end{bmatrix} & \text{for a prismatic joint} \\ \begin{bmatrix} z_{i-1} \times (p_e - p_{i-1}) \\ z_{i-1} \end{bmatrix} & \text{for a revolute joint.} \end{cases} \tag{14}$$

3.2.2.1. Forward differential kinematics

The joint angles q_1, q_2, and q_3 define the IRB 140 end-effector position in space, while joint angles q_4, q_5, and q_6 describe the end-effector orientation. Using the effector velocity (15), tabled D-H parameters, and the transformation matrices, the Jacobin matrix will be obtained for the three proximal links [210].

$$v_e = \begin{pmatrix} \dot{p}_e \\ \omega_e \end{pmatrix} = J(q)\dot{q} \tag{15}$$

The transformation matrix representing the reference frame and end-effector position for an articulated robotic arm with six degrees of freedom is defined as follows:

$$ {}^{0}_{6}\mathrm{T} = \begin{pmatrix} \mathrm{r}_{11} & \mathrm{r}_{12} & \mathrm{r}_{13} & \mathrm{x} \\ \mathrm{r}_{21} & \mathrm{r}_{22} & \mathrm{r}_{23} & \mathrm{y} \\ \mathrm{r}_{31} & \mathrm{r}_{32} & \mathrm{r}_{33} & \mathrm{z} \\ 0 & 0 & 0 & 1 \end{pmatrix} \tag{16} $$

The Jacobian matrix is defined as follows:

$$ J = \begin{pmatrix} J_v \\ J_w \end{pmatrix} \tag{17} $$

Such as:

J_v The linear velocity

J_w The angular velocity

$$ J_v = \begin{pmatrix} \frac{\delta x}{\delta q_1} & \frac{\delta x}{\delta q_2} & \frac{\delta x}{\delta q_3} \\ \frac{\delta y}{\delta q_1} & \frac{\delta y}{\delta q_2} & \frac{\delta y}{\delta q_3} \\ \frac{\delta z}{\delta q_1} & \frac{\delta z}{\delta q_2} & \frac{\delta z}{\delta q_3} \end{pmatrix} \tag{18} $$

Matrix J_w is obtained from the transformation matrices ${}^{1}_{0}T$, ${}^{2}_{0}T$ and ${}^{3}_{0}T$, such that r_{13}, r_{23} and r_{33} in each of the transformation matrixes correspond to, ${}^{2}_{0}Z$ and ${}^{3}_{0}Z$

$$ J_w = \begin{pmatrix} {}^{1}_{0}Z & {}^{2}_{0}Z & {}^{3}_{0}Z \end{pmatrix} \tag{19} $$

$$J = \begin{pmatrix} J_v \\ J_w \end{pmatrix} = \begin{pmatrix} \frac{\delta x}{\delta q_1} & \frac{\delta x}{\delta q_2} & \frac{\delta x}{\delta q_3} \\ \frac{\delta y}{\delta q_1} & \frac{\delta y}{\delta q_2} & \frac{\delta y}{\delta q_3} \\ \frac{\delta z}{\delta q_1} & \frac{\delta z}{\delta q_2} & \frac{\delta z}{\delta q_3} \\ {}^{1}_{0}Z & {}^{2}_{0}Z & {}^{3}_{0}Z \end{pmatrix} \quad (20)$$

3.2.2.2. Inverse differential kinematics

Suppose the relationship between the joint space variable and the orientation space variable is highly nonlinear. In that case, the inverse kinematics solution will be redundant and closed-form or even non-existent. The inverse kinematics problem begins with the linear mapping of the joint velocity space and the operational velocity space using differential equations. Depending on the desired end-effector position and orientation, the desired joint velocity can be obtained via simple inversion of the Jacobian matrix, which must be invertible. J is square, and its determinant is not equal to zero. As mentioned above, the Jacobian matrix can be of any dimension and is not always square or invertible. In this case, the pseudo inverse of the generalized inverse can be used, as defined in equations (21) and (22) below [210].

$$\mathrm{v_e} = \begin{pmatrix} \dot{\mathrm{p}}_e \\ \omega_e \end{pmatrix} = \mathrm{J(q)\dot{q}} \quad (21)$$

$$\dot{\mathrm{q}} = \mathrm{J^{-1}(q)v_e}. \quad (22)$$

J^{-1} inversion of the Jacobian matrix

3.2.3. Dynamic model

A dynamic model allows the expression of robot function in terms of joint acceleration forces and torque. The method most used to determine this model is the Euler-Lagrange approach. The model of an n-jointed robotic arm can be expressed as in equation 23 [211]:

$$\sum_{j=1}^{n} M_{ij}\ddot{q}_j + V_i + G_i = Q_i = \tau_i \quad \text{para} \quad i = 1, 2, ..., n. \tag{23}$$

Where $\ddot{q}$ is the joint acceleration vector, M is the inertia matrix, Vi the Coriolis vector, G is the gravitational vector, and τ is the force and torque vector.

3.3. Mathematical models of the robot

Figure 8 shows the frame assignments, and Table 3 lists the D-H parameters of the ABB IRB 140 industrial robot, with the global coordinate system shown below [212]:T

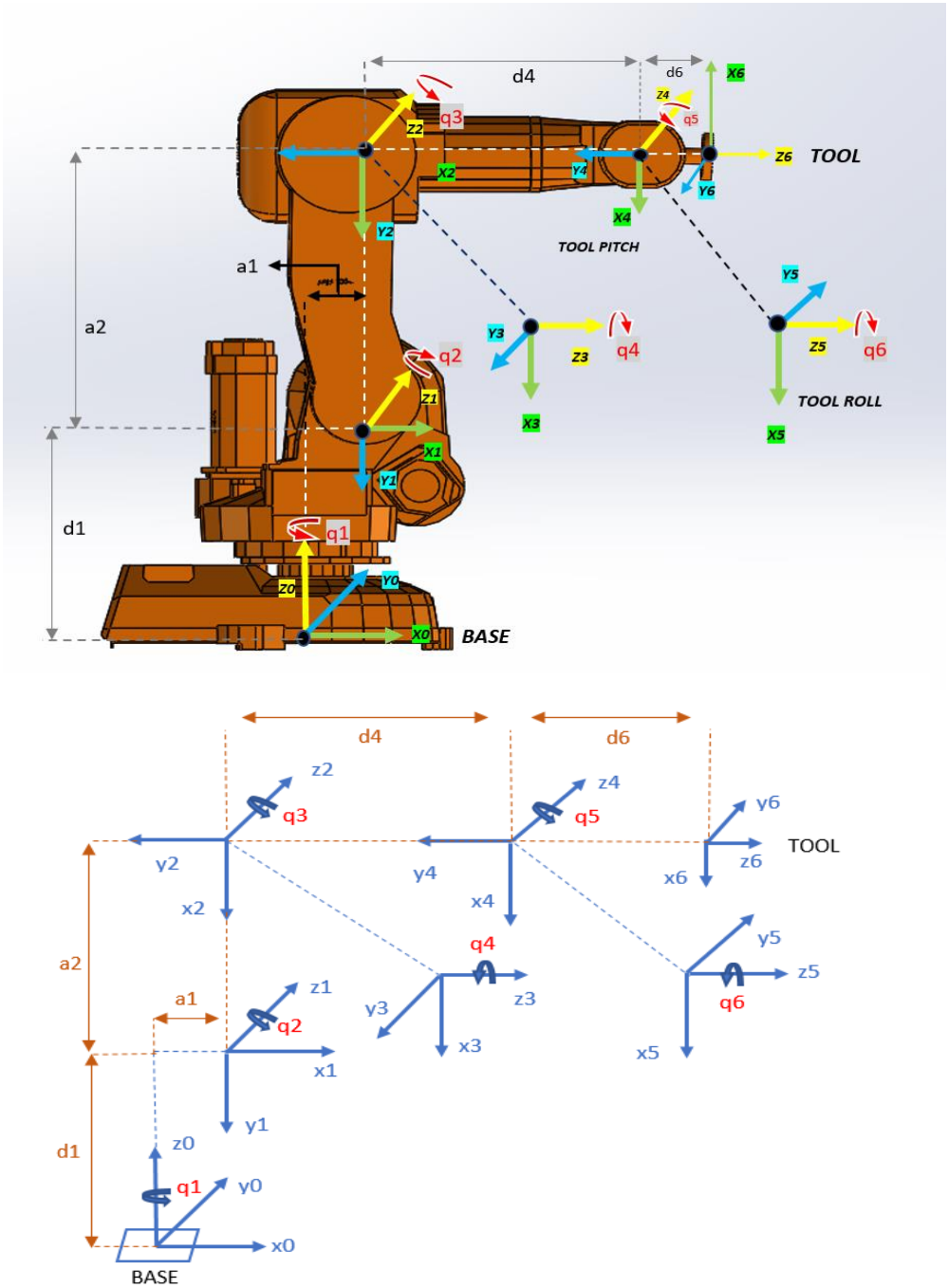

Figure 8: ABB IRB 140 frame assignments.

Based on the frame assignment, modified D-H parameters are defined as follows:

Table 3: DENAVIT-HARTENBERG parameters for the ABB IRB 140 robotic arm.

LINK	a (mm)	α (˚)	d (mm)	q (˚)
1	$a_1 = 70$	-90	$d_1 = 352$	q_1
2	$a_2 = -360$	0	0	$q_2 + 90$
3	0	-90	0	q_3
4	0	90	$d_4 = 380$	q_4
5	0	-90	0	q_5
6	0	0	$d_6 = 65$	q_6

With D-H parameters, we can achieve the individual transformation matrix for each link by substituting the link parameters into the relationship (9), giving:

$$q_2' = 2' = q_2 + \pi/2 \qquad (24)$$

$$T_0^1 = \begin{pmatrix} C1 & 0 & -S1 & a1.C1 \\ S1 & 0 & C1 & a1.S1 \\ 0 & -1 & 0 & d1 \\ 0 & 0 & 0 & 1 \end{pmatrix} \quad (25)$$

$$T_1^2 = \begin{pmatrix} C2 & -S2' & 0 & -a2.C2' \\ S2 & C2' & 0 & -a2.S2' \\ 0 & 0 & 1 & 0 \\ 0 & 0 & 0 & 1 \end{pmatrix} \quad (26)$$

$$T_2^3 = \begin{pmatrix} C3 & 0 & S3 & 0 \\ S3 & 0 & -C3 & 0 \\ 0 & 1 & 0 & 0 \\ 0 & 0 & 0 & 1 \end{pmatrix} \quad (27)$$

$$T_3^4 = \begin{pmatrix} C4 & 0 & -S4 & 0 \\ S4 & 0 & C4 & 0 \\ 0 & -1 & 0 & d4 \\ 0 & 0 & 0 & 1 \end{pmatrix} \quad (28)$$

$$T_4^5 = \begin{pmatrix} C5 & 0 & S5 & 0 \\ S5 & 0 & -C5 & 0 \\ 0 & 1 & 0 & 0 \\ 0 & 0 & 0 & 1 \end{pmatrix} \quad (29)$$

$$T_5^6 = \begin{pmatrix} C6 & -S6 & 0 & 0 \\ S6 & C6 & 0 & 0 \\ 0 & 0 & 1 & d6 \\ 0 & 0 & 0 & 1 \end{pmatrix} \quad (30)$$

After obtaining a homogeneous transformation matrix for each link, position and orientation are achieved by applying the forward kinematic chain in the global frame. The pose matrix of the end-effector relative to its base frame is obtained as shown below:

$${}_6^0T = {}_1^0T.\ {}_2^1T.\ {}_3^2T.\ {}_4^3T.\ {}_5^4T.\ {}_6^5T \qquad {}_6^0\mathrm{T} = \begin{pmatrix} \mathrm{r11} & \mathrm{r12} & \mathrm{r13} & \mathrm{x} \\ \mathrm{r21} & \mathrm{r22} & \mathrm{r23} & \mathrm{y} \\ \mathrm{r31} & \mathrm{r32} & \mathrm{r33} & \mathrm{z} \\ 0 & 0 & 0 & 1 \end{pmatrix} \quad (31)$$

Such that:

$$r_{11} = -S_6(S_4C_1C_{2'3} + C_4S_1) - C_6(C_5(S_1S_4 - C_4C_1C_{2'3}) + S_5C_1C_{2'3}) \quad (32.1)$$

$$r_{12} = S_6(C_5(S_1S_4 - C_4C_1C_{2'3}) + S_5C_1C_{2'3}) - C_6(S_4C_1C_{2'3} + C_4S_1) \quad (32.2)$$

$$r_{13} = C_5C_1S_{2'3} - S_5(S_1S_4 - C_4C_1C_{2'3}) \quad (32.3)$$

$$r_{21} = C_6(C_5(C_4S_1C_{2'3} + C_1S_4) - S_5S_1S_{2'3}) - S_6(S_4S_1C_{2'3} - C_1C_4) \quad (32.4)$$

$$r_{22} = -S_6(C_5(C_4S_1C_{2'3} + C_1S_4) - S_5S_1S_{2'3}) - C_6(S_4S_1C_{2'3} - C_1C_4) \quad (32.5)$$

$$r_{23} = C_5S_1S_{2'3} + S_5(C_4S_1C_{2'3} + C_1S_4) \quad (32.6)$$

$$r_{31} = -C_6(S_5C_{2'3} + C_4C_5S_{2'3}) + S_4S_6S_{2'3} \quad (32.7)$$

$$r_{32} = C_6S_4S_{2'3} + S_6(S_5C_{2'3} + C_4C_5S_{2'3}) \quad (32.8)$$

$$r_{33} = C_5C_{2'3} - C_4S_5S_{2'3} \quad (32.9)$$

The X, Y, and Z position coordinates of the IRB140 robot relative to the base frame are computed as follows:

$$X = C_1a_1 + d_6(C_5C_1S_{2'3} - S_5(S_1S_4 - C_4C_1C_{2'3})) + d_4C_1S_{2'3} - C_1C_2a_2 \quad (33)$$

$$Y = S_1a_1 + d_6(C_5S_1S_{2'3} - S_5(C_4S_1C_{2'3} + C_1S_4)) + d_4S_1S_{2'3} - C_2S_1a_2 \quad (34)$$

$$Z = d_1 + d_4C_{2'3} + a_2S_2 + d_6(C_5C_{2'3} - C_4S_5S_{2'3}) \quad (35)$$

C_i and S_i stand for the cosine and sine of the joint angle q_i.

C_{ij} and S_{ij} stand for the cosine and sine of the sum $q_i + q_j$.

There are generally two approaches to solving inverse kinematics, analytical and geometrical. The Pieper solution is selected in the present case because of its simplicity and ease of implementation. For q_1, q_2, and q_3, which define the end-effector position in space, a geometrical approach is implemented to determine the joint variables. An analytical solution is then applied to calculate angles q_4, q_5, and q_6, which define the end-effector orientation [213]. According to Figure 8, robot frame assignments, 0 and 1 have the same x and y axes, having different offsets only in the z-direction. Therefore, the wrist component projections will be the same on frames 0 and 1 [214, 215]. To obtain the first joint angle q_1, the arctangent function is used, which gives two solutions:

$$q_1 = atan2(p_y, p_x),\ q_1' = \pi + q_1 \quad \text{(two possible answers)} \qquad (36)$$

Since the second and third links are planar, changes in the position vector in the y-axis direction only concern q_1. The solutions for q_2 and q_3 are obtained by considering Figure 9:

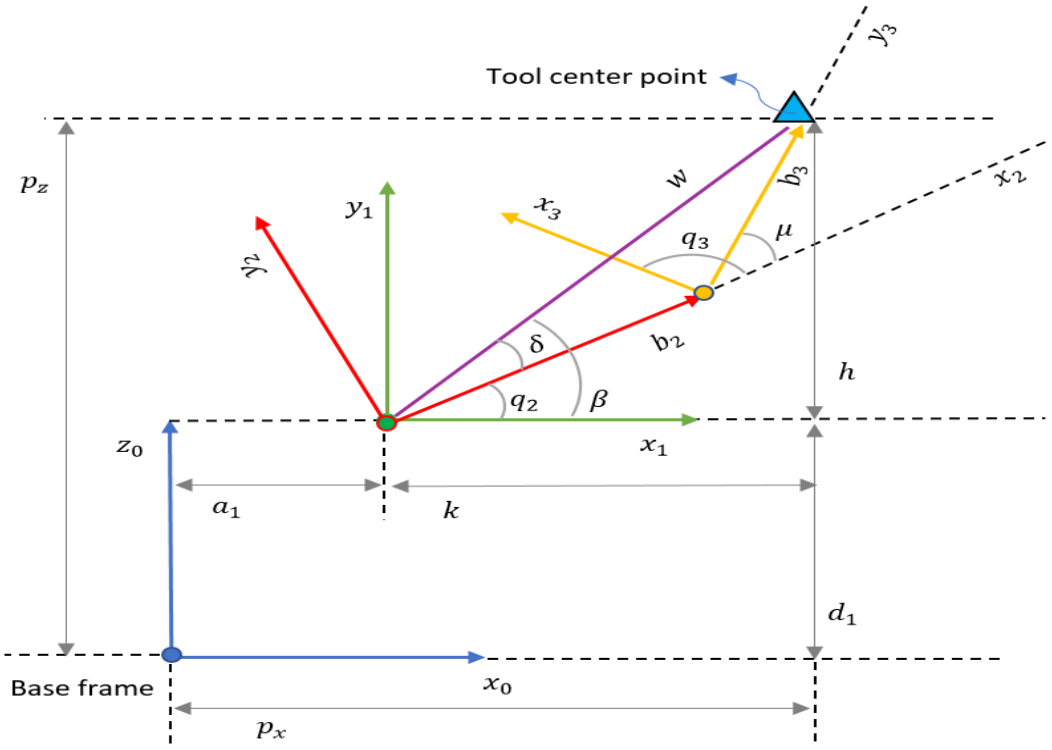

Figure 9**:** Projection of the second and third links on the x–y plane of the tool center point.

The value of q_3 is obtained by applying the cosine law:

$$w^2 = b_2^2 + b_3^2 - 2b_2b_3\cos(180 - \mu) \quad (37)$$

$b_3 = d_4 + d_6$ (d_6 is the distance from joint 6 to the tool center point)

$$b_2 = a_2 \quad (38)$$

$$w^2 = h^2 + k^2 \quad (39)$$

$$cos\,(180 - \mu) = -\,cos\,(\mu) \quad (40)$$

$$h^2 + k^2 = a_2^2 + (d_4 + d_6)^2 + 2a_2(d_4 + d_6)\cos\,(\mu) \quad (41)$$

$$\cos\,(\mu) = h^2 + k^2 - a_2^2 - (d_4 + d_6)^2/2a_2(d_4 + d_6) \quad (42)$$

The values of h and k in terms of the tool center point (p_x, p_y, p_z) and q_1 are as follows:

$$h = p_z - d_1 \quad (43)$$

$$k = \pm\,[(p_z - a_1\cos(q_1))^2 + (p_y - a_1\sin(q_1))^2]^{1/2} \quad (44)$$

$$\cos(\mu) = (p_z - d_1)^2 + (p_x - a_1\cos(q_1))^2 + (p_y - a_1\sin(q_1))^2 - a_2^2 - (d_4 + d_6)^2/2a_2(d_4 + d_6) \quad (45)$$

$$\sin(\mu) = \pm(1 - cos^2\,(\mu))^{1/2} \quad (46)$$

$$\mu = atan2(\sin\mu \;\; \cos\mu) \quad (47)$$

Finally, $q_3 = -\,(\frac{\pi}{2} + \mu)$ rotation occurs in the opposite direction (four possible answers).

Using similar trigonometric relationships to solve q_2:

$$q_2 = \beta - \delta \quad (48)$$

$$\beta = atan2(h, k) \tag{49}$$

$$\delta = atan2((d_4 + d_6)sin\mu\,, a_2 + (d_4 + d_6)cos\mu) \tag{50}$$

$$q_2 = atan2(h, k) - atan2((d_4 + d_6)sin\mu\,,\ a_2 + (d_4 + d_6)cos\mu) \tag{51}$$

Substituting the values of *h* and *k* gives:

$$q_2 = atan2[(p_z - d_1), 1), \pm ((p_z - a_1\cos(q_1))^2 + (p_y - a_1\sin(q_1))^2]^{1/2} - atan2((d_4 + d_6)sin\mu, a_2 + (d_4 + d_6)cos\mu) \tag{52}$$

$$q_2 = -((\beta - \delta) - \frac{\pi}{2}) \quad \text{(eight possible answers)} \tag{53}$$

Joint angles q_4, q_5, and q_6, corresponding to the wrist section of the manipulator, define the orientation of the end effector. Euler's formula determines these angles in the following inverse kinematics solution. We need a transformation matrix (^3_6R) between joints 3 and 6.

The Z-Y-X Euler rotation will take an axis whose location depends on the previous rotation. Furthermore, we must describe this tool's frame rotation relative to the global frame. The Euler angles and their corresponding equations are given below [204].

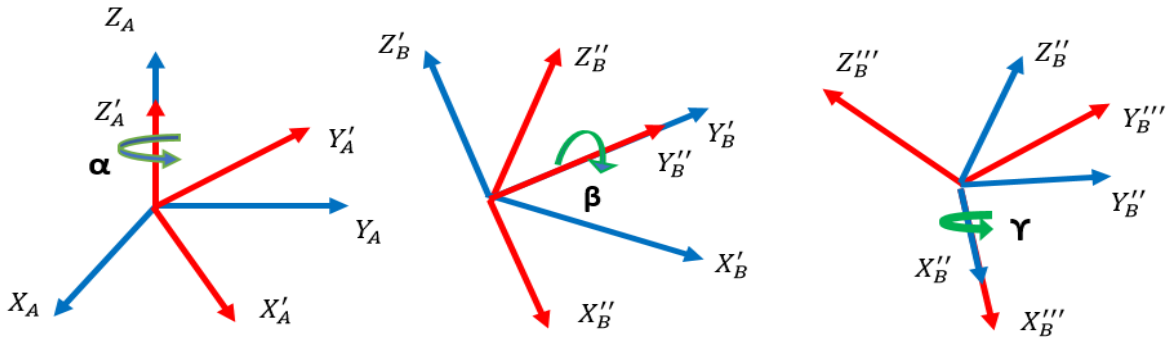

Figure 10: Z-Y-X Euler rotations of the distal joints.

For final rotation

$$ {}^{0}_{6}R = R_{z',y',x'} = R_z(\alpha)\, R_y(\beta)\, R_x(\gamma) \tag{54.1} $$

$$ {}^{0}_{6}R = \begin{pmatrix} c_\alpha & -s_\alpha & 0 \\ s_\alpha & c_\alpha & 0 \\ 0 & 0 & 1 \end{pmatrix} X \begin{pmatrix} c_\beta & 0 & s_\beta \\ 0 & 1 & 0 \\ -s_\beta & 0 & c_\beta \end{pmatrix} X \begin{pmatrix} 1 & 0 & 0 \\ 0 & c_\gamma & -s_\gamma \\ 0 & s_\gamma & c_\gamma \end{pmatrix} \tag{54.2} $$

$R_z(\alpha)$ is rotation around axis z by the α

$R_y(\beta)$ is rotation around axis y by the β

$R_x(\gamma)$ is rotation around axis x by the γ

$$ {}^{0}_{6}R = \begin{pmatrix} c_\alpha c_\beta & c_\alpha s_\beta s_\gamma - s_\alpha c_\gamma & c_\alpha s_\beta c_\gamma + s_\alpha s_\gamma \\ s_\alpha c_\beta & s_\alpha s_\beta s_\gamma + c_\alpha c_\gamma & s_\alpha s_\beta c_\gamma - c_\alpha s_\gamma \\ -s_\beta & c_\beta s_\gamma & c_\beta c_\gamma \end{pmatrix} \tag{55} $$

With reference to the forward kinematics equations:

$$ {}^{0}_{3}R = \begin{pmatrix} c_1 c_{23} & -c_1 s_{23} & -s_1 \\ s_1 c_{23} & -s_1 s_{23} & c_1 \\ -s_{23} & -c_{23} & 0 \end{pmatrix} \tag{56.1} $$

$$ {}^{3}_{6}R = \left({}^{0}_{3}R \right)^{T} {}^{0}_{6}R \tag{56.2} $$

$$ {}^{3}_{6}R = \begin{pmatrix} c_1 c_{23} & -s_1 c_{23} & -s_{23} \\ -c_1 s_{23} & -s_1 s_{23} & -c_{23} \\ -s_1 & c_1 & 0 \end{pmatrix} x \begin{pmatrix} c_\alpha c_\beta & c_\alpha s_\beta s_\gamma - s_\alpha c_\gamma & c_\alpha s_\beta c_\gamma + s_\alpha s_\gamma \\ s_\alpha c_\beta & s_\alpha s_\beta s_\gamma + c_\alpha c_\gamma & s_\alpha s_\beta c_\gamma - c_\alpha s_\gamma \\ -s_\beta & c_\beta s_\gamma & c_\beta c_\gamma \end{pmatrix} \tag{57.1} $$

$$ {}^{3}_{6}R = \begin{pmatrix} A_{11} & A_{12} & A_{13} \\ A_{21} & A_{22} & A_{23} \\ A_{31} & A_{32} & A_{33} \end{pmatrix} \tag{57.2} $$

On the other hand, for frames 4, 5, and 6, the Euler angle can be considered a Z-Y-Z set. The transform matrix (^3_6R) for this set will be found as follows:

$$R_{z'y'x'} = {}^3_6R = R_z(\alpha)R_y(\beta)R_x(\gamma) \tag{58.1}$$

$$^3_6R = \begin{pmatrix} c_\alpha & -s_\alpha & 0 \\ s_\alpha & c_\alpha & 0 \\ 0 & 0 & 1 \end{pmatrix} X \begin{pmatrix} c_\beta & 0 & s_\beta \\ 0 & 1 & 0 \\ -s_\beta & 0 & c_\beta \end{pmatrix} X \begin{pmatrix} c_\gamma & -s_\gamma & 0 \\ s_\gamma & c_\gamma & 0 \\ 0 & 0 & 1 \end{pmatrix} \tag{58.2}$$

$$^3_6R = \begin{pmatrix} c_\alpha c_\beta c_\gamma - s_\alpha s_\gamma & -c_\alpha c_\beta s_\gamma - s_\alpha c_\gamma & c_\alpha s_\beta \\ s_\alpha c_\beta c_\gamma + c_\alpha s_\gamma & -s_\alpha c_\beta s_\gamma + c_\alpha c_\gamma & s_\alpha s_\beta \\ -s_\beta c_\gamma & s_\beta s_\gamma & c_\beta \end{pmatrix} \tag{59}$$

Where ^3_6R is given above as matrix (57.2) and can be considered as follows:

$$^3_6R = \begin{pmatrix} A_{11} & A_{12} & A_{13} \\ A_{21} & A_{22} & A_{23} \\ A_{31} & A_{32} & A_{33} \end{pmatrix}$$

As a result, the solution for q_4, q_5, and q_6 will be:

$$q_5 = \beta = \text{atan2}\left(+\sqrt{A_{31}^2 + A_{32}^2}\ ,\ A_{33}\right) \tag{60}$$

$$q_4 = \alpha = \alpha\text{tan2}\left(\frac{A_{32}}{s_\beta}, \frac{-A_{31}}{s_\beta}\right) \tag{61}$$

$$q_6 = \gamma = \alpha\text{tan2}\left(\frac{A_{23}}{s_\beta}\ ,\ \frac{A_{13}}{s_\beta}\right) \tag{62}$$

$$q_5' = \beta' = \text{atan2}\left(-\sqrt{A_{31}^2 + A_{32}^2}\ ,\ A_{33}\right) \text{ or } q_5' = -q_5 \tag{63}$$

$$q_4^{'} = \alpha^{'} = \alpha\tan2\left(\frac{A_{32}}{s_\beta^{'}}\ ,\ \frac{-A_{31}}{s_\beta^{'}}\right) \text{ or } q_4^{'} = 180 + q_4 \tag{64}$$

$$q_6^{'} = \gamma = \alpha\tan2\left(\frac{A_{23}}{s_\beta^{'}}\ ,\ \frac{A_{13}}{s_\beta^{'}}\right) \text{ or } q_6^{'} = 180 + q_6 \tag{65}$$

$q_4 = \alpha$ = rotation of axis 4

$q_5 = \beta$ = rotation of axis 5

$q_6 = \gamma$ = rotation of axis 6

If $\beta = q_5 = 0$ or $q_5 = \beta = 180°$ then $q_5 = \beta$ and $q_6 = \gamma$ (will be in a parallel configuration)

If $\beta = q_5 = 0$, as result $q_4 = \alpha = 0$, and finally $q_6 = \gamma = atan2\ (-A_{12}\ ,\ A_{11})$

If $\beta = q_5 = 180°$, as result $q_4 = \alpha = 0$, and finally $q_6 = \gamma = atan2\ (A_{12}, -A_{11})$

The inertial data and mass center position for our purposes are obtained via 3D CAD modeling software (SolidWorks) for the detailed, semi-detailed (rectangular) and simplified models, which consider factors such as geometry, the density of each link (assumed to be uniform in all models), their significant values related to mass and other physical properties such as mass center position and inertia matrices represented in their respective reference frames for the three proximal links.

$$^1p_{c1} = \begin{bmatrix} x_{c1} \\ y_{c1} \\ z_{c1} \end{bmatrix},\ ^2p_{c2} = \begin{bmatrix} x_{c2} \\ y_{c2} \\ z_{c2} \end{bmatrix},\ ^3p_{c3} = \begin{bmatrix} x_{c3} \\ y_{c3} \\ z_{c3} \end{bmatrix} \tag{66}$$

$$^1I_1 = \begin{bmatrix} I_{xx1} & I_{xy1} & I_{xz1} \\ I_{xy1} & I_{yy1} & I_{yz1} \\ I_{xz1} & I_{yz1} & I_{zz1} \end{bmatrix},\ ^2I_2 = \begin{bmatrix} I_{xx2} & I_{xy2} & I_{xz2} \\ I_{xy2} & I_{yy2} & I_{yz2} \\ I_{xz2} & I_{yz2} & I_{zz2} \end{bmatrix},\ ^3I_3 = \begin{bmatrix} I_{xx3} & 0 & I_{xz3} \\ 0 & I_{yy3} & I_{yz3} \\ I_{xz3} & I_{yz3} & I_{zz3} \end{bmatrix} \tag{67}$$

so that ${}^{i}p_{ci}$ is the mass center position of each link and ${}^{i}I_{i}$ are inertia matrices.

Assuming a constant and homogeneous density, a comparative estimate of the mass of each link is possible. The volume of each link is determined using SolidWorks software. The relationship of an element's volume to the robot's total volume is multiplied by the total mass to give a supposed link mass value.

Position vectors ${}^{j-1}\mathbf{p}_{i}^{*}$ calculated from the origin of the link frame j-1 to the mass center of link i, expressed in the base reference frame, and unit vectors that point to rotation axes $\mathbf{z}_{j-1}$ for the three proximal links of the robotic arm, are obtained as follows [211]:

$$ {}^{0}\mathbf{p}_{c1}^{*} = {}^{0}p_{1} + \left[{}^{0}R_{1} \right] {}^{1}p_{c1}, \tag{68.1} $$

$$ {}^{1}\mathbf{p}_{c2}^{*} = \left[{}^{0}R_{1} \right] {}^{1}p_{2} + \left[{}^{0}R_{1}\,{}^{1}R_{2} \right] {}^{2}p_{c2}, \tag{68.2} $$

$$ {}^{0}\mathbf{p}_{c2}^{*} = {}^{0}p_{2} + \left[{}^{0}R_{1}\,{}^{1}R_{2} \right] {}^{2}p_{c2}, \tag{68.3} $$

$$ {}^{2}\mathbf{p}_{c3}^{*} = \left[{}^{0}R_{1}\,{}^{1}R_{2} \right] {}^{2}p_{3} + \left[{}^{0}R_{1}\,{}^{1}R_{2}\,{}^{2}R_{3} \right] {}^{3}p_{c3}, \tag{68.4} $$

$$ {}^{1}\mathbf{p}_{c3}^{*} = \left[{}^{0}R_{1} \right] {}^{1}p_{3} + \left[{}^{0}R_{1}\,{}^{1}R_{2}\,{}^{2}R_{3} \right] {}^{3}p_{c3}, \tag{68.5} $$

$$ {}^{0}\mathbf{p}_{c3}^{*} = {}^{0}p_{3} + \left[{}^{0}R_{1}\,{}^{1}R_{2}\,{}^{2}R_{3} \right] {}^{3}p_{c3}, \tag{68.6} $$

$$ \mathbf{z}_{0} = \begin{bmatrix} 0 & 0 & 1 \end{bmatrix}, \tag{69.1} $$

$$ \mathbf{z}_{1} = \left[{}^{0}R_{1} \right] z_{0}, \tag{69.2} $$

$$ \mathbf{z}_{2} = \left[{}^{0}R_{1}\,{}^{1}R_{2} \right] z_{0} \tag{69.3} $$

The following Jacobian submatrices $\mathbf{J_{vi}}$ and $\mathbf{J_{wi}}$ for the proximal links express the partial rate of change of the linear velocities of the mass centers and angular velocities of each link [210]:

$$J_{v1} = \begin{bmatrix} | & 0 & 0 & 0 & 0 \\ \mathbf{z}_0 \times {}^0\mathbf{p}^*_{c1} | & 0 & 0 & 0 & 0 \\ | & 0 & 0 & 0 & 0 \end{bmatrix}, \quad (70.1) \qquad J_{\omega 1} = \begin{bmatrix} | & 0 & 0 & 0 & 0 \\ \mathbf{z}_0 | & 0 & 0 & 0 & 0 \\ | & 0 & 0 & 0 & 0 \end{bmatrix}, \quad (70.2)$$

$$J_{v2} = \begin{bmatrix} | & | 0 & 0 & 0 \\ \mathbf{z}_0 \times {}^0\mathbf{p}^*_{c2} | \mathbf{z}_1 \times {}^1\mathbf{p}^*_{c2} | & 0 & 0 & 0 \\ | & | 0 & 0 & 0 \end{bmatrix}, \quad (70.3) \qquad J_{\omega 2} = \begin{bmatrix} | & | 0 & 0 & 0 \\ \mathbf{z}_0 | \mathbf{z}_1 | & 0 & 0 & 0 \\ | & | 0 & 0 & 0 \end{bmatrix}, \quad (70.4)$$

$$J_{v3} = \begin{bmatrix} | & | & | & 0 & 0 \\ \mathbf{z}_0 \times {}^0\mathbf{p}^*_{c3} | \mathbf{z}_1 \times {}^1\mathbf{p}^*_{c3} | \mathbf{z}_2 \times {}^2\mathbf{p}^*_{c3} | & 0 & 0 \\ | & | & | & 0 & 0 \end{bmatrix}, \quad (70.5) \qquad J_{\omega 3} = \begin{bmatrix} | & | & | & 0 & 0 \\ \mathbf{z}_0 | \mathbf{z}_1 | \mathbf{z}_2 | & 0 & 0 \\ | & | & | & 0 & 0 \end{bmatrix} \quad (70.6)$$

The following matrices I_i correspond to the inertia tensors of the proximal links over their mass centers and are expressed relative to the base reference frame [216]:

$$I_1 = \left[{}^0R_1 \right] {}^1I_1 + \left[{}^0R_1 \right]^T, \quad (71.1)$$

$$I_2 = \left[{}^0R_1 \, {}^1R_2 \right] {}^2I_2 \left[{}^0R_1 \, {}^1R_2 \right]^T, \quad (71.2)$$

$$I_3 = \left[{}^0R_1 \, {}^1R_2 \, {}^2R_3 \right] {}^3I_3 \left[{}^0R_1 \, {}^1R_2 \, {}^2R_3 \right]^T \quad (71.3)$$

In the dynamic analysis of this manipulator, friction in joints was not considered. For the tracking of a path, the vector of generalized forces was deemed to be shown below:

$$\sum_{j=1}^{n} M_{ij}\ddot{q}_j + V_i + G_i = Q_i = \tau_i \quad \text{para} \quad i = 1, 2, ..., n. \quad (72)$$

The first term in the equation represents the inertial forces, the second term centrifugal and Coriolis forces, and the third term gravitational forces. This equation may be written as follows [211]:

$$M\ddot{q} + V + G = Q. \tag{73}$$

So that,

$$M = \sum_{i=1}^{n} \left(J_{vi}^{T} m_i J_{vi} + J_{\omega i}^{T} I_i J_{\omega i} \right), \tag{74}$$

$$V_i = \sum_{j=1}^{n} \sum_{k=1}^{n} \left(\frac{\partial M_{ij}}{\partial q_k} - \frac{1}{2} \frac{\partial M_{jk}}{\partial q_i} \right) \dot{q}_j \dot{q}_k, \tag{75}$$

$$G_i = -\sum_{j=1}^{n} m_j g^{T} J_{vj}^{i}. \tag{76}$$

The inertia matrix of the manipulator is symmetric, positive definite, and therefore always invertible [217].

3.4. CAD designs of the robot

To investigate the kinematic and dynamic behavior, the ABB IRB 140 arm industrial robot was first modeled in SolidWorks using three methods. To design the robotic arm models, referenced the dimensional and physical specifications available in the company's documents [201] and the actual model of the robot in the Mechatronics laboratory of the UQTR university were used. An accurate and detailed model is shown in Figure 11, the less detailed rectangular model in Figure 12, and the simplified model in Figure 13. SolidWorks provides the mass and inertia characteristics for the three different models of the robotic arm (mass center positions and inertia matrices). Density was assumed uniform and constant in all parts and links. Details of each model and results for the proximal links are summarized in Table 4.

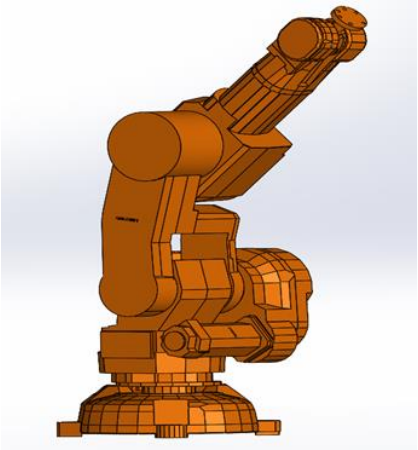

Figure 11: Detailed SolidWorks model of the ABB IRB 140 robotic arm.

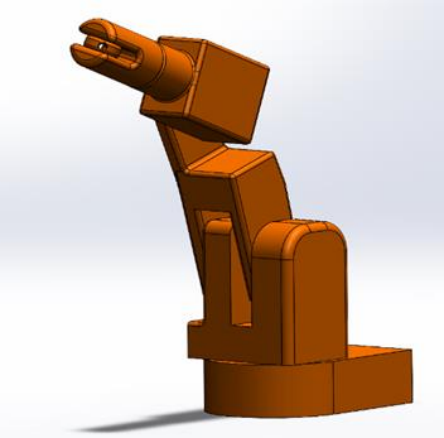

Figure 12: Semi-detailed rectangular SolidWorks model of the ABB IRB 140 robotic arm.

Figure 13: Simplified SolidWorks model of the ABB IRB 140 robotic arm.

Table 4: Mass property results of each model provided using SolidWorks software.

Links	Parameter (unit)	Detailed Model	Rectangular Model	Simplified Model
Link 1	*Weight (kg)*	35	35	35
	X_c *(mm)*	277.87	17.87	0
	Y_c	373.12	103.12	181.37
	Z_c	-199.03	-79.03	0
	I_{xx} $(kg.m^2)$	6.5	1.5	1.1
	I_{xy}	1.1	0.1	0
	I_{xz}	3.05	0.05	0
	I_{yy}	2.02	0.002	0
	I_{yz}	5.07	0.07	0.1e-5
	I_{zz}	1.4	0.04	1.1
Link 2	*Weight (kg)*	25	25	25
	X_c *(mm)*	218.29	178.29	0
	Y_c	229.73	9.73	255.24
	Z_c	112.43	72.43	0
	I_{xx} $(kg.m^2)$	0.9	0.1	1.6
	I_{xy}	-0.03	-0.03	0.1e-5
	I_{xz}	0.1	0.01	0
	I_{yy}	1.3	0.03	0
	I_{yz}	-0.01	-0.01	0
	I_{zz}	0.95	0.05	1.6
Link 3	*Weight (kg)*	18	18	18
	X_c *(mm)*	-24.56	14.56	0
	Y_c	-219.96	-199.96	195.69
	Z_c	-25.86	-15.86	0
	I_{xx} $(kg.m^2)$	2.5	1.5	0.6
	I_{xy}	-0.001	-0.001	0.3e-5
	I_{xz}	0.09	0.09	0
	I_{yy}	2.7	0.7	0
	I_{yz}	-0.8	-0.02	0
	I_{zz}	0.5	0.2	0.6

3.5. Evaluation of robot performance

To evaluate the predictive skill of the three models, we focused on energy consumption by the three proximal joints and total energy consumption by the robot over the same time and path of movement. In the proposed modeling, it is possible to calculate energy consumption by each joint at a specific time using joint torque and angular velocity with equation (77). The integrated energy consumption by the robot is presumed to be the sum of all energy consumption by the joints.

$$E_i = \int_{t_0}^{t_f} \tau_i\,(t).\,\dot{q}_i(t)\,dt \qquad (77)$$

3.6. Control Strategy - Sliding Mode Control (SMC)

One method of robust control technique for controlling a complicated and nonlinear mechanism like a manipulator robotic arm is called sliding mode control (SMC) methodology, a type of variable structure control system (VSCS). The most crucial feature of the sliding mode control is the complete insensitivity to parametric uncertainty and external disturbances during the sliding process. The VSCS utilizes a high-speed switching control law to perform two purposes. First of all, it forces the nonlinear system's form trajectory along a user-defined surface in the state space, named the sliding or switching surface [218]. The control approach has one gain if the state trajectory of the mechanism is above the surface and a different gain if the controlling object, such as trajectory in robotics, drops below the surface, and because of this named sliding surface. Secondly, it keeps the mechanism state control object on this surface by following the time [219]. During the controlling process, the control system's structure differs from one to another, and thus it donates the name variable structure control. This model also permits the elimination of

interactions among the joints of the manipulator. A general equation of the motion can represented in the space state by [210]:

$$\dot{x} = f(x,t) + g(x,t).u \quad (78)$$

Where u is the control input, x is the output, and the functions f (x , t) and g(x, t) are nonlinear functions.

The control input variable is :

$$u_i(x,t) = \begin{cases} u_i^+(x,t) & if \ S_i(x,t) > 0 \\ u_i^-(x,t) & if \ S_i(x,t) < 0 \end{cases} \quad (79)$$

Where u_i, is the ith component of u , and $S_i(x,t) = 0$ is the ith component switching hypersurfaces $S(x, t) = 0$, $S \in R^m$.

According to the presented rules with discontinuous control, the system is named a variable structure system since the controller switches alternatively based on the state of the mechanism. The sliding mode appears on a switching surface S(X) = 0, which pushes the machine to behave Type equation here.as a linear time uniform system, which can be assumed to be stable. For to be linear, the surfaces can be written as :

$$s_i(x) = x_n + \sum_{i=1}^{n} \lambda_i . x_i \quad (80)$$

The condition for the sliding mode to exist on the ith surface is provided by the following equation:

$$\lim_{s_i \to 0^+} \dot{S} < 0 \quad \text{and} \quad \lim_{s_i \to 0^-} \dot{S} > 0 \quad (81)$$

Which is the $S\dot{S} < 0$ too close of $S_i(x) = 0$, when all the trajectories shift towards the switching surface. In the perfect sliding mode on S_i the related control is the equal control issued from the equation (78) and given by the equation for $\dot{S} = 0$:

$$u_{eq} = g^{-1}(x,t)[\dot{x}(t) - f(x,t)] \quad (82)$$

So, the discontinuous control input presented in relation (79) can note as follow:

$$u_i = \begin{cases} u_{ieq}^{*} + \Delta u_i^{+} & if \;\; S_i > 0 \\ u_{ieq}^{*} + \Delta u_i^{-} & if \;\; S_i < 0 \end{cases} \quad (83)$$

Where u_{eq} illustrates the low-frequency, and Δu presented the high-frequency discontinuous term. For the functional case, the control equation is known by evaluated value due to error modelling and variation of the parameters as follows:

$$u_{eq}^{*} = u_{eq} + \Delta u_{eq} \quad (84)$$

The formula equivalent to discontinuous control input in (83), the term high frequency Δu can be represented differently, such as the equation based on the Classical Reaching Law, it's one of the methods reported in the literature for alleviating chattering in sliding mode [220]. Classical reaching law can express in four principal subcategories that are represented as the following:

Constant reaching law:

$$\dot{s} = -\varepsilon . sgn(s) \quad , \qquad \varepsilon > 0 \quad (85)$$

Exponential reaching law:

$$\dot{s} = -\varepsilon . sgn(s) \; - ks \quad , \qquad \varepsilon > 0 \qquad k > 0 \quad (86)$$

Power rate reaching law:

$$\dot{s} = -k \, |s^{\alpha}| . sgn(s) \quad , \qquad 0 < \; \alpha < 1 \qquad k > 0 \quad (87)$$

General reaching law:

$$\dot{s} = -\varepsilon . sgn(s) - f(s) \quad , \qquad \varepsilon > 0 \quad \text{where f(0)=0 and sf(s)>0 when s}\neq 0 \quad (88)$$

To obtain a robust sliding mode control based on reaching law, considering general equation motion as below:

$$\ddot{x} = f(x) + g(x)u + d(t) \quad (89)$$

where f(x) and g(x) are unknown equation and g(x)>0 and d(t) is the term of disturbance.

As sliding surface and derivative of the sliding surface, the combination of error of models and considering satisfy the Hurwitz condition can describe as follows:

$$s = \dot{e} + ce \quad , \quad c > 0$$

$$e = r - x(t)$$

$$\dot{e} = \dot{r} - \dot{x}(t) \quad (90)$$

For the derivative of the sliding surface equation considering the effect of external disturbance as d(t),

$$\dot{s} = \ddot{e} + c\dot{e} = \ddot{r} - \ddot{x} + c(\dot{r} - \dot{x}) = \ddot{r} - f(x) - g(x)u - d(t) + c(\dot{r} - \dot{x}) \quad (91)$$

In order to obtain the robust control sliding mode based on exponential reaching law, from relations of (86) and (91):

$$\ddot{r} - f(x) - g(x)u - d(t) + c(\dot{r} - \dot{x}) = -\varepsilon.sgn(s) - ks$$

$$u = \frac{1}{g(x)}(\ddot{r} - f(x) - d(t) + c(\dot{r} - \dot{x}) + \varepsilon.sgn(s) + ks \quad (92)$$

Derivative of the sliding surface equation also can be with considering (91) described with the disturbances term as follow:

$$\dot{s} = -\varepsilon.sgn(s) - ks + d_c - d \quad (93)$$

The disturbance term d_c must satisfy the conditions for reaching the sliding surface, and the term d should be limited. dl and du are lower and upper term of disturbance, respectively as:

$d_l \leq d(t) \leq d_u$

when s(t)> 0 , $\dot{s} = \varepsilon - ks + d_c - d$ we want $\dot{s}$(t)<0 , so let $d_c = d_l$

when s(t)< 0 , $\dot{s} = -\varepsilon - ks + d_c - d$ we want $\dot{s}$(t)>0 , so let $d_c = d_u$

there for, if we define $d_1 = \frac{d_u - d_l}{2}$, $d_2 = \frac{d_u + d_l}{2}$, then we can get,

$$d_c = d_2 - d_1 . sgn(s) \quad (94)$$

The discontinuity of the sign function will generate chattering in the closed loop system. for this reason, the sign function is usually substituted by a saturation function sat (s/ε), where sat(.) is described as follows:

$$sat(x) = \begin{cases} x & if\ |x| \leq 1 \\ sgn\ (x) & if\ |x| > 1 \end{cases} \quad (95)$$

Employing this alternative will present a tracking error. The trade-off between the tracking error and control bandwidth will be created by setting the boundary layer properly.

As mentioned before, the position of the robot's end-effector in this case study depends on the three first joints and links. For this reason, the control strategy implements for the first three joints of the robot. Generally, for the three links, the robot's sliding mode control can describe as follows:

$s = \dot{e} + ce$

$e = \theta_d - \theta$

$$\dot{s} = \ddot{e} + c\dot{e} = \ddot{\theta_d} - \ddot{\theta} + c\dot{e} \quad (96)$$

$$\dot{s} = -\varepsilon\, sgn(s) \tag{97}$$

(96) and (97),

$$\ddot{\theta} = \ddot{\theta_d} + c\dot{e} + \varepsilon\, sgn\,(s) \tag{98}$$

The general equation of the robot relly on the dynamics of the robot described as relation (72),

$$M\ddot{\theta} + V + G = \tau$$

So that,

$$\ddot{\theta} = M^{-1}(\tau - V - G) \tag{99}$$

With relations (98) and (99), obtain the main equation of sliding mode control as follows;

$$\tau = M\left(\ddot{\theta_d} + c\dot{e} + \ \varepsilon\, sgn(s)\right) + V + G \tag{100}$$

Assuming the presence of the disturbances for the robot in the working space to determine and track of end-effector position, considering inverse kinematics and dynamics of the robot manipulator, we can achieve the following equation for controlling in the sliding mode technique:

$$M\ddot{\theta} + V + G = \tau + d$$

$$\ddot{X} = \dot{J}(\theta)\dot{\theta} + J(\theta)\ddot{\theta}$$

$$\tau = M.J^{-1}\left(\ddot{X_d} + c\dot{e} + \ \varepsilon\, sgn(s) - \dot{J}(\theta)\dot{\theta}\right) + V + G \tag{101}$$

That J is the jacobian matrix of the robot, and X is the end-effector position matrix.

Chapter Four

Results and Discussion

4. 1. Impact of simplifications on dynamics model of the robot

Based on the mass and inertia characteristics of the robot and the calculated end-effector position, orientation, velocity and acceleration and the torque of each joint in the three proximal links (the principal determinants of the end-effector position), the dynamic kinematic model of the robot developed in SolidWorks was examined in MATLAB in full detail over a 30 second interval without a payload at the effector end of the robotic arm. Forward and robot kinematic models were derived from Denavit-Hartenberg parameters, and a procedure was developed to solve the inverse kinematics. Trajectory planning was based on a fifth-order polynomial. For each rotating joint of the robot, the values in Table 2 were used to cover all possible angles. The changes in angle over time for the three proximal links are shown in Figure 14. The velocity and acceleration diagrams are shown in Figures 15 and 16. The torque variations for a position and path corresponding to a single, uninterrupted time interval are shown in Figures 17 to 19.

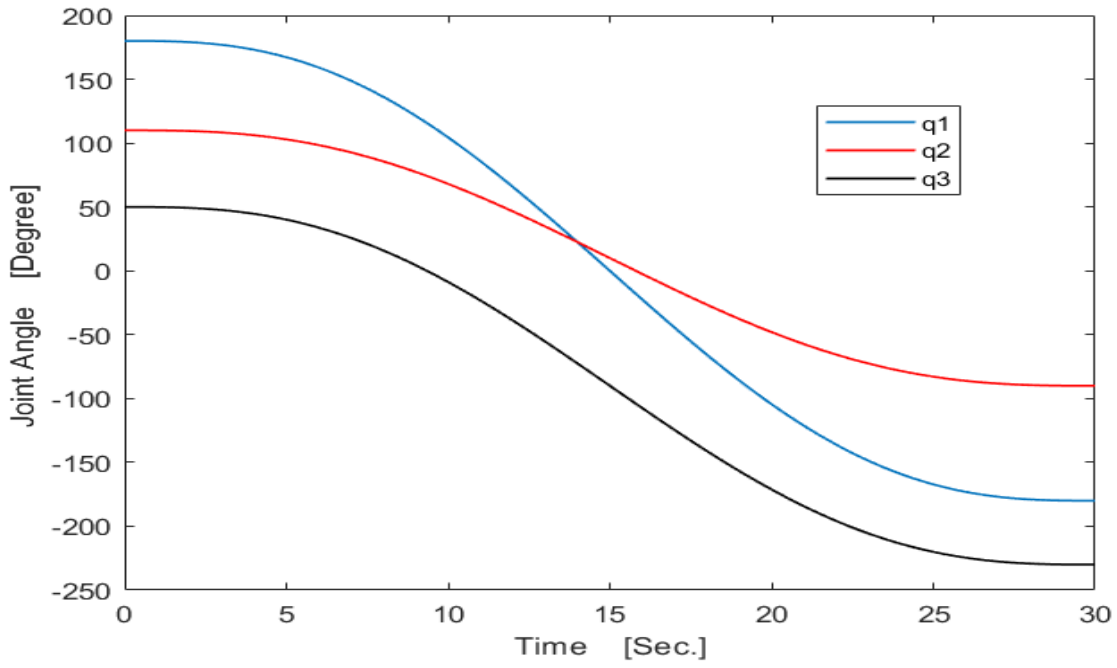

Figure 14: IRB 140 robot proximal joint angle variations.

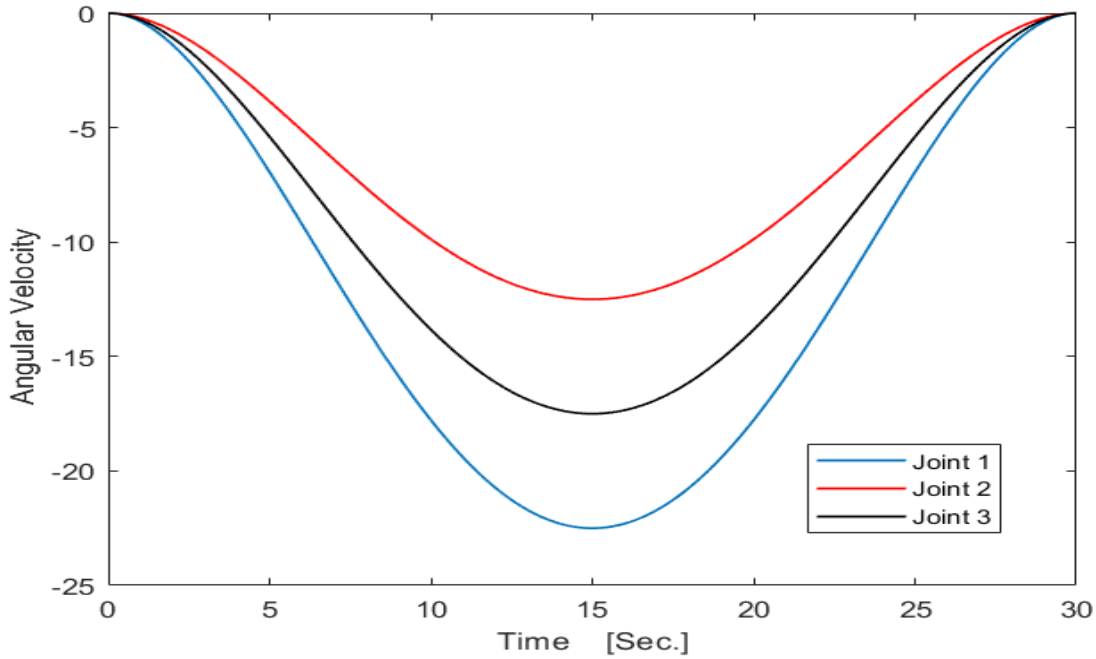

Figure 15: IRB 140 robot proximal joint angular velocity.

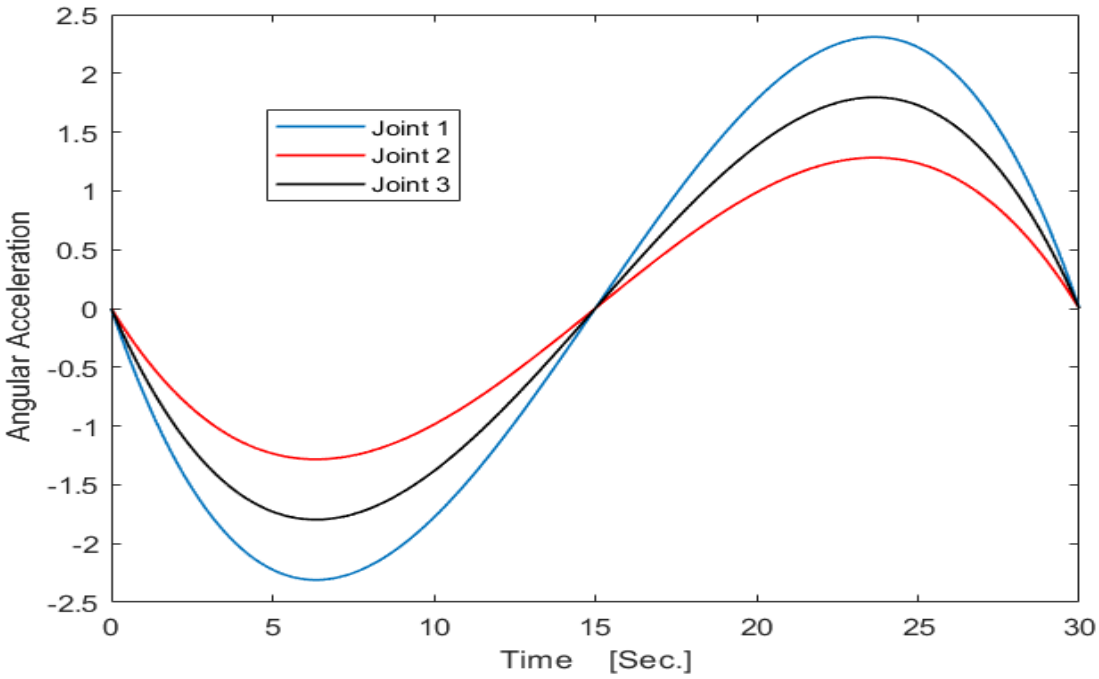

Figure 16: IRB 140 robot proximal joint angular acceleration.

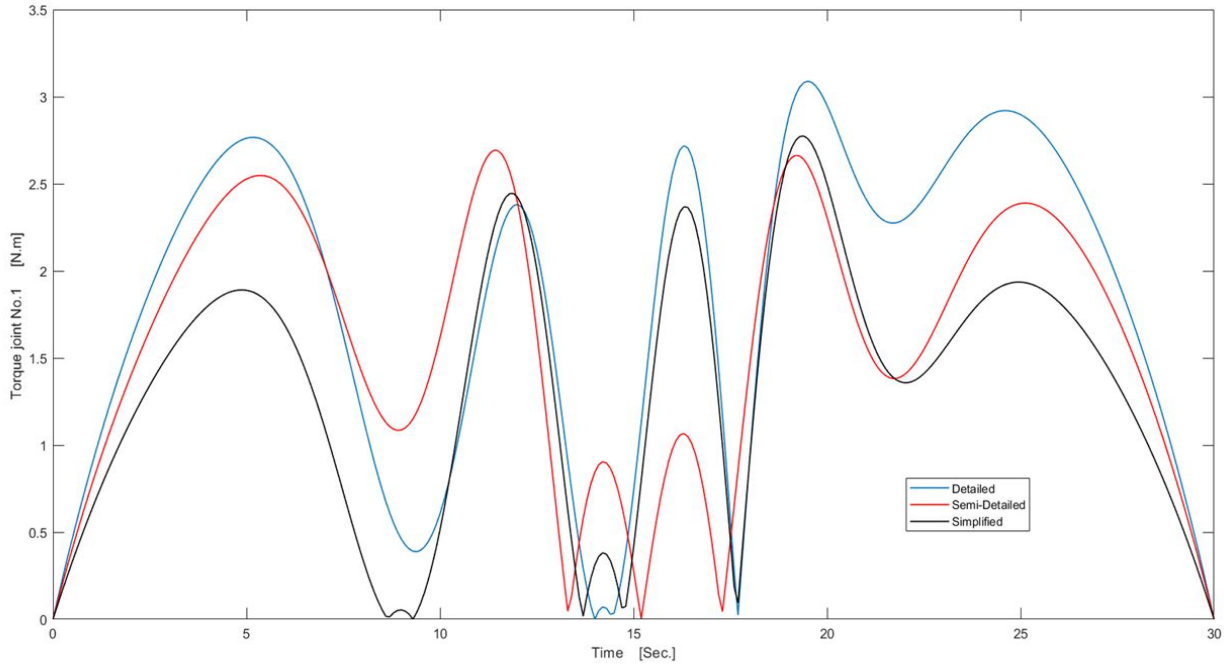

Figure 17: Torque variations for the first proximal joint of the IRB 140 robotic arm.

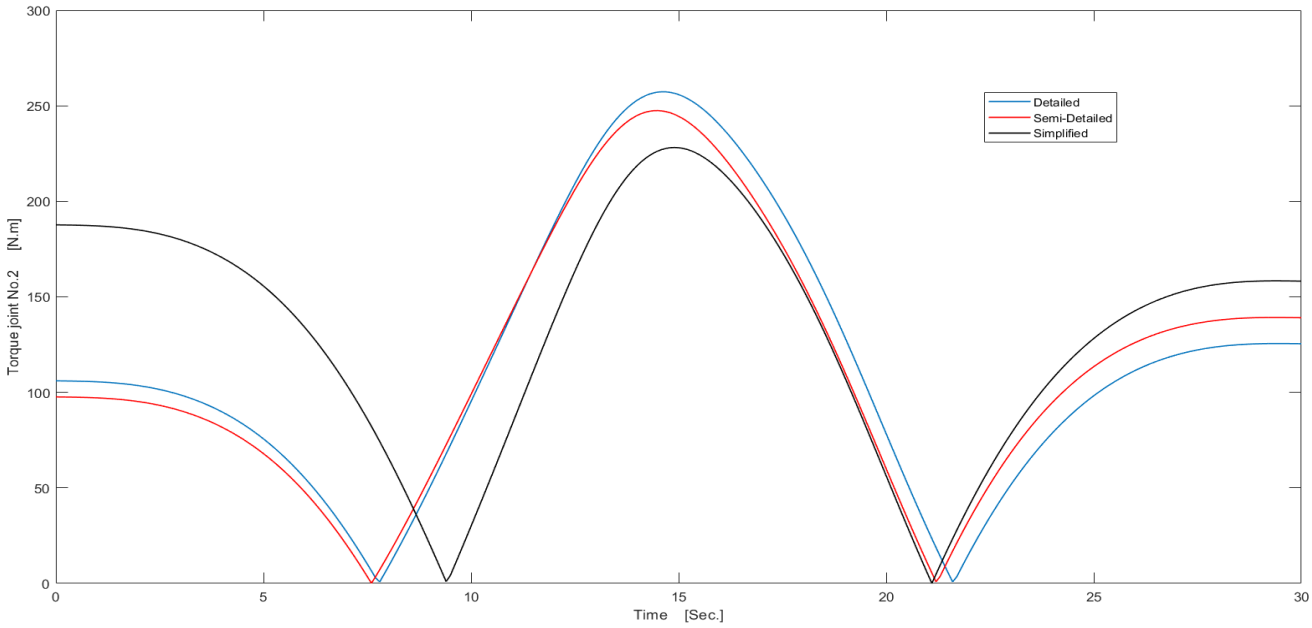

Figure 18: Torque variations for the second proximal joint of the IRB 140 robotic arm.

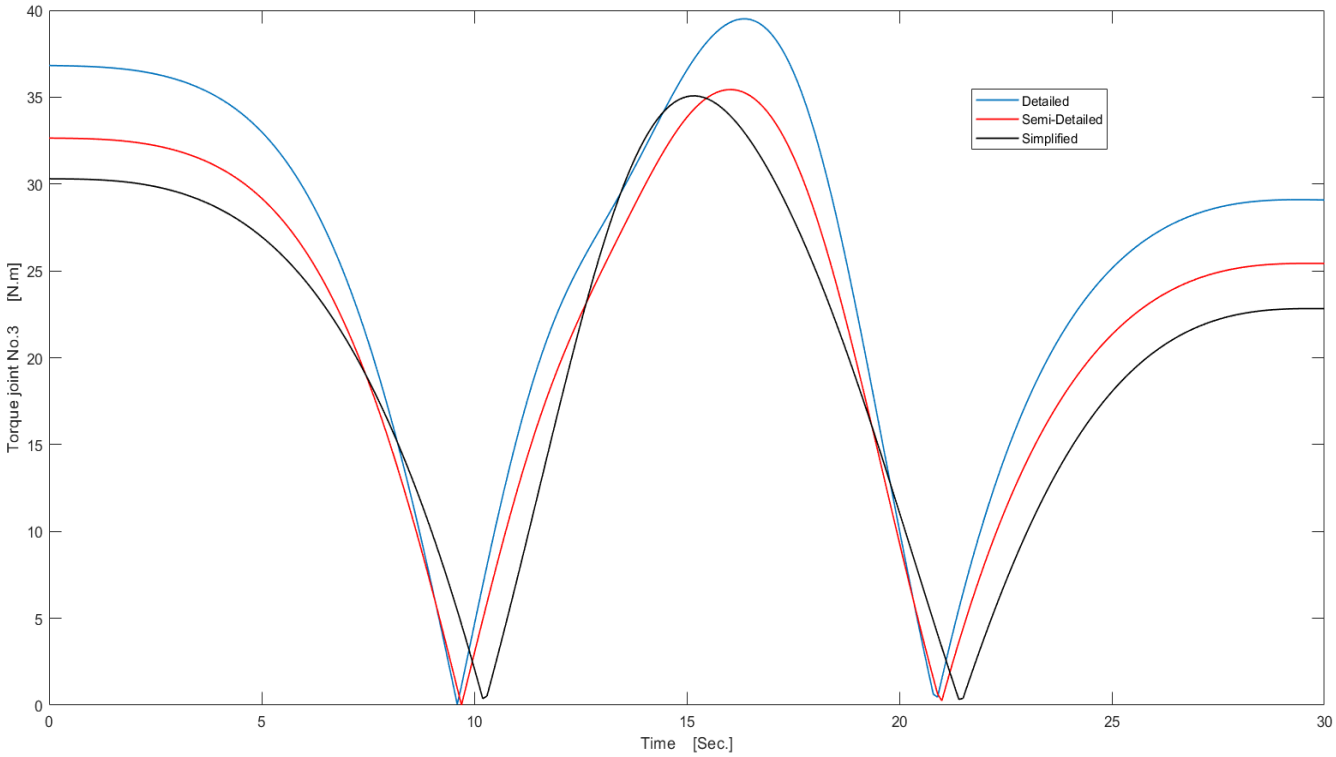

Figure 19: Torque variations for the third proximal joint of the IRB 140 robotic arm.

The results obtained for all three joints are coordinated and appear to be relatively close in the semi-detailed and simplified models. The detailed model shows higher torque for most of the time in joint 1, some of the time in joint 2, and practically all the time in joint 3. It is worth noting that the semi-detailed and simplified models both track the detailed model quite closely for at least some of the time and that this time varies from one joint to the next.

It is also clear that joint 2 experienced much more torque than the other joints. This joint provides most of the reaching capability of the robotic arm. In addition to its weight and gravitational force, the link also bears a share of the weight and gravitational force of the third link. As the robot reaches further away from the center of gravity, the mass of the remaining links creates additional torque. The bends in the torque curves are due to changes in the direction of the arm movement

based on the task path defined. In addition, these changes in direction in the defined path cause all three joints to have equal torque values at various points.

Due to the choice of a fifth-order polynomial trajectory, the joint torque curves have little or no noise in all three models. Torque starts at zero for the joint 1, rises quickly then falls back to zero smoothly overall. For joints 2 and 3, it starts at non-zero values and drops, rises to new values, and ends at other different values at the end of the path. This profile is due to the positions and movements against gravity encountered over the defined trajectory.

In the case of joints 1 and 2, the semi-detailed and simplified models show more torque than the detailed model does during some periods. The opposite is seen in general in the case of joint 3. In addition, the simplified model shows slightly less torque than the semi-detailed model at the beginning and end periods and lags the semi-detailed dynamics throughout the path. Since there is no difference in link weight and density from one model to the next, these differences in torque must reflect differences in the center of mass and inertia tensors. Differences between the torque at joint 1 and joint 2 are due likely to the effect of weight and torque imposed by other links. Both the first and second joints clearly are affected by the gravitational force of the other links, and only the third joint carries its gravitational force without much additional torque.

At the midpoint of the simulation (15 seconds), joint angular velocity has peaked, and acceleration is at its point of inflection. At this instant, link 1 is at one of its lowest torque values while the second and third joints are at their peak values. This pattern is observed for all three models and is undoubtedly related to joint acceleration and the gravitational force of the links. According to the frame assignments defined for the robotic arm, link 1 does not exert a gravitational force and only undergoes joint acceleration, and torque is therefore at its lowest value. The second and third links exert gravitational force and are subject to angular acceleration in the joints. The outcome of these

two acceleration vectors while crossing over traces the overall acceleration of these two links. When joint acceleration falls to zero, the most significant portion of the torque is expected to be gravitational, which is an opposing force resisting the movement of the robotic arm.

One of the main aims of this study is to examine how well different dynamic models predict energy consumption by each rotational joint and by the robot overall, using equation (77). These results are shown in Figure 20a - 20c (joints) and Figure 21 (robot).

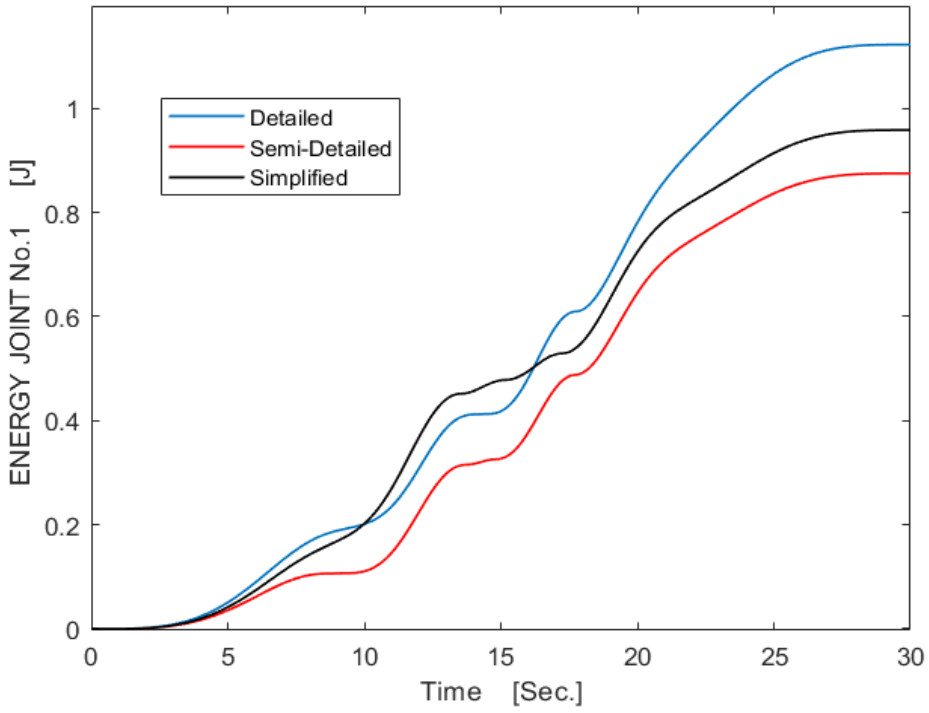

(a)

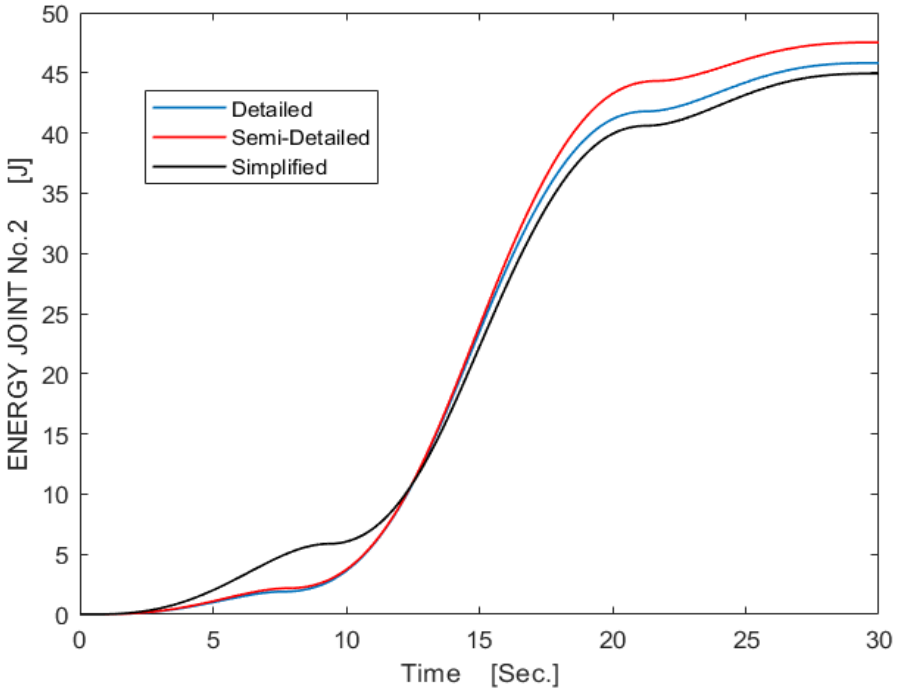
Detailed
Semi-Detailed
Simplified
ENERGY JOINT No.2 [J]
Time [Sec.]
0
5
10
15
20
25
30
35
40
45
50

(b)

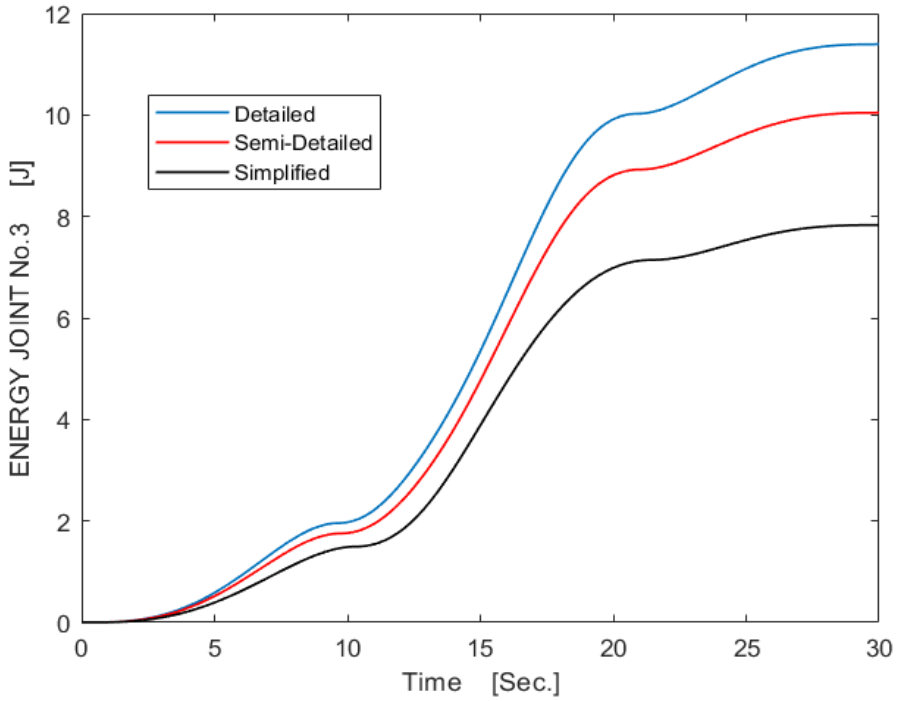
Detailed
Semi-Detailed
Simplified
ENERGY JOINT No.3 [J]
Time [Sec.]
0
2
4
6
8
10
12
0
5
10
15
20
25
30

Figure 20: Energy consumption for the joints: (a) Energy consumption by the proximal joint 1 based on three models, (b) Energy consumption by the proximal joint 2 based on three models, (c) Energy consumption by the proximal joint 3 based on three models.

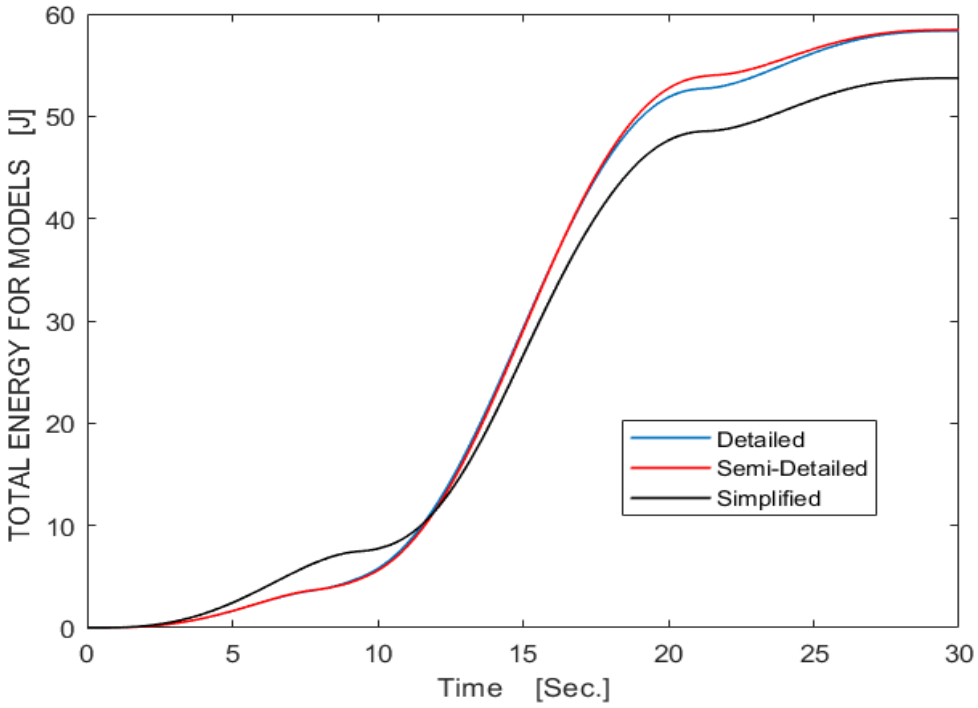

Figure 21: Energy consumption by the IRB 140 robotic arm, based on three models.

Energy consumption follows a pattern that differs in form only slightly from one joint to the next or from one model to the next. Joint 2, which has the highest torque, consumes the most energy. Over this 30-second simulation, energy consumption by the joints and by the whole robotic arm increased, but most rapidly during the middle period. The increases reflect changes in gravitational forces on the links as they move away from the initial centers of mass. Joint 2 and the arm as a whole show strikingly similar energy consumption patterns with all three models. In the case of the joint, the semi-detailed and the simplified models track each other closely, and in the case of the whole arm, the detailed and semi-detailed models do so. This may reflect the influence of the mass properties and shape characteristics of each model. The semi-detailed model gives the highest

energy consumption in both cases, whereas the simplified model gives the lowest, except for joint 1. The overall difference is 0.53% less for the detailed model and 6.8% less for the simplified model compared to the semi-detailed. Based on these results, the three dynamic models tested in this study all appear to be worthy of confidence for the prediction of energy consumption by articulated robotic arms.

4. 2. Robust controller results

The following Simulink model is employed as the Algorithm Implementation for the carried out simulation of the motion control of the robotic arm manipulator. Simulink allows creating blocks that have all of the features and capabilities of built-in any types of function, including multiple input and output ports, the ability to get vector or matrix signals of any data class supported by Simulink, real or complex signals, signal frames, the ability to operate at multiple sample rates and simple. The block function of the plant implemented all equations for the dynamic equations of motion, such as the inertia, gravity, and Coriolis Centrifugal parameters, to obtain the torque and force equation of the robot, presented in Chapter Three of this study, and the mass properties of the robot, which consist of mass center points and inertia matrixes for three different models that presented in Chapter Four of this study. A classic sliding mode controller with an approach of expositional reaching law based on the method shown in chapter Four is implemented in the controller block function, schematic diagram of the controller model is represented in figure 22.

The Sliding mode controller algorithm is used for motion control, designed basis of with and without disturbances to evaluate the model's robustness for three different robot manipulator models. The value of disturbance applied based on the sine and cosine trajectory of the joint variable is predefined as a percentage of the input signal to examine the robustness of the designed controller.

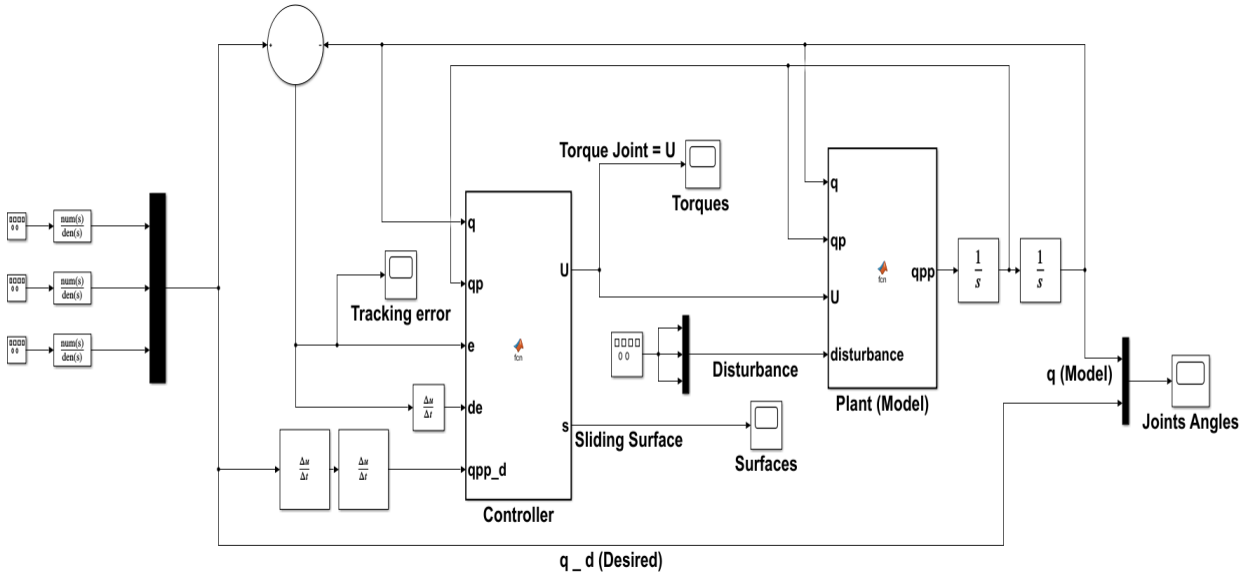

Figure 22: Simulink Model of Robot Manipulator.

The implemented algorithm examines a thorough trajectory to verify the performance and behavior of the designed sliding mode controller of the robot to execute tasks undertaking the controller. The Simulink model of the trajectory is presented in figure 23.

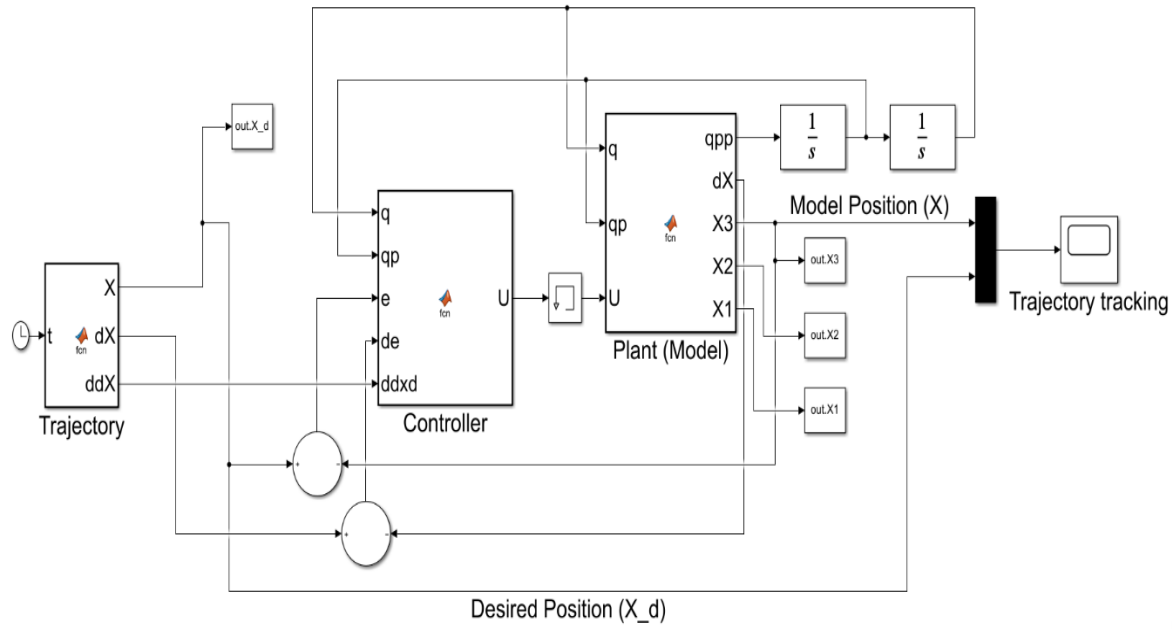

Figure 23: Simulink Trajectory Model of Robot Manipulator.

A circular trajectory is defined in the robot's working space considering avoiding singularity to perform the robot's task and estimate the chosen controller's execution. The motion of the end effector starts somewhere in the working space outside of the circular trajectory. Figures 24 and 25 present executing the assigned task of the robot under taking the SMC controller.

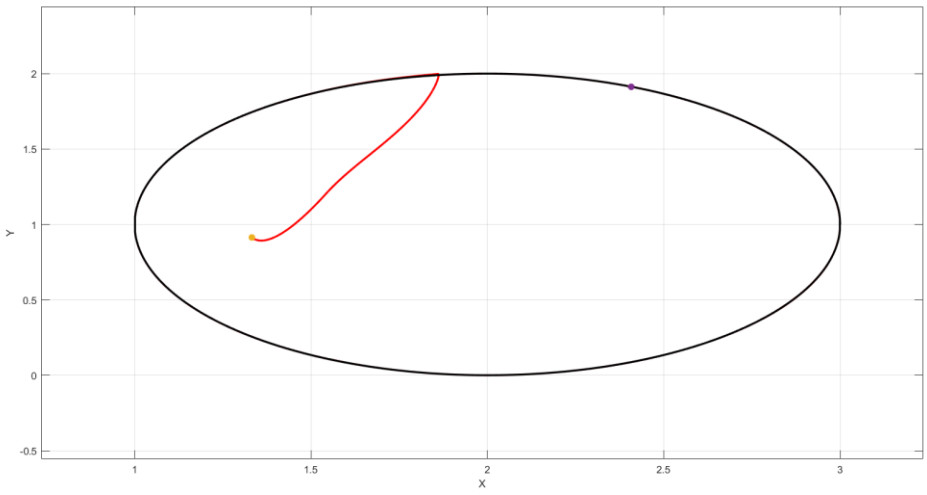

Figure 24: Projection of X-Y Trajectory of Robot Manipulator.

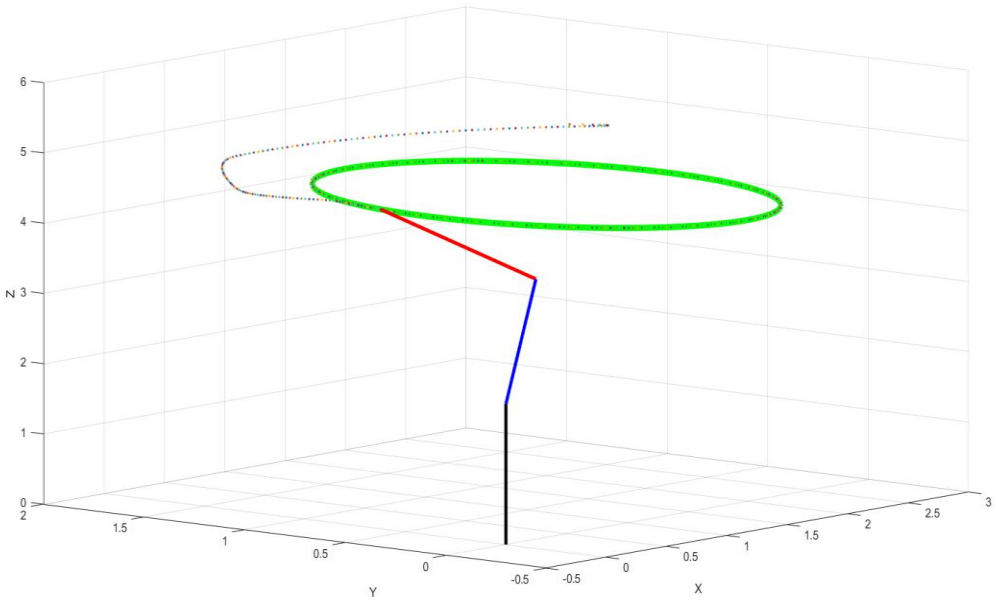

Figure 25: Projection of X-Y-Z Trajectory of Robot Manipulator.

After starting the simulation, robot effort to reach the circle path, execute a circular motion, and remain in a specified way. Getting the specified path from any starting point in the robot workspace indicates that the controller is working correctly.

The SMC response for the three different robot models (Detailed, Semi-Detailed, and Simplified) for the first three links and joints is depicted in Figures 26, 27 and 28 for angular position. Figures 29,30, and 31 illustrate the plot of angular position tracking error of the model's joints and demonstrate the steady state error. Figures 29 to 31 indicate the plot of angular position error of the models' joints that relative values demonstrate the steady state error of models. To evaluate the performance of the controller's general time and frequency performance requirements in the time domain, performance in the Steady state error, Speed of response, Rise time, and settling time. Based on figures 26 to 31, SMC's performance for the angular position, Table 5 is represented.

Table 5: Performance of SMC of angular position for the different models.

SMC Performance	**Rising time** (sec)	**Settling time** (sec)	**Overshoot** (%)	**Steady state error** (%)
Detailed				
Arm 1	0.304	0.47	1.73	0.096
Arm 2	0.301	0.78	2.01	0.076
Arm 3	0.306	0.52	1.92	0.063
Semi-Detailed				
Arm 1	0.283	0.683	1.36	0.073
Arm 2	0.276	0.765	1.48	0.051
Arm 3	0.295	0.697	1.26	0.046
Simplified				
Arm 1	0.183	0.653	1.2	0.0036
Arm 2	0.168	0.423	1.2	0.0021
Arm 3	0.146	0.389	1.2	0.002

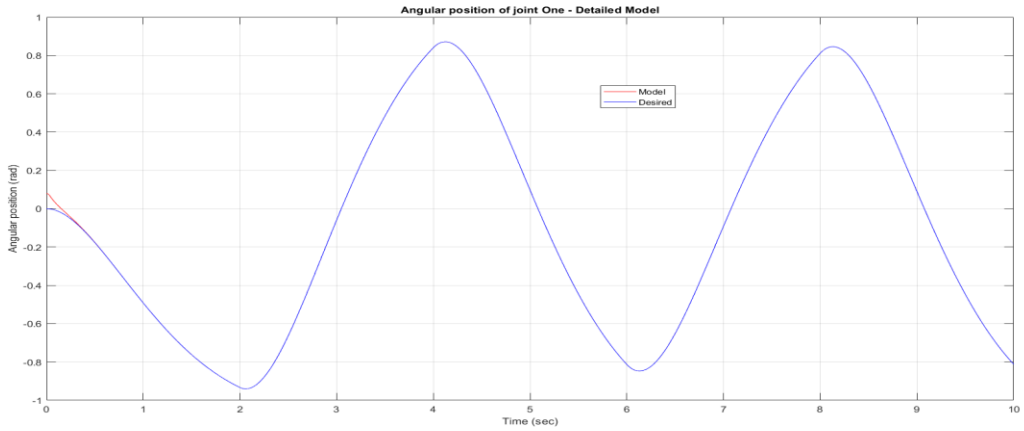
Angular position of joint One - Detailed Model
Model
Desired
Angular position (rad)
Time (sec)

(a)

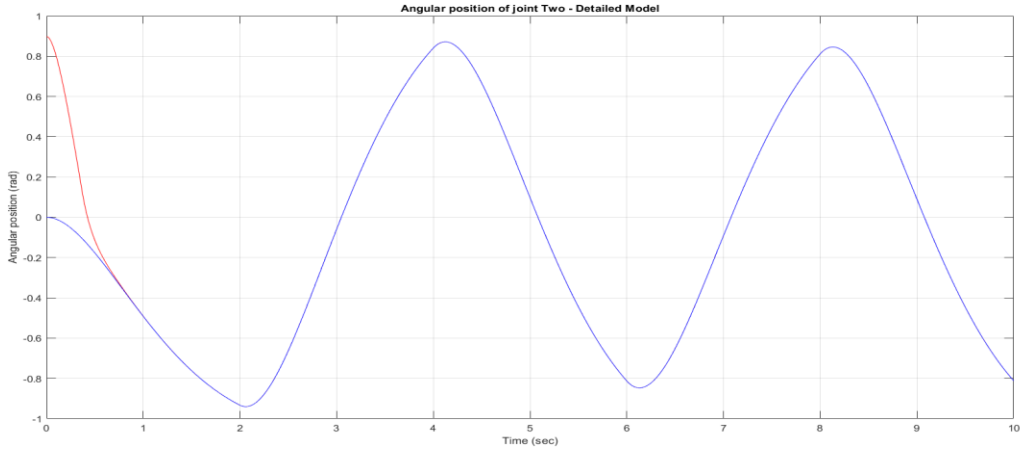
Angular position of joint Two - Detailed Model
Angular position (rad)
Time (sec)

(b)

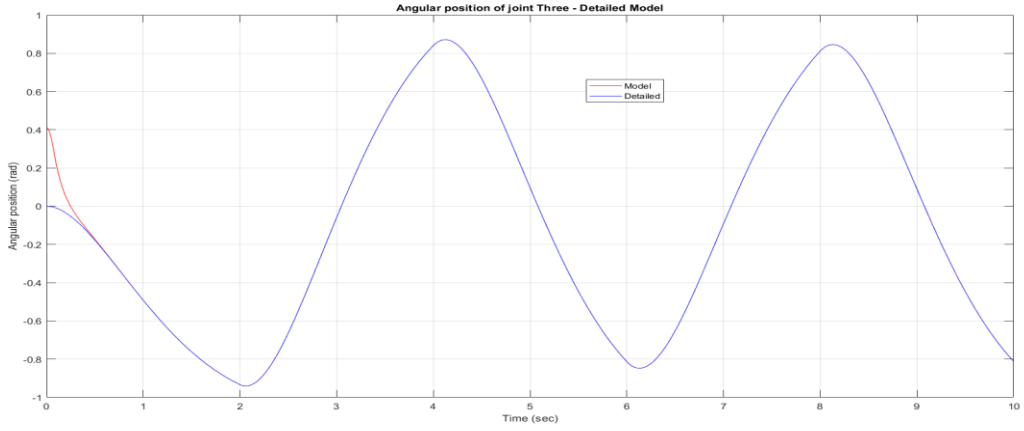
Angular position of joint Three - Detailed Model
Model
Detailed
Angular position (rad)
Time (sec)

(c)

Figure 26: Angular position of the joints for the detailed model using SMC: (a) Angular position of joint One, (b) Angular position of joint Two, (c) Angular position of joint Three.

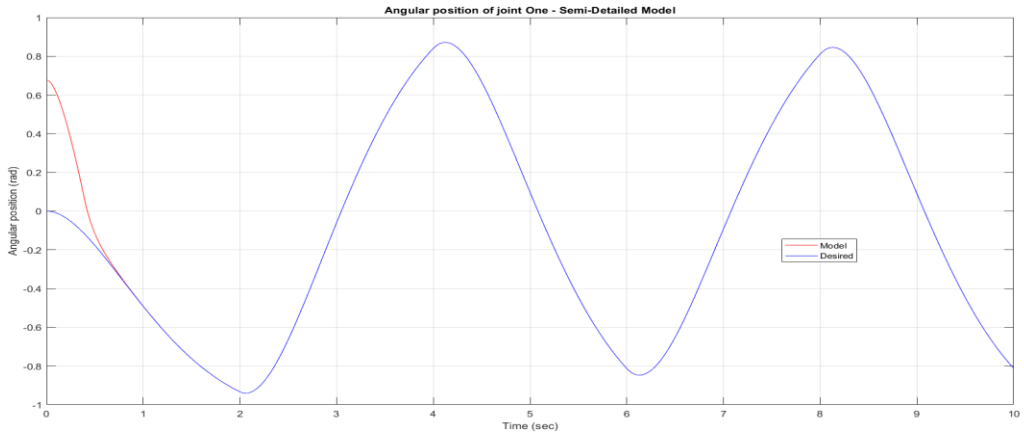

(a)

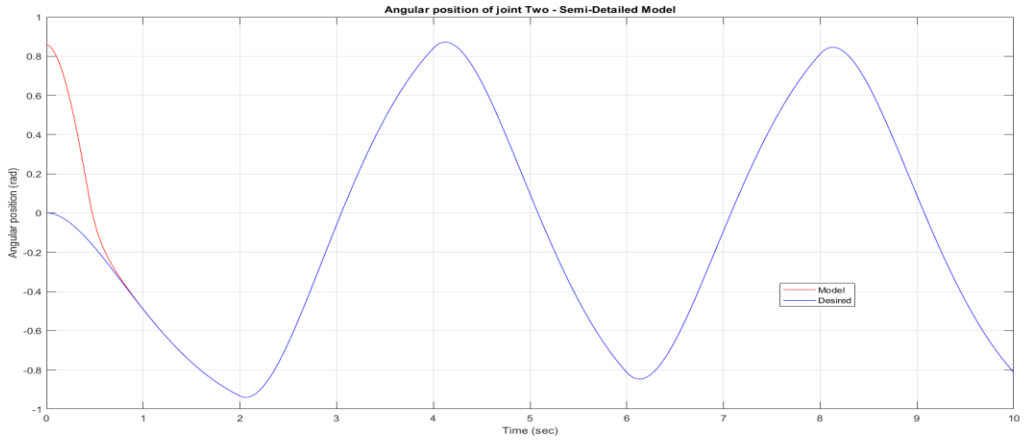

(b)

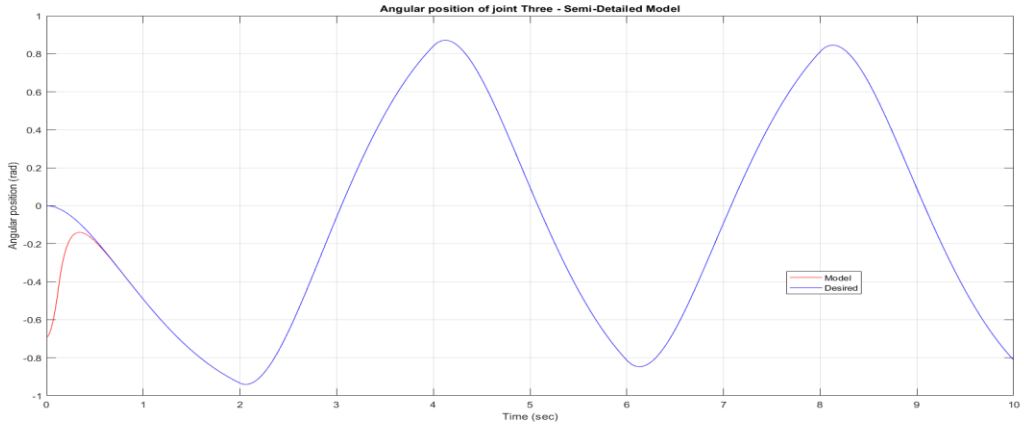

(c)

Figure 27: Angular position of the joints for Semi-Detailed Model using SMC: (a) Angular position of joint One, (b) Angular position of joint Two, (c) Angular position of joint Three.

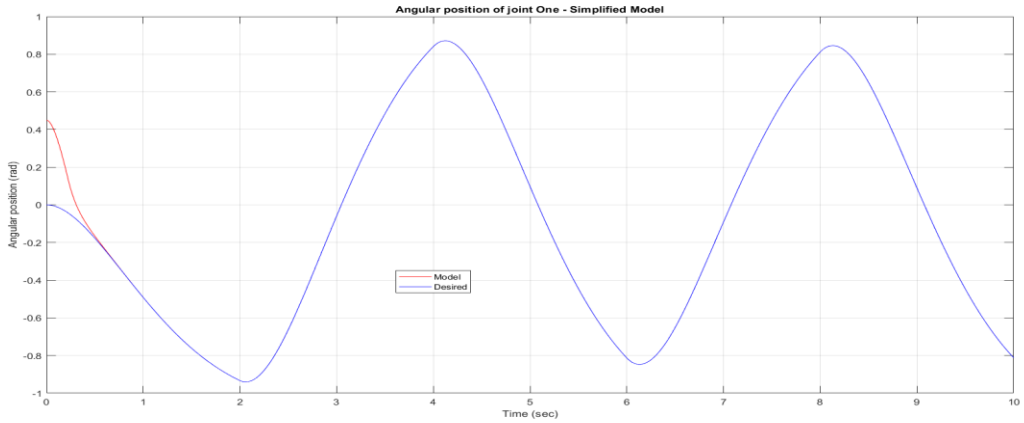

(a)

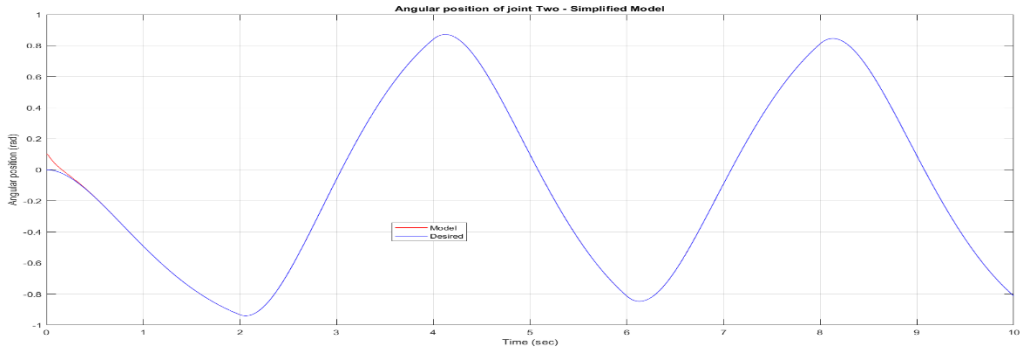

(b)

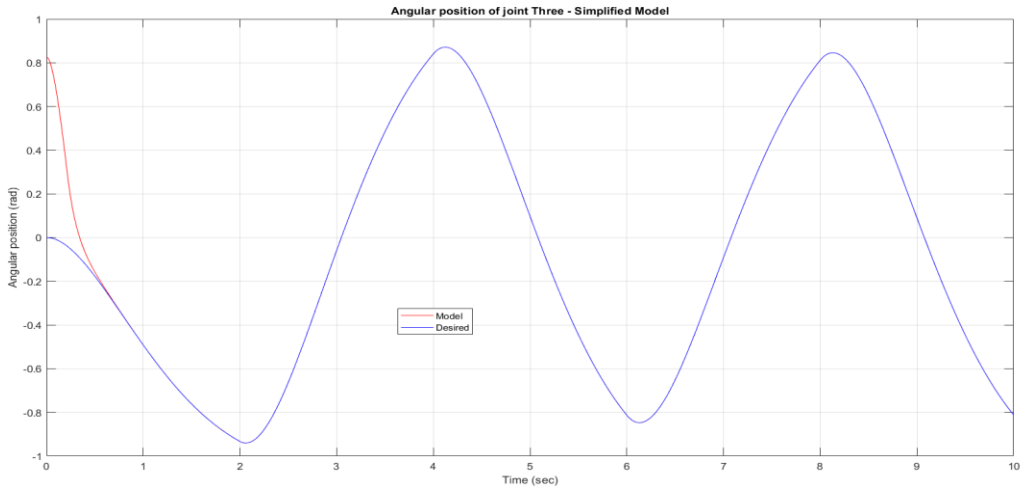

(c)

Figure 28: Angular position of the joints for the simplified model using SMC: (a) Angular position of joint One, (b) Angular position of joint Two, (c) Angular position of joint Three.

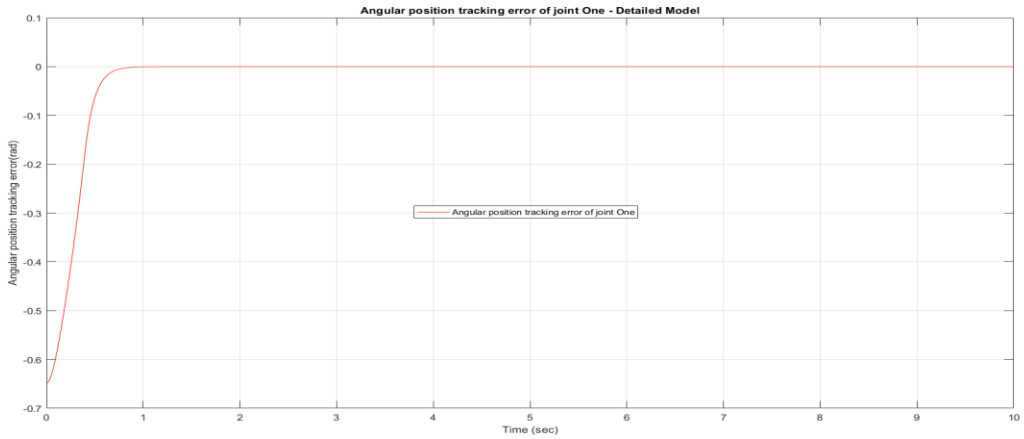

(a)

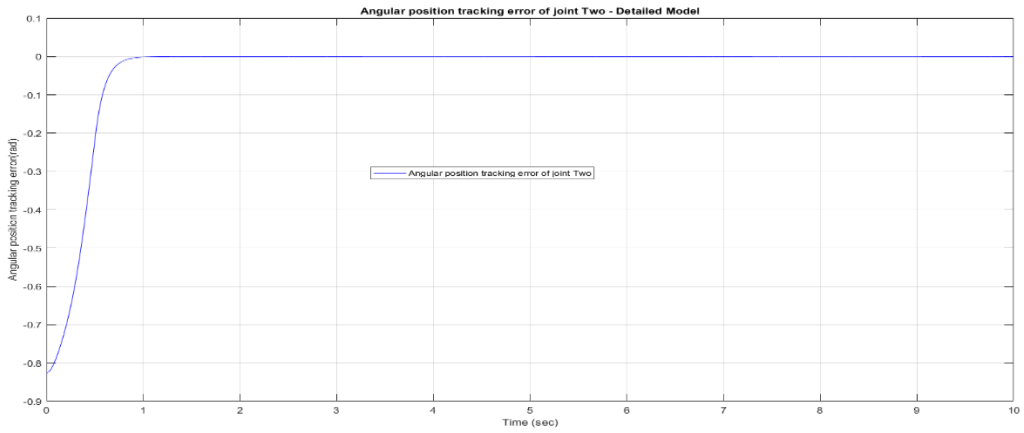

(b)

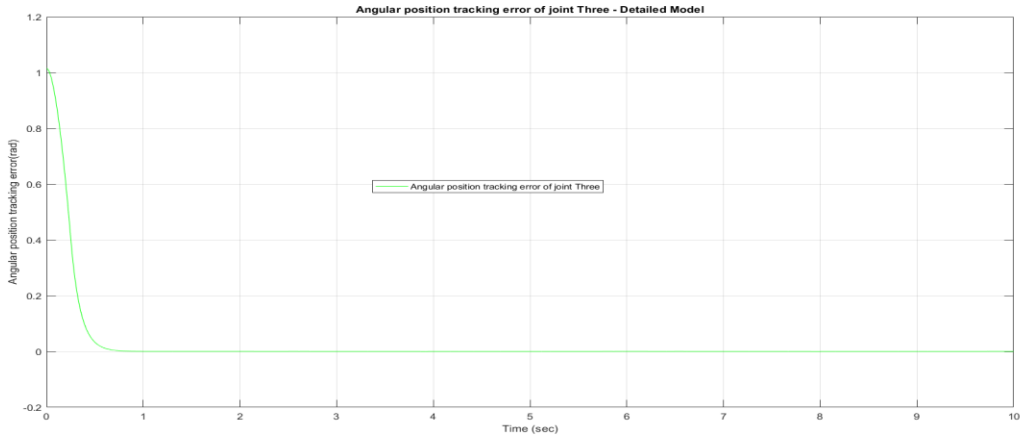

(c)

Figure 29: Angular position tracking error for Detailed Model using SMC: (a) Angular position tracking error of joint One, (b) Angular position tracking error of joint Two, (c) Angular position tracking error of joint Three.

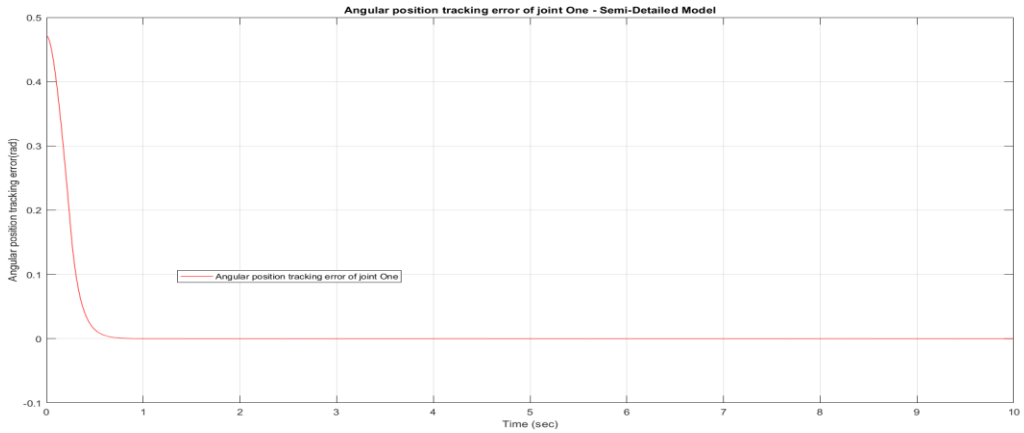

(a)

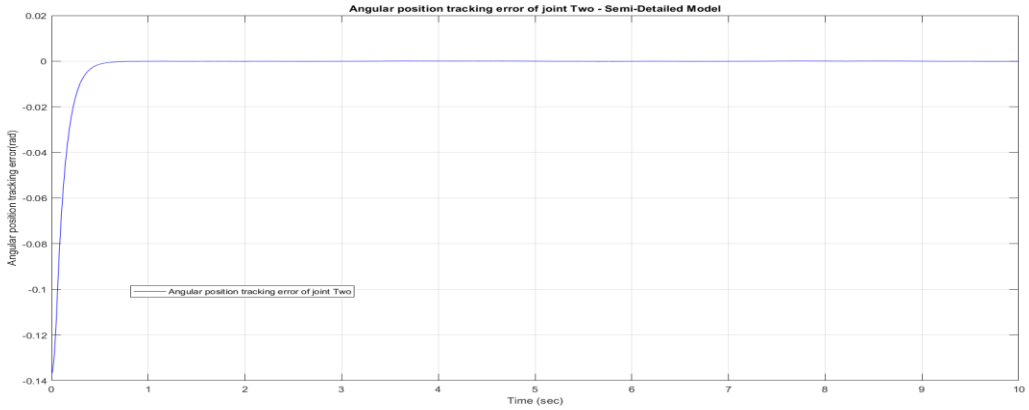

(b)

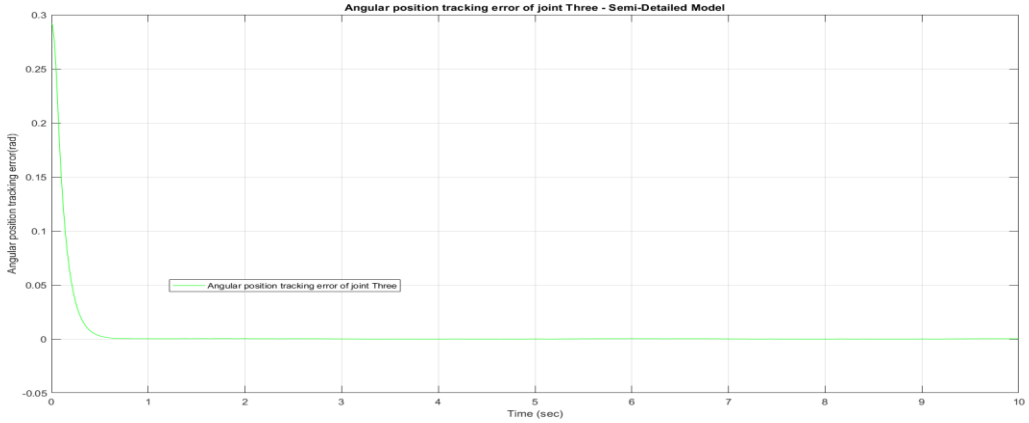

(c)

Figure 30: Angular position tracking error for Semi-Detailed Model using SMC: (a) Angular position tracking error of joint One, (b) Angular position tracking error of joint Two, (c) Angular position tracking error of joint Three.

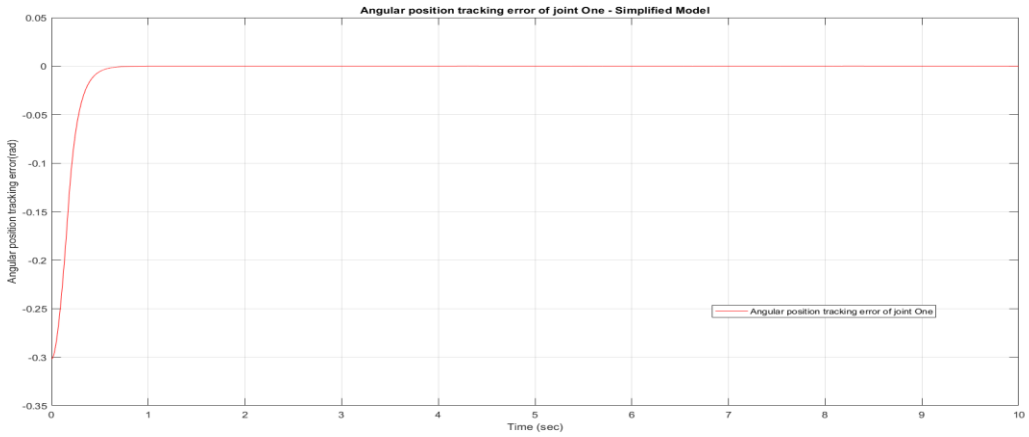

(a)

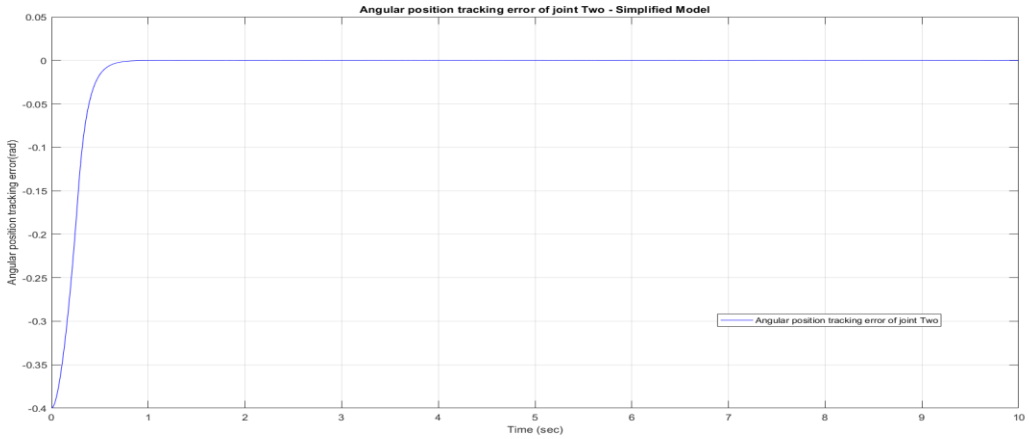

(b)

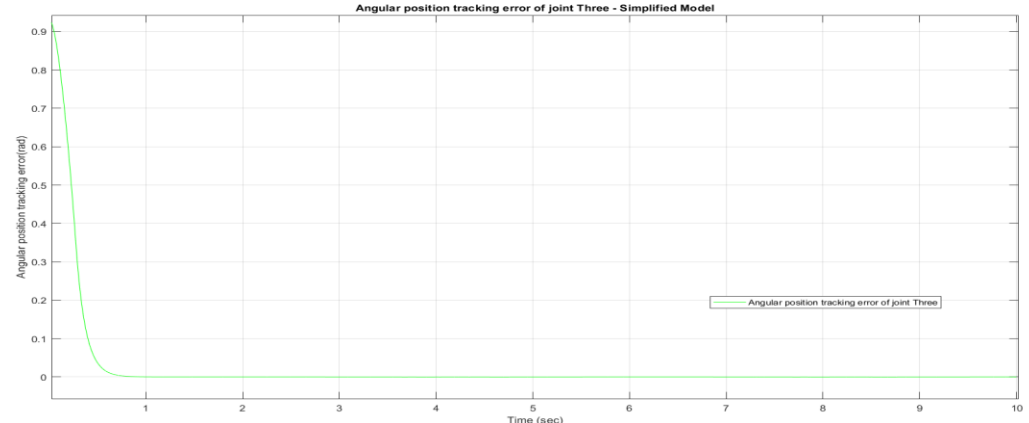

(c)

Figure 31: Angular position tracking error for Simplified Model using SMC: (a) Angular position tracking error of joint One, (b) Angular position tracking error of joint Two, (c) Angular position tracking error of joint Three.

Figures 32, 33, and 34, indicate the plot of sliding surface (s). The sliding surfaces are smooth and converge to zero as expected. The average reaching time to the sliding manifold in the simplified model is about 0.29 sec and in the semi-detailed is around 0.34 sec, and in the detailed model is about 0.49 sec. For the same controller structure and initial condition and input, the response time and reaching time for three different models are so close. The reaching time is the least for the simplified model, the semi-detailed model, and the most for the detailed model, respectively.

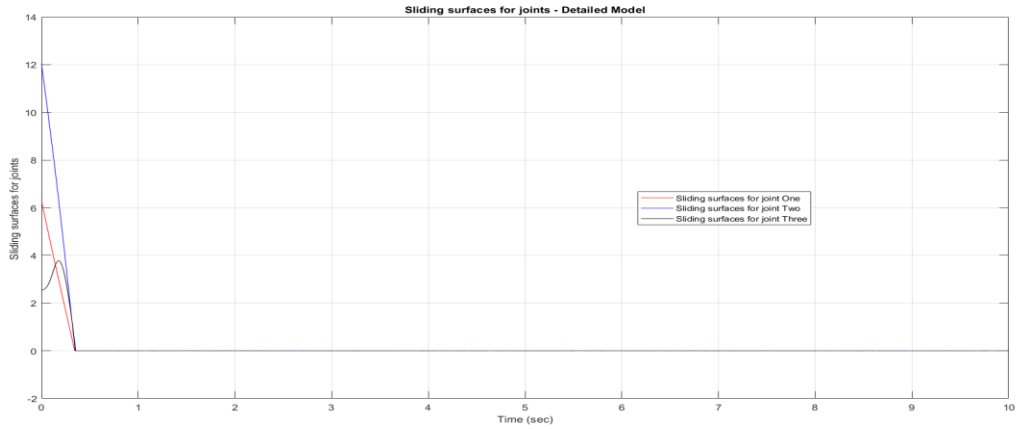

Figure 32: Sliding surfaces for Detailed Model.

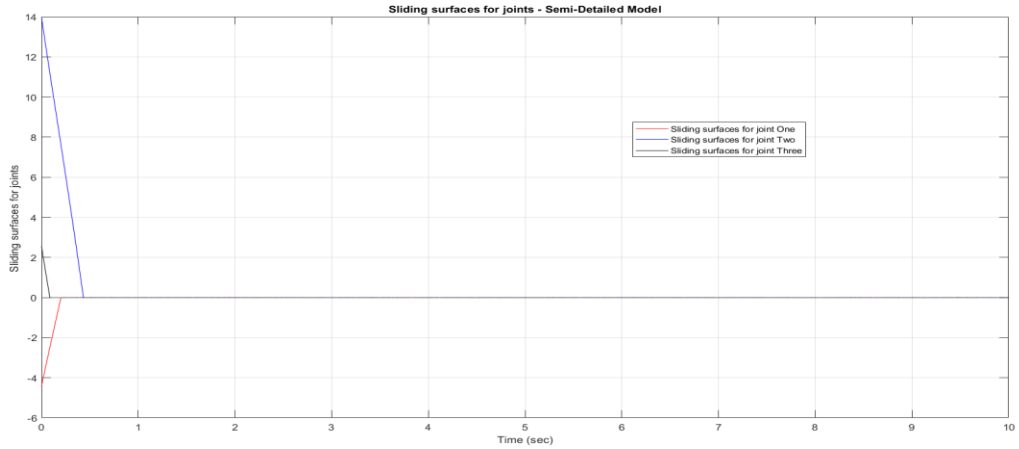

Figure 33: Sliding surfaces for Semi- Detailed Model.

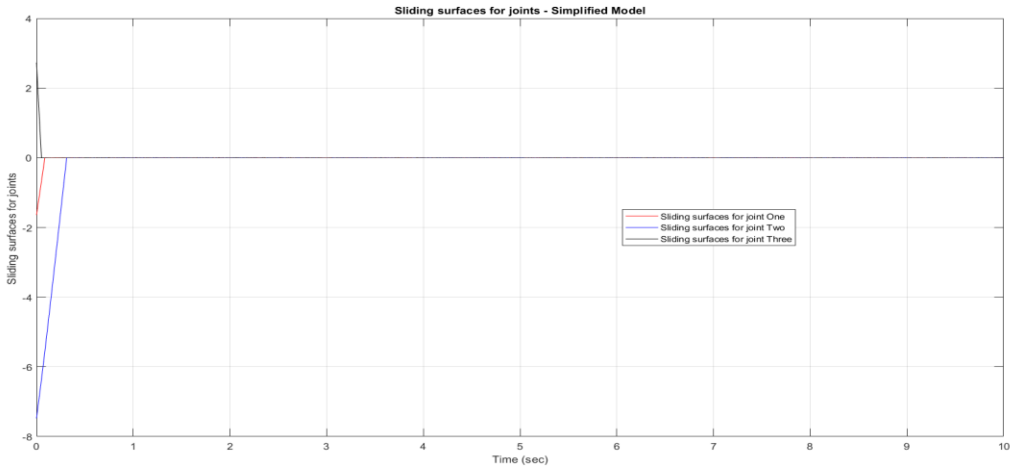

Figure 34: Sliding surfaces for Simplified Model.

Table 5 of the performance of SMC of angular position for the different models and compersion between figures 32-34 demonstrate that the three different models' performances are almost the same. Generally, considering all measured parameters for all three models underperforming the same SMC controller, the Simplified model had the best performance, and then the Semi-Detailed and detailed models, respectively.

The robustness of the SMC controller is examined based on the value of disturbance applied to the sinusoidal trajectory of the joint variable is predefined as 35% of the input signal. The SMC with disturbance response for the three different robot models (Detailed, Semi-Detailed, and Simplified) for the first three links and joints is shown in Figures 35, 36, and 37 for angular position. Figures 38, 39, and 40 depict the model's angular position tracking error plot and present the steady state error. Figures 41, 42, and 43 indicate the diagram of sliding surfaces for the SMC controller with disturbances term.

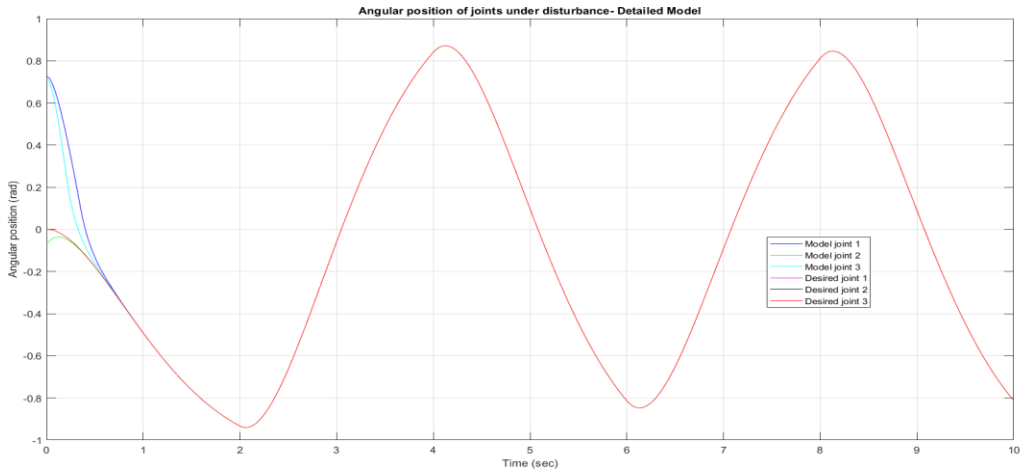

Figure 35 : Angular position of joints for Detailed Model with disturbance.

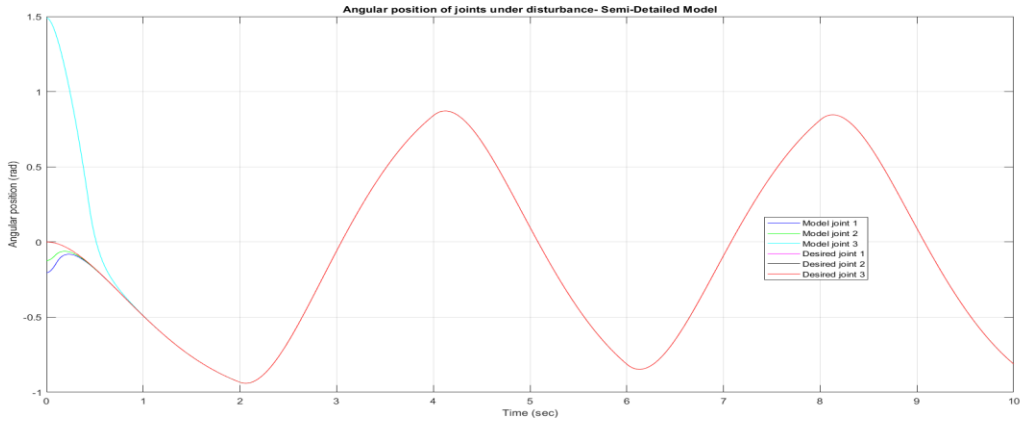

Figure 36: Angular position of joints for Semi-Detailed Model with disturbance.

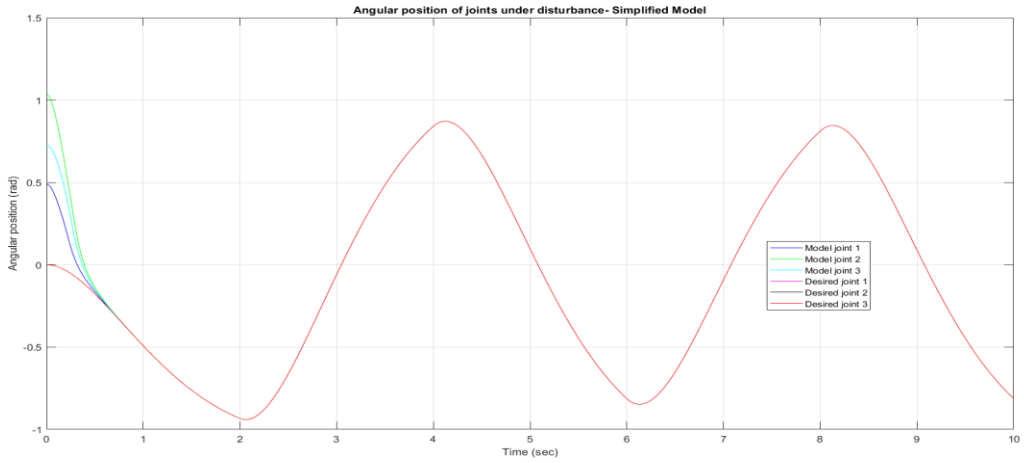

Figure 37: Angular position of joints for Simplified Model with disturbance.

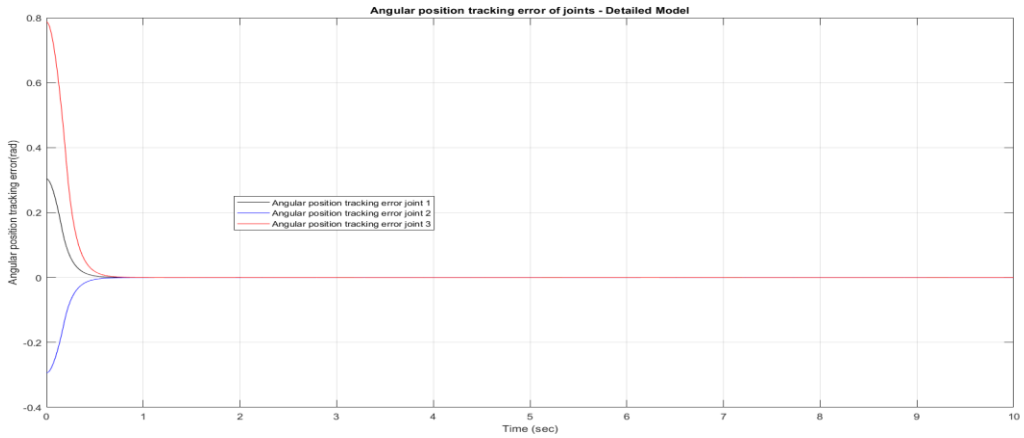

Figure 38: Angular position tracking error of joints for Detailed Model with disturbance.

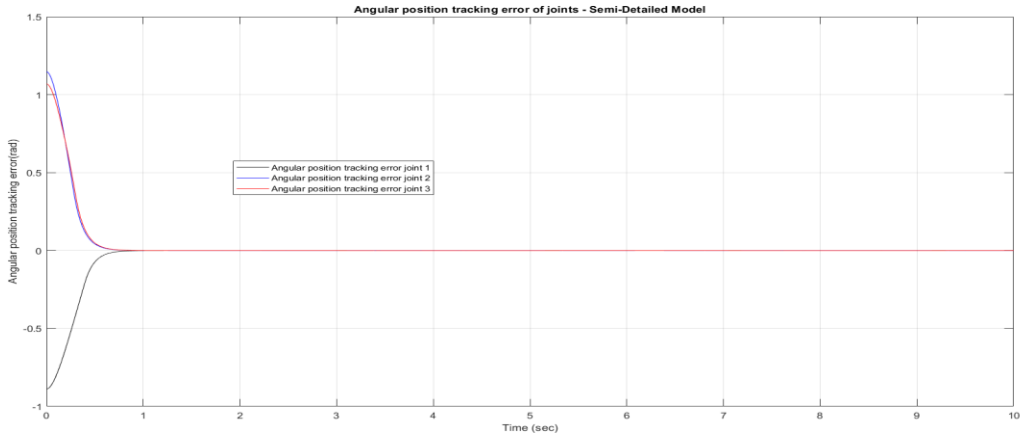

Figure 39: Angular position tracking error of joints for Semi-Detailed Model with disturbance.

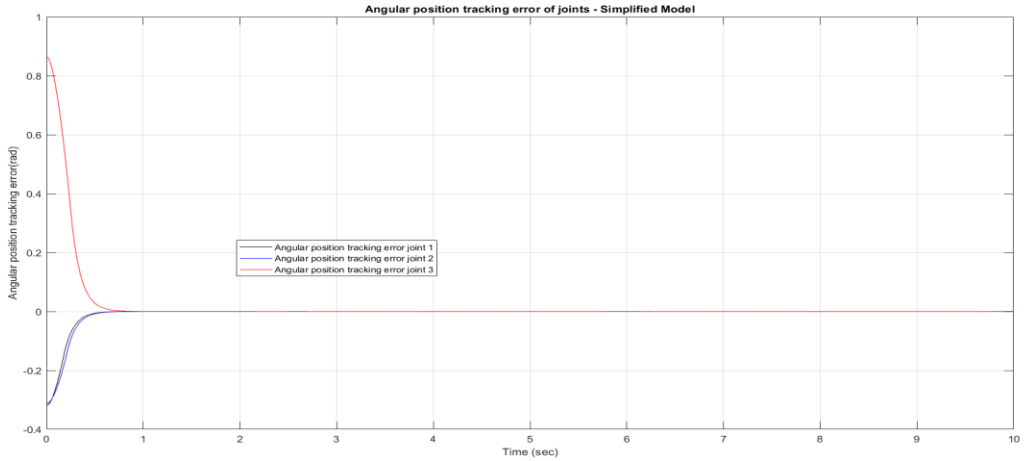

Figure 40: Angular position tracking error of joints for Simplified Model with disturbance.

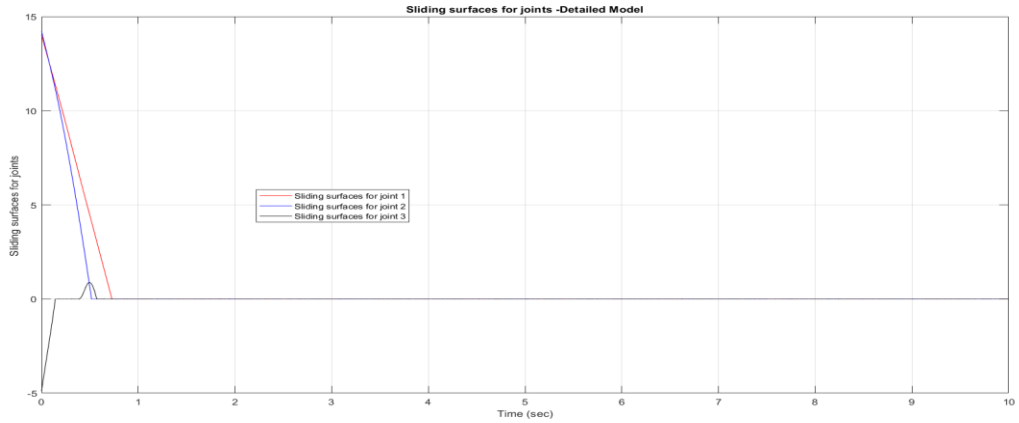

Figure 41: Sliding surfaces with disturbance for Detailed Model.

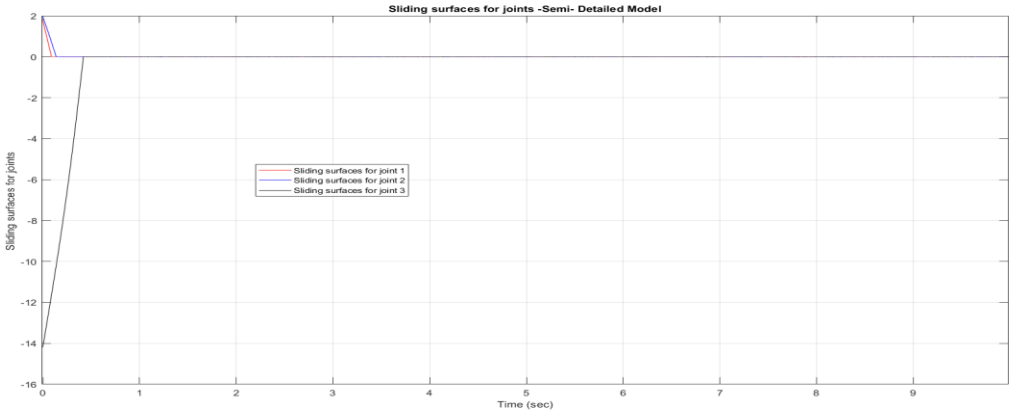

Figure 42: Sliding surfaces with disturbance for Semi-Detailed Model.

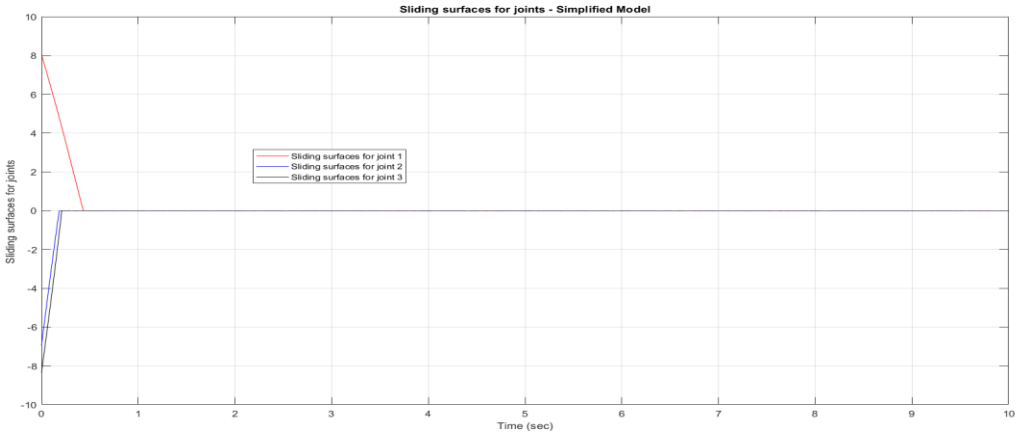

Figure 43: Sliding surfaces with disturbance for Simplified Model.

Based on figures 35 to 40, the SMC controller under the disturbance of 35% of input amplitude result indicates a good performance response. Performance for the angular position is represented in Table 6.

Table 6: Performance of SMC of angular position for three different models under disturbance.

SMCPerformance under disturbance	**Rising time** (sec)	**Settling time** (sec)	**Overshoot** (%)	**Steady state error** (%)
Detailed				
Arm 1	0.524	0.379	1.84	0.0999
Arm 2	0.661	0.768	2.01	0.0804
Arm 3	0.516	0.497	1.96	0.0692
Semi-Detailed				
Arm 1	0.455	0.693	1.34	0.0786
Arm 2	0.481	0.662	1.47	0.0553
Arm 3	0.467	0.629	1.29	0.0512
Simplified				
Arm 1	0.343	0.608	1.2	0.0038
Arm 2	0.398	0.333	1.2	0.0027
Arm 3	0.384	0.299	1.2	0.0031

According to Table 5, the SMC considered disturbances outcomes, and the performances with disturbance and without disturbance are almost the same. Nevertheless, results with disturbances show that the Steady State error is increased to 4.5% and 6%, and 7% for the Simplified and Semi-detailed and Detailed models, respectively. Overshoot remains the same. Rise times are increased on average by 0.31sec, and settling times are decreased on average by 0.09sec.

Figures 41, 42, and 43 show the diagram of the sliding surface under disturbance. The sliding surfaces for the controller with disturbance, the same as the controller without disturbance, are smooth and converge to zero as expected. The average reaching time to the sliding manifold in the simplified model is about 0.39 sec and in the semi-detailed is around 0.47 sec, and in the detailed model is about 0.63 sec. Same as the simple SMC controller, controller under disturbance for the same controller structure and initial condition and input, the response time and reaching time for three different models are close. The reaching time is the least for the simplified model, the semi-detailed model, and the most for the detailed model, respectively.

Conclusion

The dynamics of an industrial robotic manipulator arm having six degrees of freedom or articulations (the ABB IRB 140) were studied using detailed, semi-detailed, and simplified models in SolidWorks. Using mass and inertial data, forward/inverse kinematic characterization, end-effector position and orientation, and joint torque associated with the three proximal links (the most critical determinants of the accuracy of the robotic arm movement), the dynamic model thus developed was examined in MATLAB in full detail. Forward kinematics of the robot were derived from Denavit-Hartenberg parameters, and a procedure was developed to solve the inverse kinematics, with trajectory planning based on fifth-order polynomial and forward and inverse differential kinematics in Spong formulation [216]. The steps of this development are described in detail herein. Energy consumption on a path of movement over a fixed time interval was examined to evaluate the three dynamic models as predictors of the robot's performance.

Our most notable finding is that link dimensions and geometry directly affect how the center of mass position and inertial characteristics change and hence the suitability of the torque equations. The position of the center of mass in dynamic calculations and models must be chosen carefully. On the other hand, the simplified model used in classical computational methods provides acceptable results. How close these results are to the behavior of the real robot remains to be seen. However, any data of mass properties for mechanical mechanisms like inertia matrices, mass center points, friction, and gravity forces provided by any software indicates an error percentage that must be considered in the dynamics equation calculus.

MATLAB is a helpful tool for implementing algorithms, estimating and validating models, and simulating system responses. Still, the computational time for the calculus of algebraic equations in robotics is not very efficient. Another valuable result of this study is that the three models reach nearly the same values for the total energy consumption by the robot executing a path of movement

over a single time interval, suggesting that they all could give acceptable results in different situations. In some cases, with more degree of freedom in the robotic field, results are heavy and slow-performing a simulation or generating equations such as torque and energy equations with a high number of points. For this reason, using a simplified state of the actual model improves and optimizes the calculus process. The torque requirement for different robot positions and operations may be computed over different periods and paths. The quality of the approach developed in this study could be tested further by comparing energy consumption by the robot during different tasks.

A control module and a robustness controller (SMC) included to minimize the impact of the error in the property inputs to the controller. The simulation results show that the sliding mode control method is robust and performs satisfactorily even in external disturbances. Sliding mode control offers suitable performances for control of robot models with unmodeled disturbances. Generally, the controller results examined on three models (detailed, semi-detailed, and simplified) are close with a slight percentage difference. The controller under disturbance also had relatively close results compared to the controller without disturbance. The sliding mode control methodology has an appropriate dynamic response and minimum tracking error performance from simulation results. The most significant disadvantage of this technique is the chattering phenomenon effect with control input, but the overall results for the models are satisfactory.

The study of significant issues, such as the impacts of different mathematical and dynamic models of a chain mechanism such as a robotic arm, has not been attended to in the literature review. Since the equations related to torque and force in robotic arms with more than three degrees of freedom are heavy equations with many mathematical and trigonometric elements, analyzing these equations for software such as MATLAB with high equation-solving capabilities is also time-consuming. Therefore, simplifying force and torque equations will increase the calculation speed

and decrease the calculation time. One of the ways to simplify the equations and dynamic models of the manipulator robotic arms is to suppose the robotic arm mechanism in simpler geometric shapes such as a rod. The advantage of this assumption is to eliminate the techniques of finding the center of mass and the equations based on the moment of inertia. Analyzing the impact of these assumptions on the final accuracy of robot models and to what extent these results will be acceptable was one of the objectives of this research that had not been addressed so far. For the investigation, in this case, powerful design software such as SolidWorks was employed to design according to the actual mechanism of the case of the studied robotic arm. Although in this study, as much as possible, an accurate model of the arm of the robot is prepared, and it is also considered that the manufacturer's material and the weight of the parts match the real robot, this information is the exclusive property of the robotic arms manufacturer companies. Although reliable details are available to researchers in this field that provide by official companies, these points can be counted as one of the limitations of this research.

As a follow-up to our work, we intend to study a novel kinematics model based on quantum computing for the same case of study, an articulated six-jointed IRB 140 ABB robotic arm. The model establishes the position and the orientation expressions using quantum tools. The robot's position is determined through the successive elementary translations and rotations starting from the end-effector until the base frame. In contrast, the orientation model of the robot is extracted from the quaternion's representation of the orientation. The presented quantum model is based on the equivalence between the quaternions and the Pauli matrices or gates. The main advantage of this novel model is that it utilizes only one qubit to model the position and orientation. A novel kinematics model based on quantum computing denotes a massive saving in computing resources and time. This quantum kinematics model is a step ahead of future quantum models and simulation

software adapted to future quantum computers. The proposed techniques and results can also be used in the classic computing theories for robotic arms kinematics modeling [212].

References

1. Goel, Ruchi, and Pooja Gupta. "Robotics and Industry 4.0." In A Roadmap to Industry 4.0: Smart Production, Sharp Business and Sustainable Development, pp. 157-169. Springer, Cham, 2020.

2. Oztemel, Ercan, and Samet Gursev. "Literature review of Industry 4.0 and related technologies." Journal of Intelligent Manufacturing 31, no. 1 (2020): 127-182.

3. Karabegović, Isak. "THE ROLE OF INDUSTRIAL AND SERVICE ROBOTS IN THE 4th INDUSTRIAL REVOLUTION–" INDUSTRY 4.0"." Acta Technica Corviniensis-Bulletin of Engineering 11, no. 2 (2018): 11-16.

4. Chen, Qingrong, Wenming Cheng, Lingchong Gao, and Johannes Fottner. "A pure neural network controller for double-pendulum crane anti-sway control: Based on Lyapunov stability theory." Asian Journal of Control 23, no. 1 (2021): 387-398.

5. Gambhire, Shankar J., Dondapati Ravi Kishore, Pandurang S. Londhe, and Sushant N. Pawar. "Robust trajectory tracking with non-singular terminal sliding mode control of a mobile manipulator." Bulletin of Electrical Engineering and Informatics 11, no. 1 (2022): 134-142.

6. Mishra, S., Pandurang S. Londhe, S. Mohan, Santosh Kumar Vishvakarma, and B. M. Patre. "Robust task-space motion control of a mobile manipulator using a nonlinear control with an uncertainty estimator." Computers & Electrical Engineering 67 (2018): 729-740.

7. Huang, Chin-I., Kuang-Yow Lian, Chian-Song Chiu, and Li-Chen Fu. "Smooth sliding mode control for constrained manipulator with joint flexibility." IFAC Proceedings Volumes 38, no. 1 (2005): 91-96.

8. Wang, Yanmin, and Lanxin Sun. "On the optimized continuous nonsingular terminal sliding mode control of flexible manipulators." In 2014 Fourth International Conference on Instrumentation and Measurement, Computer, Communication and Control, pp. 324-329. IEEE, 2014.

9. Jun, Liu, Wang Xiaoguang, Wang Yuqi, and Lin Qi. "Continuous terminal sliding mode control of a 6-DOF wire-driven parallel robot." In 2017 IEEE International Conference on Robotics and Biomimetics (ROBIO), pp. 1757-1762. IEEE, 2017.

10. Yu, Xinghuo, and Okyay Kaynak. "Sliding-mode control with soft computing: A survey." IEEE transactions on industrial electronics 56, no. 9 (2009): 3275-3285.

11. Wang, Liangyong, Tianyou Chai, and Lianfei Zhai. "Neural-network-based terminal sliding-mode control of robotic manipulators including actuator dynamics." IEEE Transactions on Industrial Electronics 56, no. 9 (2009): 3296-3304.

12. Tran, Minh-Duc, and Hee-Jun Kang. "A novel adaptive finite-time tracking control for robotic manipulators using nonsingular terminal sliding mode and RBF neural networks." International journal of precision engineering and manufacturing 17, no. 7 (2016): 863-870.

13. Tran, Minh-Duc, and Hee-Jun Kang. "A novel adaptive finite-time tracking control for robotic manipulators using nonsingular terminal sliding mode and RBF neural networks." International journal of precision engineering and manufacturing 17, no. 7 (2016): 863-870.

14. Si, Yanna, Jiexin Pu, and Lifan Sun. "A fast terminal sliding mode control of two-link flexible manipulators for trajectory tracking." In 2017 Chinese Automation Congress (CAC), pp. 6387-6391. IEEE, 2017.

15. Moreno, Jaime A., and Marisol Osorio. "A Lyapunov approach to second-order sliding mode controllers and observers." In 2008 47th IEEE conference on decision and control, pp. 2856-2861. IEEE, 2008.

16. Liu, Lei, Quanmin Zhu, Lei Cheng, Yongji Wang, and Dongya Zhao. Applied Methods and Techniques for Mechatronic Systems. Springer, 2014.

17. Choi, Seung-Bok, Dong-Won Park, and Suhada Jayasuriya. "A time-varying sliding surface for fast and robust tracking control of second-order uncertain systems." Automatica 30, no. 5 (1994): 899-904.

18. Asif, Muhammad, Muhammad Junaid Khan, and Attaullah Y. Memon. "Integral terminal sliding mode formation control of non-holonomic robots using leader follower approach." Robotica 35, no. 7 (2017): 1473-1487.

19. Parra-Vega, Vicente, Suguru Arimoto, Yun-Hui Liu, Gerd Hirzinger, and Prasad Akella. "Dynamic sliding PID control for tracking of robot manipulators: Theory and experiments." IEEE Transactions on Robotics and Automation 19, no. 6 (2003): 967-976.

20. Hung, John Y., Weibing Gao, and James C. Hung. "Variable structure control: A survey." IEEE transactions on industrial electronics 40, no. 1 (1993): 2-22.

21. Camacho, Oscar. "A predictive approach based-sliding mode control." IFAC Proceedings Volumes 35, no. 1 (2002): 381-385.

22. Levant, Arie. "Sliding order and sliding accuracy in sliding mode control." International journal of control 58, no. 6 (1993): 1247-1263.

23. Hamerlain, F., K. Achour, T. Floquet, and W. Perruquetti. "Trajectory tracking of a car-like robot using second order sliding mode control." In 2007 European Control Conference (ECC), pp. 4932-4936. IEEE, 2007.

24. Xuan, D. and J. Bae, A Precise Neural-Disturbance Learning Controller of Constrained Robotic Manipulators. IEEE Access, 2021. 9: p. 50381-50390.

25. Goubej, M., et al., Employing Finite Element Analysis and Robust Control Concepts in Mechatronic System Design-Flexible Manipulator Case Study. Applied Sciences, 2021. 11(8): p. 3689.

26. Sage, H. G., De Mathelin, M. F., & Ostertag, E. (1999). Robust control of robot manipulators: a survey. International Journal of control, 72(16), 1498-1522.

27. Park, Y. (2021). An Automatic Program of Generation of Equation of Motion and Dynamic Analysis for Multi-body Mechanical System using GNU Octave. Journal of Applied and Computational Mechanics, 7(3), 1687-1697.

28. Trojanová, M. and T. Cakurda, VALIDATION OF THE DYNAMIC MODEL OF THE PLANAR ROBOTIC ARM WITH USING GRAVITY TEST.

29. Zhuang, C., et al., A convolution neural network based semi-parametric dynamic model for industrial robot. Proceedings of the Institution of Mechanical Engineers, Part C: Journal of Mechanical Engineering Science, 2021: p. 09544062211039875.

30. Deng, J., et al. Dynamic Model Identification of Collaborative Robots Using a Three-Loop Iterative Method. in 2021 6th IEEE International Conference on Advanced Robotics and Mechatronics (ICARM). 2021. IEEE.

31. Leboutet, Q., et al., Inertial Parameter Identification in Robotics: A Survey. Applied Sciences, 2021. 11(9): p. 4303.

32. Han, Y., et al., An iterative approach for accurate dynamic model identification of industrial robots. IEEE Transactions on Robotics, 2020. 36(5): p. 1577-1594.

33. Bottin, M., et al., Modeling and identification of an industrial robot with a selective modal approach. Applied Sciences, 2020. 10(13): p. 4619.

34. Zimmermann, S.A., et al. Dynamic modeling of robotic manipulators for accuracy evaluation. in 2020 IEEE International Conference on Robotics and Automation (ICRA). 2020. IEEE.

35. Romero, J. G., Ortega, R., & Bobtsov, A. (2021). Parameter estimation and adaptive control of Euler–Lagrange systems using the power balance equation parameterisation. International Journal of Control, 1-13.

36. Muñoz-Vázquez, A. J., Parra-Vega, V., Sánchez-Orta, A., & Sánchez-Torres, J. D. (2022). High-gain PI-like control of Euler–Lagrange mechanical systems: Simulations and experiments in 2DoF robotic manipulators. Proceedings of the Institution of Mechanical Engineers, Part I: Journal of Systems and Control Engineering, 236(4), 857-869.

37. He, X., Lu, M., & Deng, F. (2021, December). Trajectory Tracking Control of Uncertain Euler-Lagrange Systems: A Robust Control Approach. In 2021 IEEE International Conference on Robotics and Biomimetics (ROBIO) (pp. 1855-1860). IEEE.

38. Kong, L., S. Zhang, and X. Yu, Approximate optimal control for an uncertain robot based on adaptive dynamic programming. Neurocomputing, 2021. 423: p. 308-317.

39. Caccavale, F., B. Siciliano, and L. Villani, The Tricept robot: dynamics and impedance control. IEEE/ASME transactions on mechatronics, 2003. 8(2): p. 263-268.

40. Vargas, F.J.T., E. De Fieri, and E.B. Castelan. Identification and friction compensation for an industrial robot using two degrees of freedom controllers. in ICARCV 2004 8th Control, Automation, Robotics and Vision Conference, 2004. 2004. IEEE.

41. Zou, Q., et al., Kinematic and dynamic analysis of a 3-DOF parallel mechanism. International Journal of Mechanics and Materials in Design, 2021: p. 1-13.

42. Gaponenko, E., L. Rybak, and D. Malyshev, Numerical Method for Determining the Operating Area of a Robot with Relative Manipulation Mechanisms. Journal of Machinery Manufacture and Reliability, 2020. 49(6): p. 474-489.

43. Grassmann, R. and J. Burgner-Kahrs. On the Merits of Joint Space and Orientation Representations in Learning the Forward Kinematics in SE (3). in Robotics: science and systems. 2019.

44. Li, J., Wang, Y., Liu, Z., Jing, X., & Hu, C. (2021). A new recursive composite adaptive controller for robot manipulators. Space: Science & Technology, 2021.

45. Trotti, F., Ghignoni, E., & Muradore, R. (2021, June). A Modified Recursive Newton-Euler Algorithm Embedding a Collision Avoidance Module. In 2021 European Control Conference (ECC) (pp. 1150-1155). IEEE.

46. Petrović, G. R., & Mattila, J. (2022). Mathematical modelling and virtual decomposition control of heavy-duty parallel–serial hydraulic manipulators. Mechanism and Machine Theory, 170, 104680.

47. Schilling, R.J., Fundamentals of robotics: analysis and control. 1996: Simon & Schuster Trade.

48. Hamet, Pavel, and Johanne Tremblay. "Artificial intelligence in medicine." Metabolism 69 (2017): S36-S40.

49. Pandilov, Zoran, and Vladimir Dukovski. "COMPARISON OF THE CHARACTERISTICS BETWEEN SERIAL AND PARALLEL ROBOTS." Acta Technica Corviniensis-Bulletin of Engineering 7, no. 1 (2014).

50. Stone, Wesley L. "The history of robotics." Robotics and automation handbook (2005): 1-12.

51. Bock, Thomas, and Thomas Linner. Robotic industrialization. Cambridge University Press, 2015.

52. Mondada, Francesco, Edoardo Franzi, and Paolo Ienne. "Mobile robot miniaturisation: A tool for investigation in control algorithms." In Experimental robotics III, pp. 501-513. Springer, Berlin, Heidelberg, 1994.

53. Zahid, Azlan, Md Sultan Mahmud, Long He, Daeun Choi, Paul Heinemann, and James Schupp. "Development of an integrated 3R end-effector with a cartesian manipulator for pruning apple trees." Computers and Electronics in Agriculture 179 (2020): 105837.

54. Koren, Yoram, and Yoram Koren. Robotics for engineers. Vol. 168. New York: McGraw-Hill, 1985.

55. Žlajpah, Leon. "Simulation in robotics." Mathematics and Computers in Simulation 79, no. 4 (2008): 879-897.

56. Ghorbel, Fathi H., Olivier Chételat, Ruvinda Gunawardana, and Roland Longchamp. "Modeling and set point control of closed-chain mechanisms: Theory and experiment." IEEE Transactions on control systems technology 8, no. 5 (2000): 801-815.

57. Jin, Xiaodong, Yuefa Fang, and Dan Zhang. "Design of a class of generalized parallel mechanisms with large rotational angles and integrated end-effectors." Mechanism and Machine Theory 134 (2019): 117-134.

58. Tsai, Lung-Wen. Robot analysis: the mechanics of serial and parallel manipulators. John Wiley & Sons, 1999.

59. Alassar, Ahmed Z., Iyad M. Abuhadrous, and Hatem A. Elaydi. "Modeling and control of 5 DOF robot arm using supervisory control." In 2010 The 2nd International Conference on Computer and Automation Engineering (ICCAE), vol. 3, pp. 351-355. IEEE, 2010.

60. Liu, Kai, John M. Fitzgerald, and Frank L. Lewis. "Kinematic analysis of a Stewart platform manipulator." IEEE Transactions on industrial electronics 40, no. 2 (1993): 282-293.

61. Craig, John J., Ping Hsu, and S. Shankar Sastry. "Adaptive control of mechanical manipulators." The International Journal of Robotics Research 6, no. 2 (1987): 16-28.

62. Arai, Tamio, Enrico Pagello, and Lynne E. Parker. "Advances in multi-robot systems." IEEE Transactions on robotics and automation 18, no. 5 (2002): 655-661.

63. Westwood, David A., Matthew Heath, and Eric A. Roy. "The effect of a pictorial illusion on closed-loop and open-loop prehension." Experimental Brain Research 134, no. 4 (2000): 456-463.

64. Lewis, Frank L., Darren M. Dawson, and Chaouki T. Abdallah. Robot manipulator control: theory and practice. CRC Press, 2003.

65. Sherkat, Nasser. High speed processing for real-time control of multiple axis continuous path manipulators. Nottingham Trent University (United Kingdom), 1989.

66. Konolige, Kurt, and Karen Myers. "The Saphira architecture for autonomous mobile robots." Artificial Intelligence and Mobile Robots: case studies of successful robot systems 9 (1998): 211-242.

67. Ang, Kiam Heong, Gregory Chong, and Yun Li. "PID control system analysis, design, and technology." IEEE transactions on control systems technology 13, no. 4 (2005): 559-576.

68. Glad, Torkel, and Lennart Ljung. Control theory. CRC press, 2018.

69. Findeisen, Rolf, and Frank Allgöwer. "An introduction to nonlinear model predictive control." In 21st Benelux meeting on systems and control, vol. 11, pp. 119-141. 2002.

70. Dobson, Annette J., and Adrian G. Barnett. An introduction to generalized linear models. Chapman and Hall/CRC, 2018.

71. Kashyap, Abhishek Kumar, and Dayal R. Parhi. "Particle swarm optimization aided pid gait controller design for a humanoid robot." ISA transactions 114 (2021): 306-330.

72. Vukobratovic, Miomir. Dynamics and robust control of robot-environment interaction. Vol. 2. World Scientific, 2009.

73. Singh, Mandeep, and M. K. Shukla. "Intelligent and Hybrid Control Techniques for Robotic Manipulator." In International Conference on Intelligent Computing and Smart Communication 2019, pp. 1535-1545. Springer, Singapore, 2020.

74. Yu, Wen. PID Control with Intelligent Compensation for Exoskeleton Robots. Academic Press, 2018.

75. Wen, John T., and Steve H. Murphy. "PID control for robot manipulators." (1990).

76. Saridis, George. "Intelligent robotic control." IEEE Transactions on Automatic Control 28, no. 5 (1983): 547-557.

77. Anderson, Russell L. A robot ping-pong player: experiment in real-time intelligent control. MIT press, 1988.

78. Li, Lei, Shuming Rong, Rui Wang, and Shuili Yu. "Recent advances in artificial intelligence and machine learning for nonlinear relationship analysis and process control in drinking water treatment: A review." Chemical Engineering Journal 405 (2021): 126673.

79. Piltan, Farzin, MohammadHossain Yarmahmoudi, Mina Mirzaie, Sara Emamzadeh, and Zahra Hivand. "Design novel fuzzy robust feedback linearization control with application to robot manipulator." International Journal of Intelligent Systems and Applications 5, no. 5 (2013): 1.

80. Al Saidi, Riyadh. "Model based control of a reconfigurable robot." (2015).

81. Song, Zuoshi, Jianqiang Yi, Dongbin Zhao, and Xinchun Li. "A computed torque controller for uncertain robotic manipulator systems: Fuzzy approach." Fuzzy sets and systems 154, no. 2 (2005): 208-226.

82. Norsahperi, N. M. H., and K. A. Danapalasingam. "An improved optimal integral sliding mode control for uncertain robotic manipulators with reduced tracking error, chattering, and energy consumption." Mechanical Systems and Signal Processing 142 (2020): 106747.

83. Behal, Aman, Warren Dixon, Darren M. Dawson, and Bin Xian. Lyapunov-based control of robotic systems. CRC Press, 2009.

84. Liu, Changxin, Jian Gao, and Demin Xu. "Lyapunov-based model predictive control for tracking of nonholonomic mobile robots under input constraints." International Journal of Control, Automation and Systems 15, no. 5 (2017): 2313-2319.

85. Salehi, Ahmad, Mohammad Hosein Kazemi, and Omid Safarzadeh. "The μ–synthesis and analysis of water level control in steam generators." Nuclear Engineering and Technology 51, no. 1 (2019): 163-169.

86. Riaz, Umar, Muhammad Tayyeb, and Arslan A. Amin. "A review of sliding mode control with the perspective of utilization in fault tolerant control." Recent Advances in Electrical & Electronic Engineering (Formerly Recent Patents on Electrical & Electronic Engineering) 14, no. 3 (2021): 312-324.

87. Ran, Chenyang, Yicheng Zhu, and Jianbo Su. "Sliding mode control with extended state observer for a class of nonlinear uncertain systems." International Journal of Control (2022): 1-17.

88. Al-hadithy, Dina, and Ahmed Hammoudi. "Two-Link Robot Through Strong and Stable Adaptive Sliding Mode Controller." In 2020 13th International Conference on Developments in eSystems Engineering (DeSE), pp. 121-127. IEEE, 2020.

89. Hung, John Y., Weibing Gao, and James C. Hung. "Variable structure control: A survey." IEEE transactions on industrial electronics 40, no. 1 (1993): 2-22.

90. Ghabi, Jalel. "A novel sliding mode controller scheme for a class of nonlinear uncertain systems." International Journal of Modelling, Identification and Control 29, no. 2 (2018): 127-135.

91. Gambier, Adrian. "Control in Partial Load Operation." In Control of Large Wind Energy Systems, pp. 119-154. Springer, Cham, 2022.

92. Khalil, Wisama, and Etienne Dombre. Modeling identification and control of robots. CRC Press, 2002.

93. Isidori, Alberto. "Local decompositions of control systems." In Nonlinear control systems, pp. 1-76. Springer, London, 1995.

94. Slotine, Jean-Jacques E., and Weiping Li. Applied nonlinear control. Vol. 199, no. 1. Englewood Cliffs, NJ: Prentice hall, 1991.

95. Freeman, Randy A., M. Krstić, and P. V. Kokotović. "Robustness of adaptive nonlinear control to bounded uncertainties." Automatica 34, no. 10 (1998): 1227-1230.

96. Narendra, Kumpati S. "Neural networks for control theory and practice." Proceedings of the IEEE 84, no. 10 (1996): 1385-1406.

97. Thomas, David E., and Brian Armstrong-Helouvry. "Fuzzy logic control-a taxonomy of demonstrated benefits." Proceedings of the IEEE 83, no. 3 (1995): 407-421.

98. Guo, Chen, M. A. Simaan, and Zengqi Sun. "Neuro-fuzzy intelligent controller for ship roll motion stabilization." In Proceedings of the 2003 IEEE International Symposium on Intelligent Control, pp. 182-187. IEEE, 2003.

99. Lee, Sang Yeal, and Hyung Suck Cho. "A fuzzy controller for an electro-hydraulic fin actuator using phase plane method." Control Engineering Practice 11, no. 6 (2003): 697-708.

100. Chen, Zheng, Ya-Jun Pan, and Jason Gu. "Integrated adaptive robust control for multilateral teleoperation systems under arbitrary time delays." International Journal of Robust and Nonlinear Control 26, no. 12 (2016): 2708-2728.

101. Khosla, Pradeep K., and Takeo Kanade. "Real-time implementation and evaluation of computed-torque scheme." IEEE Transactions on Robotics and Automation 5, no. 2 (1989): 245-253.

102. Akhrif, O., and G. L. Blankenship. "Robust stabilization of feedback linearizable systems." In Proceedings of the 27th IEEE Conference on Decision and Control, pp. 1714-1719. IEEE, 1988.

103. Lee, Hong Jae, Sung Eun Kim, Il Keun Kwon, Chiyoung Park, Chulhee Kim, Jaemoon Yang, and Sang Cheon Lee. "Spatially mineralized self-assembled polymeric nanocarriers with enhanced robustness and controlled drug-releasing property." Chemical communications 46, no. 3 (2010): 377-379.

104. Ding, BaoCang, HeXu Sun, and Peng Yang. "Further studies on LMI-based relaxed stabilization conditions for nonlinear systems in Takagi–Sugeno's form." Automatica 42, no. 3 (2006): 503-508.

105. Pranayanuntana, Poramate, and Riewruja Vanchai. "Nonlinear backstepping control design applied to magnetic ball control." In 2000 TENCON Proceedings. Intelligent Systems and Technologies for the New Millennium (Cat. No. 00CH37119), vol. 3, pp. 304-307. IEEE, 2000.

106. Shieh, Hsin-Jang, and Chia-Hsiang Hsu. "An adaptive approximator-based backstepping control approach for piezo actuator-driven stages." IEEE Transactions on Industrial Electronics 55, no. 4 (2008): 1729-1738.

107. Lin, S. M., C. J. Lin, C. C. Lin, C. W. Hsu, and Y. C. Chen. "Randomised controlled trial comparing percutaneous radiofrequency thermal ablation, percutaneous ethanol injection, and percutaneous acetic acid injection to treat hepatocellular carcinoma of 3 cm or less." Gut 54, no. 8 (2005): 1151-1156.

108. Liang, Yew-Wen, Li-Wei Ting, and Li-Gang Lin. "Study of reliable control via an integral-type sliding mode control scheme." IEEE Transactions on Industrial Electronics 59, no. 8 (2011): 3062-3068.

109. Fnaiech, Mohamed Amine, Franck Betin, Gérard-André Capolino, and Farhat Fnaiech. "Fuzzy logic and sliding-mode controls applied to six-phase induction machine with open phases." IEEE Transactions on Industrial Electronics 57, no. 1 (2009): 354-364.

110. Orlowska-Kowalska, Teresa, Grzegorz Tarchala, and Mateusz Dybkowski. "Sliding-mode direct torque control and sliding-mode observer with a magnetizing reactance estimator for the field-weakening of the induction motor drive." Mathematics and Computers in Simulation 98 (2014): 31-45.

111. Emelyanov, S. V. "Control of first order delay systems by means of an astatic controller and nonlinear correction." Autom. Remote Control 8 (1959): 983-991.

112. Utkin, Vadim. "Variable structure systems with sliding modes." IEEE Transactions on Automatic control 22, no. 2 (1977): 212-222.

113. Young, K. David, Vadim I. Utkin, and Umit Ozguner. "A control engineer's guide to sliding mode control." IEEE transactions on control systems technology 7, no. 3 (1999): 328-342.

114. Šabanovic, Asif. "Variable structure systems with sliding modes in motion control—A survey." IEEE Transactions on Industrial Informatics 7, no. 2 (2011): 212-223.

115. Hung, John Y., Weibing Gao, and James C. Hung. "Variable structure control: A survey." IEEE transactions on industrial electronics 40, no. 1 (1993): 2-22.

116. Utkin, Vadim, Jürgen Guldner, and Jingxin Shi. Sliding mode control in electro-mechanical systems. CRC press, 2017.

117. Zinober, Alan SI, ed. Variable structure and Lyapunov control. Vol. 193. Berlin: Springer, 1994.

118. Utkin, Vadim I., and I. Vadim. "Sliding mode control." Variable Structure Systems, from Principles To Implementation 66 (2004).

119. Iordanou, Harry N., and Brian W. Surgenor. "Experimental evaluation of the robustness of discrete sliding mode control versus linear quadratic control." IEEE Transactions on control systems technology 5, no. 2 (1997): 254-260.

120. Edwards, Christopher, and Sarah Spurgeon. Sliding mode control: theory and applications. Crc Press, 1998.

121. Utkin, Vadim, Jürgen Guldner, and Jingxin Shi. Sliding mode control in electro-mechanical systems. CRC press, 2017.

122. Barkana, Itzhak. "Adaptive control? But is so simple!." Journal of Intelligent & Robotic Systems 83, no. 1 (2016): 3-34.

123. Wang, Yu-Long, and Guang-Hong Yang. "Robust H∞ model reference tracking control for networked control systems with communication constraints." International Journal of Control, Automation and Systems 7, no. 6 (2009): 992-1000.

124. Zhang, Yangming, Peng Yan, and Zhen Zhang. "Robust adaptive backstepping control for piezoelectric nano-manipulating systems." Mechanical Systems and Signal Processing 83 (2017): 130-148.

125. Shtessel, Yuri, Christopher Edwards, Leonid Fridman, and Arie Levant. Sliding mode control and observation. Vol. 10. New York: Springer New York, 2014.

126. Ding, Shihong, Ju H. Park, and Chih-Chiang Chen. "Second-order sliding mode controller design with output constraint." Automatica 112 (2020): 108704.

127. Li, Jianxiong, Xinjian Liu, Miao Xu, and Yiming Fang. "Continuous Higher-Order Sliding Mode Control for A Class of n-th Order Perturbed Systems." IEEE Transactions on Circuits and Systems II: Express Briefs (2022).

128. Zhang, Cheng, and Franck Plestan. "Adaptive sliding mode control of floating offshore wind turbine equipped by permanent magnet synchronous generator." Wind Energy 24, no. 7 (2021): 754-769.

129. Zhang, Cheng, and Franck Plestan. "Individual/collective blade pitch control of floating wind turbine based on adaptive second order sliding mode." Ocean Engineering 228 (2021): 108897.

130. Truong, Thanh Nguyen, Anh Tuan Vo, and Hee-Jun Kang. "A backstepping global fast terminal sliding mode control for trajectory tracking control of industrial robotic manipulators." IEEE Access 9 (2021): 31921-31931.

131. Qian, Dianwei, and Jianqiang Yi. "Hierarchical sliding mode control for under-actuated cranes." Heidelberg, Ber: Springer (2016).

132. Utkin, Vadim, Alex Poznyak, Yury Orlov, and Andrey Polyakov. "Conventional and high order sliding mode control." Journal of the Franklin Institute 357, no. 15 (2020): 10244-10261.

133. Veselić, Boban, Čedomir Milosavljević, Branislava Peruničić-Draženović, Senad Huseinbegović, and Milutin Petronijević. "Discrete-time sliding mode control of linear systems with input saturation." International Journal of Applied Mathematics and Computer Science 30, no. 3 (2020).

134. Behera, Abhisek K., Bijnan Bandyopadhyay, Michele Cucuzzella, Antonella Ferrara, and Xinghuo Yu. "A survey on event-triggered sliding mode control." IEEE Journal of Emerging and Selected Topics in Industrial Electronics 2, no. 3 (2021): 206-217.

135. Qian, Dianwei, and Jianqiang Yi. "Hierarchical sliding mode control for under-actuated cranes." Heidelberg, Ber: Springer (2016).

136. Tabatabaee-Nasab, Fahimeh S., and Naser Naserifar. "Nanopositioning control of an electrostatic MEMS actuator: adaptive terminal sliding mode control approach." Nonlinear Dynamics 105, no. 1 (2021): 213-225.

137. Lv, Chengkun, Juntao Chang, Wen Bao, and Daren Yu. "Recent research progress on airbreathing aero-engine control algorithm." Propulsion and Power Research (2022).

138. Adamiak, Katarzyna. "Trajectory Following Quasi-Sliding Mode Control for Arbitrary Relative Degree Systems." In Advanced, Contemporary Control, pp. 27-38. Springer, Cham, 2020.

139. Tang, Rongchuan, Ke Shao, Feng Xu, Xueqian Wang, and Bin Liang. "Adaptive chattering-free terminal sliding mode control for a coordinate measuring machine system." Computers & Electrical Engineering 96 (2021): 107486.

140. Li, Chunli, Chao Ren, Yutong Ding, Tong Zhang, Wei Li, Xinshan Zhu, and Shugen Ma. "Non-singular terminal sliding mode control of an omnidirectional mobile manipulator based on extended state observer." International Journal of Intelligent Robotics and Applications 5, no. 2 (2021): 219-234.

141. Zhang, Lu, and Jun Yang. "Continuous nonsingular terminal sliding mode control for nonlinear systems subject to mismatched terms." Asian Journal of Control 24, no. 2 (2022): 885-894.

142. Sun, Zhe, Hao Xie, Jinchuan Zheng, Zhihong Man, and Defeng He. "Path-following control of Mecanum-wheels omnidirectional mobile robots using nonsingular terminal sliding mode." Mechanical Systems and Signal Processing 147 (2021): 107128.

143. Zhou, Shizhao, Chong Shen, Yangxiu Xia, Zheng Chen, and Shiqiang Zhu. "Adaptive robust control design for underwater multi-dof hydraulic manipulator." Ocean Engineering 248 (2022): 110822.

144. Saidi, Imen, and Nahla Touati. "Sliding Mode Control of a 2 DOF Robot Manipulator: A Simulation Study Using Artificial Neural Networks with Minimum Parameter Learning." Recent Patents on Mechanical Engineering 15, no. 2 (2022): 241-253.

145. Yousufzai, Imran Khan, Farrukh Waheed, Qudrat Khan, Aamer Iqbal Bhatti, Rahat Ullah, and Rini Akmeliawati. "A Linear Parameter Varying Strategy Based Integral Sliding Mode Control Protocol Development and Its Implementation on Ball and Beam Balancer." IEEE Access 9 (2021): 74437-74445.

146. Xiao, Yunfei, Yuan Feng, Tao Liu, Xiuping Yu, and Xianfeng Wang. "Integral Sliding Mode Based Finite-Time Tracking Control for Underactuated Surface Vessels with External Disturbances." Journal of Marine Science and Engineering 9, no. 11 (2021): 1204.

147. Rehman, Fazal Ur, Nadir Mehmood, Sami Ud Din, Muhammad Rafiq Mufti, and Humaira Afzal. "Adaptive Sliding Mode Based Stabilization Control for the Class of Underactuated Mechanical Systems." IEEE Access 9 (2021): 26607-26615.

148. Zhou, Weixiang, Yueying Wang, and Yinzheng Liang. "Sliding mode control for networked control systems: A brief survey." ISA transactions (2021).

149. Mehta, Axaykumar, and Bijnan Bandyopadhyay, eds. Emerging Trends in Sliding Mode Control: Theory and Application. Singapore: Springer, 2021.

150. Ullah, Safeer, Qudrat Khan, Adeel Mehmood, Syed Abdul Mannan Kirmani, and Omar Mechali. "Neuro-adaptive fast integral terminal sliding mode control design with variable gain robust exact differentiator for under-actuated quadcopter UAV." ISA transactions 120 (2022): 293-304.

151. Kali, Yassine, Khalid Benjelloun, Maarouf Saad, and Mohammed Benbrahim. "Non-singular terminal sliding mode with time delay control for uncertain 2 nd order nonlinear systems." In 2017 14th International Multi-Conference on Systems, Signals & Devices (SSD), pp. 625-630. IEEE, 2017.

152. Fallaha, Charles. "Design of a sliding mode controller with model-based switching functions applied to robotic systems." PhD diss., École de technologie supérieure, 2021.

153. Vernekar, Pratik, and Vitthal Bandal. "Robust Sliding Mode Control of a Magnetic Levitation System: Continuous-Time and Discrete-Time Approaches." arXiv preprint arXiv:2110.12363 (2021).

154. Derakhshannia, Mehran, and Seyyed Sajjad Moosapour. "Disturbance observer-based sliding mode control for consensus tracking of chaotic nonlinear multi-agent systems." Mathematics and Computers in Simulation 194 (2022): 610-628.

155. Parra-Vega, Vicente, Alejandro Rodríguez-Angeles, and Gerhard Hirzinger. "Perfect position/force tracking of robots with dynamical terminal sliding mode control." Journal of Robotic Systems 18, no. 9 (2001): 517-532.

156. Tang, Yuangang, Fuchun Sun, and Zengqi Sun. "Neural network control of flexible-link manipulators using sliding mode." Neurocomputing 70, no. 1-3 (2006): 288-295.

157. Wang, Liangyong, Tianyou Chai, and Lianfei Zhai. "Neural-network-based terminal sliding-mode control of robotic manipulators including actuator dynamics." IEEE Transactions on Industrial Electronics 56, no. 9 (2009): 3296-3304.

158. Guo, Bao-Zhu, and Feng-Fei Jin. "The active disturbance rejection and sliding mode control approach to the stabilization of the Euler–Bernoulli beam equation with boundary input disturbance." Automatica 49, no. 9 (2013): 2911-2918.

159. Nojavanzadeh, Donya, and Mohammadali Badamchizadeh. "Adaptive fractional-order non-singular fast terminal sliding mode control for robot manipulators." IET Control Theory & Applications 10, no. 13 (2016): 1565-1572.

160. Razzaghian, Amir, Reihaneh Kardehi Moghaddam, and Naser Pariz. "Adaptive neural network conformable fractional-order nonsingular terminal sliding mode control for a class of second-order nonlinear systems." IETE Journal of Research (2020): 1-10.

161. Zhu, Jiaming, Zhiqiang Cao, Yuequan Yang, and Yang Yi. "Terminal sliding mode control of Markovian jumping manipulator systems." In 2016 IEEE International Conference on Industrial Technology (ICIT), pp. 1855-1858. IEEE, 2016.

162. Asl, Reza Mohammadi, Yashar Shabbouei Hagh, and Heikki Handroos. "Adaptive extended Kalman filter designing based on non-singular fast terminal sliding mode control for robotic manipulators." In 2017 IEEE International Conference on Mechatronics and Automation (ICMA), pp. 1670-1675. IEEE, 2017.

163. Luong, Tuan Anh, Sungwon Seo, Jeongmin Jeon, Jeongyeol Park, Ja Choon Koo, Hyouk Ryeol Choi, and Hyungpil Moon. "Continuous terminal sliding mode control with perturbation

estimation for a stewart platform." In 2017 14th International Conference on Ubiquitous Robots and Ambient Intelligence (URAI), pp. 360-365. IEEE, 2017.

164. Rsetam, Kamal, Zhenwei Cao, and Zhihong Man. "Hierarchical non-singular terminal sliding mode controller for a single link flexible joint robot manipulator." In 2017 IEEE 56th Annual Conference on Decision and Control (CDC), pp. 6677-6682. IEEE, 2017.

165. Nguyen, Van-Cuong, Anh-Tuan Vo, and Hee-Jun Kang. "A finite-time fault-tolerant control using non-singular fast terminal sliding mode control and third-order sliding mode observer for robotic manipulators." IEEE Access 9 (2021): 31225-31235.

166. Nair, Ranjith Ravindranathan, Hamad Karki, Amit Shukla, Laxmidhar Behera, and Mo Jamshidi. "Fault-tolerant formation control of nonholonomic robots using fast adaptive gain nonsingular terminal sliding mode control." IEEE Systems Journal 13, no. 1 (2018): 1006-1017.

167. Liu, Yang, and Hongnian Yu. "A survey of underactuated mechanical systems." IET Control Theory & Applications 7, no. 7 (2013): 921-935.

168. Mallem, Ali, Slimane Nourredine, and Walid Benaziza. "Mobile robot trajectory tracking using PID fast terminal sliding mode inverse dynamic Control." In 2016 4th International Conference on Control Engineering & Information Technology (CEIT), pp. 1-6. IEEE, 2016.

169. Chen, Gang, and Yong-Duan Song. "Robust fault-tolerant cooperative control of multi-agent systems: A constructive design method." Journal of the Franklin Institute 352, no. 10 (2015): 4045-4066.

170. Zheng, Naijia, Yu Zhang, Yuanbo Guo, and Xiaohua Zhang. "Hierarchical fast terminal sliding mode control for a self-balancing two-wheeled robot on uneven terrains." In 2017 36th Chinese Control Conference (CCC), pp. 4762-4767. IEEE, 2017.

171. Khoo, S., L. Xie, and Z-hong Man. "Integral terminal sliding mode cooperative control of multi-robot networks." In 2009 IEEE/ASME International Conference on Advanced Intelligent Mechatronics, pp. 969-973. IEEE, 2009.

172. Shen, Henghua, Ya-Jun Pan, Usman Ahmad, Steven Liu, Min Wu, and Yanhao He. "Tracking Performance Evaluations on the Robust Teleoperative Control of Multiple Manipulators." In 2019 IEEE 28th International Symposium on Industrial Electronics (ISIE), pp. 1268-1273. IEEE, 2019.

173. Wu, Hsiao-Lang, Ching-Chih Tsai, and Feng-Chun Tai. "Adaptive nonsingular terminal sliding-mode formation control using ORFWNN for uncertain networked heterogeneous mecanum-wheeled omnidirectional robots." In 2017 IEEE International Conference on Systems, Man, and Cybernetics (SMC), pp. 3317-3322. IEEE, 2017.

174. Zhao, Dongya, and Quanmin Zhu. "Position synchronised control of multiple robotic manipulators based on integral sliding mode." International Journal of Systems Science 45, no. 3 (2014): 556-570.

175. Bennehar, Moussab, Gamal El-Ghazaly, Ahmed Chemori, and François Pierrot. "A novel adaptive terminal sliding mode control for parallel manipulators: Design and real-time experiments." In 2017 IEEE International Conference on Robotics and Automation (ICRA), pp. 6086-6092. IEEE, 2017.

176. Khan, Muhammad Fayaz, Raza ul Islam, and Jamshed Iqbal. "Control strategies for robotic manipulators." In 2012 International Conference of Robotics and Artificial Intelligence, pp. 26-33. IEEE, 2012.

177. Laghrouche, Salah, Franck Plestan, and Alain Glumineau. "Higher order sliding mode control based on integral sliding mode." Automatica 43, no. 3 (2007): 531-537.

178. Ding, Shihong, and Shihua Li. "Second-order sliding mode controller design subject to mismatched term." Automatica 77 (2017): 388-392.

179. Basin, Michael, Chandrasekhara Bharath Panathula, and Yuri Shtessel. "Adaptive uniform finite-/fixed-time convergent second-order sliding-mode control." International Journal of Control 89, no. 9 (2016): 1777-1787.

180. Ferrara, Antonella, and Gian Paolo Incremona. "Design of an integral suboptimal second-order sliding mode controller for the robust motion control of robot manipulators." IEEE Transactions on Control Systems Technology 23, no. 6 (2015): 2316-2325.

181. Incremona, Gian Paolo, Michele Cucuzzella, and Antonella Ferrara. "Adaptive suboptimal second-order sliding mode control for microgrids." International Journal of Control 89, no. 9 (2016): 1849-1867.

182. Ling, Rui, Dragan Maksimovic, and Ramon Leyva. "Second-order sliding-mode controlled synchronous buck DC–DC converter." IEEE Transactions on power electronics 31, no. 3 (2015): 2539-2549.

183. Beltran, Brice, Mohamed El Hachemi Benbouzid, and Tarek Ahmed-Ali. "Second-order sliding mode control of a doubly fed induction generator driven wind turbine." IEEE Transactions on Energy Conversion 27, no. 2 (2012): 261-269.

184. Khan, M. Khalid, Keng Boon Goh, and Sarah K. Spurgeon. "Second order sliding mode control of a diesel engine." Asian Journal of Control 5, no. 4 (2003): 614-619.

185. Khan, Mohammad Khalid. Design and application of second order sliding mode control algorithms. University of Leicester (United Kingdom), 2003.

186. Van, Mien. "Higher-order terminal sliding mode controller for fault accommodation of Lipschitz second-order nonlinear systems using fuzzy neural network." Applied Soft Computing 104 (2021): 107186.

187. Kaplan, Orhan, and Ferhat Bodur. "Second-order sliding mode controller design of buck converter with constant power load." International Journal of Control (2022): 1-17.

188. Stepanenko, Yury, and Chun-Yi Su. "Variable structure control of robot manipulators with nonlinear sliding manifolds." International Journal of Control 58, no. 2 (1993): 285-300.

189. Yao, Meibao, Xueming Xiao, Yang Tian, and Hutao Cui. "A fast terminal sliding mode control scheme with time-varying sliding mode surfaces." Journal of the Franklin Institute 358, no. 10 (2021): 5386-5407.

190. Van, Mien. "Higher-order terminal sliding mode controller for fault accommodation of Lipschitz second-order nonlinear systems using fuzzy neural network." Applied Soft Computing 104 (2021): 107186.

191. Li, Huijie, and Yuanli Cai. "Fixed-time non-singular terminal sliding mode control with globally fast convergence." IET Control Theory & Applications (2022).

192. Rsetam, Kamal, Zhenwei Cao, and Zhihong Man. "Design of robust terminal sliding mode control for underactuated flexible joint robot." IEEE Transactions on Systems, Man, and Cybernetics: Systems (2021).

193. Ghadiri, Hamid, Alireza Mohammadi, and Hamed Khodadadi. "Fast terminal sliding mode control based on SDRE observer for two-axis gimbal with external disturbances." Journal of the Brazilian Society of Mechanical Sciences and Engineering 44, no. 2 (2022): 1-23.

194. Huang, Sunhua, Jie Wang, Chen Huang, Lidan Zhou, Linyun Xiong, Jiayan Liu, and Penghan Li. "A fixed-time fractional-order sliding mode control strategy for power quality enhancement of PMSG wind turbine." International Journal of Electrical Power & Energy Systems 134 (2022): 107354.

195. Mobayen, Saleh, Khalid A. Alattas, and Wudhichai Assawinchaichote. "Adaptive continuous barrier function terminal sliding mode control technique for disturbed robotic manipulator." IEEE Transactions on Circuits and Systems I: Regular Papers 68, no. 10 (2021): 4403-4412.

196. Camacho, Oscar, Rubén Rojas, and Winston García. "Variable structure control applied to chemical processes with inverse response." ISA transactions 38, no. 1 (1999): 55-72.

197. Kelkoul, Bahia, and Abdelmadjid Boumediene. "Stability analysis and study between classical sliding mode control (SMC) and super twisting algorithm (STA) for doubly fed induction generator (DFIG) under wind turbine." Energy 214 (2021): 118871.

198. Vo, Anh Tuan, Thanh Nguyen Truong, and Hee-Jun Kang. "A novel tracking control algorithm with finite-time disturbance observer for a class of second-order nonlinear systems and its applications." IEEE Access 9 (2021): 31373-31389.

199. Alattas, Khalid A., Javad Mostafaee, Abdullah K. Alanazi, Saleh Mobayen, Mai The Vu, Anton Zhilenkov, and Hala M. Abo-Dief. "Nonsingular Terminal Sliding Mode Control Based on Adaptive Barrier Function for n th-Order Perturbed Nonlinear Systems." Mathematics 10, no. 1 (2021): 43.

200. Brahmi, Brahim, Ibrahim El Bojairami, Tanvir Ahmed, Mohammad Habibur Rahman, Asif Al Zubayer Swapnil, and Javier Sanjuan De Caro. "New Adaptive Sliding Mode for Unperturbed Forearm and Wrist Rehabilitation Robot." In 2021 18th International Multi-Conference on Systems, Signals & Devices (SSD), pp. 1160-1165. IEEE, 2021.

201. ABB Robotics, I.M.P.S., Retrieved from http://www.abb.com/ 2021, ABB Products. ABB IRB 140 - Robots (Robotics).

202. Toquica, J.S. and J.M.S. Motta, A methodology for industrial robot calibration based on measurement sub-regions. The International Journal of Advanced Manufacturing Technology, 2021: p. 1-18.

203. Schilling, R.J., Fundamentals of robotics: analysis and control. 1996: Simon & Schuster Trade.

204. Craig, J.J., Introduction to Robotics: Mechanics and Control (3-rd Edition). PEARSON Prentice Hall, 2005: p. 41-46.

205. Almaged, M., Forward and inverse kinematic analysis and validation of the ABB IRB 140 industrial robot. Journal of Mechanical Engineering and Technology (JMET), 2017. 9(2): p. 1-20.

206. Dahari, M. and J.-D. Tan. Forward and inverse kinematics model for robotic welding process using KR-16KS KUKA robot. in 2011 Fourth International Conference on Modeling, Simulation and Applied Optimization. 2011. IEEE.

207. Kucuk, S. and Z. Bingul, Robot kinematics: Forward and inverse kinematics. 2006: INTECH Open Access Publisher.

208. Pieper, D.L., The kinematics of manipulators under computer control. 1969: Stanford University.

209. Kostic, D., et al. Closed-form kinematic and dynamic models of an industrial-like RRR robot. in Proceedings 2002 IEEE International Conference on Robotics and Automation (Cat. No. 02CH37292). 2002. IEEE.

210. Sciavicco, L. and B. Siciliano, Modelling and control of robot manipulators. 2001: Springer Science & Business Media.

211. Suárez, M.B. and R.R. Heredia. Kinematics, dynamics and evaluation of energy consumption for ABB IRB-140 serial robots in the tracking of a path. in The 2nd International Congress of Engineering Mechatron-ics and Automation. 2013.

212. Fazilat, Mehdi, Nadjet Zioui, and Jonathan St-Arnaud. "A novel quantum model of forward kinematics based on quaternion/Pauli gate equivalence: Application to a six-jointed industrial robotic arm." Results in Engineering 14 (2022): 100402.

213. Pires, J.N., Industrial robots programming: building applications for the factories of the future. 2007: Springer Science & Business Media.

214. Vicente, D.B., Modeling and Balancing of Spherical Pendulum Using a Parallel Kinematic Manipulator. 2007: Department of Automatic Control, Lund University.

215. Carter, T.J., The Modeling of a Six Degree-of-freedom Industrial Robot for the Purpose of Efficient Path Planning. 2009.

216. Spong, M.W., S. Hutchinson, and M. Vidyasagar, Robot modeling and control, jon wiley & sons. Inc, ISBN-100-471-649, 2005.

217. Baturone, A.O., Robótica: manipuladores y robots móviles. 2005: Marcombo.

218. Utkin, Vadim, Jürgen Guldner, and Jingxin Shi. Sliding mode control in electro-mechanical systems. CRC press, 2017.

219. Vaidyanathan, Sundarapandian, and Chang-Hua Lien, eds. Applications of sliding mode control in science and engineering. Vol. 709. Springer, 2017.

220. Sharma, Sandeep, Dhananjay Srivastava, Keyur Patel, and Axaykumar Mehta. "Design and implementation of second order sliding mode controller for 2-DOF flexible robotic link." In 2018 2nd International Conference on Power, Energy and Environment: Towards Smart Technology (ICEPE), pp. 1-6. IEEE, 2018.